STRATIGRAPHIC ARCHITECTURE AND DEPOSITIONAL HISTORY OF LATERALLY–ACCRETED CHANNEL FILLS IN THE LOWER ISAAC FORMATION, WINDERMERE SUPERGROUP, BRITISH COLUMBIA, CANADA

By

Iain Gerald Dumouchel

Thesis presented to the

Faculty of Graduate and Postdoctoral Studies

in partial fulfillment of the requirements for the

degree of Master of Science in Earth Sciences

Department of Earth Sciences

Faculty of Science

University of Ottawa

ABSTRACT

Continental slope channels, which serve as the primary conduits for sediment transport into the deep marine, occasionally become sites of sediment deposition with excellent reservoir potential. Increasingly reported in the literature are subsurface channel fills exhibiting shingled seismic reflectors that are interpreted to have formed by lateral channel migration. In lower Isaac Formation channels inclined strata are observed but at a lateral scale that is far below industry-seismic detection. Distinctively these flat-based channels are filled with coarse-grained sandstone that transitions abruptly and obliquely upwards into thin, fine grained turbidites. Like rivers, lateral accretion in Isaac channels is interpreted to be the result of the interaction of inertial and pressure forces, but in highly turbulent, highly density-stratified turbidity currents. This resulted in the formation of two superimposed secondary circulation cells that caused enhanced erosion on the outer bank and preferential deposition of coarse-grained sediment along the inner bank.

ACKNOWLEDGEMENTS

This thesis was completed during an interesting period in my life, and the time I spent working on it encompassed both emotional highs and lows. Its completion would ultimately not have been possible without a lot of support, either academic, financial, or personal, for which I am incredibly grateful. First and foremost, I would like to thank Dr. Bill Arnott, who has been the greatest supervisor I could have possibly asked for. Bill's enthusiasm for all things geology is very refreshing and, after sitting in his 2nd year lecture, his charisma had me hooked for both an Honour's and Master's project. He is very committed to his students, is extremely approachable, almost always available, and was also incredibly understanding when I decided to take a leave of absence for personal reasons.

A hearty 'thank-you!' is also owed to the rest of the Windermere Research Group – I will miss our (sometimes extended) talks on Friday afternoons. Dr. Viktor Terlaky and soon-to-be-Drs Mike Tilston and Lilian Navarro were extremely helpful for this project. Dave Lowe, another soon-to-be-Dr, always had insightful comments and was very patient to deal with the never-ending 'flow' of deep-marine sedimentology. Best of luck to my office-mate and partner in vodka and crime Natasa Popovic, and to all of Bill's new(er) Master's students: Derrick Midwinter, Katrina Angus, and Anika Bergen – your work is really excellent and it's too bad I won't be around to see its completion. I'm very grateful to James Randall, Alain Mauviel, Alex Gaucher-Loksts, and Kim Delauney who helped me out with fieldwork. A huge thank-you as well to Genevieve Huyer who drew up some strat logs for me while I was away – they are much nicer than my own! This research would not have been possible without grants from NSERC, as well as the generous contributions from the companies that make up the Windermere Consortium: BP, Chevron, Statoil, Canadian Natural, Nexen, Apache, Anadarko, and Husky Energy.

I also need to extend a massive thank-you to my family, who have always been supportive, and especially to my parents, Bryan and Peigi, and my sister Meaghan. Your steadfast support has meant the world to me. I want to say thanks as well to my other colleagues in the Department of Earth Sciences, the administrative staff and technicians (looking at you George for the excellent thin sections), and to my friends and climbing partners who were most encouraging and supportive.

Lastly, thanks very much to my thesis committee of Drs. Don Cummings and Quentin Gall for taking the time to read my work.

TABLE OF CONTENTS

ABSTRACT ii
ACKNOWLEDGEMENTS iii
TABLE OF CONTENTS iv
LIST OF FIGURES vi
LIST OF TABLES vii
1 INTRODUCTION 1
1.1 Thesis Objectives 1
1.2 Geological Setting and Regional Geology 2
1.3 Local Stratigraphy 9
1.4 Study Area and Methodology 9
1.5 Previous Work 12
1.6 Theoretical Overview 13
1.6.1 Sediment Gravity Flows 13
1.6.2 Sedimentation Mechanisms 19
1.6.3 Sinuous Channels and Lateral Accretion 21
1.6.4 Secondary Flow in Deep-Marine Sinuous Channels 25
1.6.5 Effects of Relative Sea-Level Change on Deep-Marine Sedimentation 26
2 FACIES DESCRIPTIONS AND INTERPRETATIONS 30
2.1 LF1: Thin to very-thick bedded, ungraded and normally-graded sandstone and conglomerate 30
2.1.1 Description 30
2.1.2 Interpretation 32
2.2 LF2: Medium to very-thick bedded, ungraded and normally-graded sandstone and conglomerate with mudstone clasts 33
2.2.1 Description 33
2.2.2 Interpretation 34
2.3 LF3: Thin- and very-thinly bedded sandstone, siltstone, and mudstone 35
2.3.1 Description 35
2.3.2 Interpretation 37
2.4 LF4: Medium-scale cross-bedded sandstone 38
2.4.1 Description 38
2.4.2 Interpretation 38
2.5 LF5: Very-thick bedded poorly-sorted silty granular mudstone 40

2.5.1 Description 40
2.5.2 Interpretation 40
3 CHANNEL FILL DESCRIPTIONS 42
3.1 Classification Hierarchy 42
3.2 Channel 2.3 42
3.3 Unit 14 48
3.4 Unit 21 49
4 REVIEW OF LATERALLY-ACCRETED CHANNEL FILL OUTCROPS 54
4.1 Introduction 54
4.2 Examples 54
4.2.1 Rosario Formation, San Fernando Canyon, Mexico 54
4.2.2 Solitary Channel, Tabernas Basin, Spain 60
4.2.3 Beacon Channel Complex, Brushy Canyon Formation, Delaware Basin, Texas 61
4.2.4 Makarska Flysch, Croatia 63
4.2.5 Ross and Gull Island Formations, Shannon Basin, Ireland 64
4.2.6 Jackfork Group, Ouachita Basin, Arkansas 67
4.3 Summary 68
5 DISCUSSION 71
5.1 Characteristic Attributes of Laterally-Accreted Channels at Castle Creek 71
5.1.1 Abundance of coarse-grained sediments 71
5.1.2 Abrupt transition to fine-grained upper division turbidites 72
5.1.3 Channel filled with inclined strata 73
5.1.4 Relatively Flat Basal Contacts 74
5.1.5 Presence of injection complexes 75
5.2 Lateral accretion model 77
5.3 Depositional History 83
5.3.1 Channel 2.3 83
5.3.2 Unit 14 84
5.3.3 Unit 21 85
6 CONCLUSIONS 87
BIBLIOGRAPHY 91

LIST OF FIGURES

Figure 1.1 Distribution of strat from the Neoproterozoic Windermere Supergroup along western North America 4
Figure 1.2: Schematic stratigraphy of the Windermere Supergroup in the southern Canadian Cordillera. 6
Figure 1.3: Geologic map of the southern Canadian Cordillera including the Castle Creek study area. 8
Figure 1.4: Photograph of the Castle Creek study area 10
Figure 1.5: Aerial photographs of (A) Isaac Channel 2.3, (B) Isaac Unit 14, and (C) Isaac Unit 21 .. 11
Figure 1.6: Schematic of the idealized Bouma turbidite sequence 14
Figure 1.7: Physically-based classification scheme for subaqueous sedimentary density flows by Mulder and Alexander (2001). 15
Figure 1.8: High-resolution (65 Hz) (A) seismic cross-section of the Green Channel Complex (B) amplitude map (C) cartoon of a laterally-migrating channel 23
Figure 1.9: Cartoon illustrating the differences in scale between an individual lateral accretion deposit (LAD), a laterally-accreted channel fill composed of lateral accretion deposits, and a lateral accretion package (LAP) composed of laterally-accreted channel fills. 25
Figure 1.10: Idealized model relating characteristics of sediment transport and deposition to positions of relative sea level 28
Figure 2.1: Welded contact between two Ta beds. 31
Figure 2.2: Photomicrograph of LF1 strata in plane (A) and cross (B) polarized light. 31
Figure 2.3: LF2 bed 34
Figure 2.4: LF3a bed with Bouma Tabcd divisions 36
Figure 2.5: LF4 bed abruptly overlying Ta bed 39
Figure 2.6: Debrite bed 41
Figure 3.1: Isaac Channel 2.3 channel element boundaries overlain on an aerial photomosaic. 45
Figure 3.2: Isaac Channel 2.3 channel element boundaries overlain on stratigraphic logs. 45
Figure 3.3: Isaac Channel 2.3 lithologies overlain on aerial photomosaic. 46
Figure 3.4: (A) photograph and (B) correlated stratigraphic logs of a lateral accretion deposit 46
Figure 3.5: (A) Photograph and photomicrographs (B = PPL, C = XPL) from medium-bedded green sandstone interval with high chlorite content. 47
Figure 3.6: Isaac Unit 14 lithologies overlain on an aerial photomosaic. 49
Figure 3.7: Isaac Unit 14 channel element boundaries overlain on an aerial photomosaic. 50
Figure 3.8: Isaac Unit 14 channel element boundaries overlain on stratigraphic logs. 50
Figure 3.9: Isaac Unit 21 lithologies overlain on an aerial photomosaic. 52
Figure 3.10: Isaac Unit 21 channel element boundaries overlain on an aerial photomosaic. 52
Figure 3.11: Isaac Unit 21 channel element boundaries overlain on stratigraphic logs. 53
Figure 4.1: Photomosaic and line drawing of the Pelican Point North Outcrop in the Rosario Formation 56
Figure 4.2: Photomosaic and line drawing fo the Pelican Point South Outcrop 57
Figure 4.3: Outcrop photograph and overlay drawing for a laterally-accreted channel fill in the Rosario Formation (Janocko, 2011, fig 4.12) 59
Figure 4.4: Photograph and overlay drawing for two laterally-accreted channel fills in the Rosario Formation (Janocko, 2011, fig 4.18). 60

Figure 4.5: Wide-angle photograph and overlay drawing for a laterally accreted channel fill in the Makarska Flysch (Janocko, 2011, fig 4.17). 64
Figure 4.6: Photograph and line diagram of interpreted lithologies for the Rehy Cliffs outcrop of the Ross Formation (Abreu et al., 2003, fig 22). 66
Figure 4.7: Photograph and line drawing of interpreted lithologies for the Big Rock Quarry outcrop of the Jackfork Group (Abreu et al., 2003, fig 23). 68
Figure 5.1: Cartoon illustrating the difference in the dip of laterally-accreted strata as a function of the orientation of the outcrop face versus dip direction of the LADs. 73
Figure 5.2: Aerial photomosaic of CE 21-1 overlain by injected sandstone, conglomerate, and mudclast breccia originating from CE 21-2. 75
Figure 5.3: Aerial photomosaic of Isaac Channel 2.2 overlain by thinly-bedded turbidites that along the step at the base of CE 2.3-2 were injected by coarse-grained sand and mudclast breccia originating from CE 2.3-2. 76
Figure 5.4: Cartoon illustrating the forces present in an open channel flow meander bend and the resultant secondary circulation. 79
Figure 5.5: Cartoon illustrating the velocity and density profiles through a highly stratified sediment gravity flow. 80
Figure 5.6: Sequence of cartoons depicting cross-stream fluid flow in a deep-marine channel as a highly stratified sediment gravity flow travels around a meander bend. 81
Figure 5.7: Conceptual diagram of estuarine flows. 82
Figure 5.8: Cartoon illustrating the proposed depositional history of Isaac Channel 2.3. 84
Figure 5.9: Cartoon illustrating the proposed depositional history of Isaac Unit 14. 85
Figure 5.10: Cartoon illustrating the proposed depositional history of Isaac Unit 21. 86

LIST OF TABLES

Table 1.1: List of sediment support mechanisms in sediment-gravity flows. 18
Table 4.1: Summary of outcrop examples of interpreted laterally accreting deep-marine channel fills. 70

1 INTRODUCTION

1.1 Thesis Objectives

Sand-rich deposits formed on continental slopes and the deeper basin floor constitute important hydrocarbon reservoirs (Weimer et al., 2000). Due to the high-cost associated with exploration and production it is important to characterize and predict the architecture and distribution of strata in turbidite systems in order to minimize the scientific and economic risk (McHargue et al., 2011). On the continental slope, the principal reservoir units are slope channels, which are the primary conduits through which sediments bypass on their journey to the basin floor. Occasionally channels become sites of sand and gravel accumulation, and therefore have been the subject of intense sedimentological investigation. While commonly sinuous, many of channels possess an internal architecture suggesting that they filled aggradationally (e.g. Navarro, 2011; Romans et al., 2007). Recently, however, channel fills characterized by shingled reflectors in seismic surveys, and interpreted to have been formed by laterally migrating channels, have increasingly been reported in the literature (e.g. Abreu, 2003; Dykstra and Kneller, 2009). Much less commonly documented in that record are examples exhibiting meter- to several-meter-scale laterally-spaced accretion deposits that more closely resemble those observed in modern and ancient sinuous fluvial channel deposits (i.e. point bars). Several laterally accreting channel elements are superbly exposed in the Castle Creek study area. Channel elements are between 5-15 m thick and filled with anomalously coarse-grained strata, typically very-coarse sand to fine granule conglomerate, which then grade abruptly upward and obliquely-upward into fine-grained, upper-division turbidites. The objective of this study, therefore, is to document in detail the lithological

make-up and stratigraphic architecture of three of these channel elements, and then interpret their mechanisms of deposition. Ultimately, these data will provide additional insights into these enigmatic channel systems. These results could then be extrapolated to help predict the lithological make-up and stratal architecture of similar channel elements in other deep-marine systems.

1.2 Geological Setting and Regional Geology

The Late Proterozoic was a time of a number of major global events, including the assembly and break-up of the supercontinent Rodinia (Li et al., 2008), low-latitude glaciations (Kilner et al., 2005), the first rise (and extinction) of metazoan life in the Ediacarans (Knoll et al., 2006), and, for this study, deposition of the Windermere Supergroup in what is now western North America (Ross, 1995). The existence of a Precambrian supercontinent was first proposed by Valentine and Moores (1970), which they named Pangea I, based on the subsequent diversification of flora and fauna in the Cambrian and Ordovician. Some two decades later the model came into the geological mainstream with the publication of three independent papers in 1991 by Hoffman, Moores, and Dalziel that utilized similar basement rocks as 'piercing points' to assemble continental landmasses into a single composite entity. Hoffman (1991) argued that although any pre-Mesozoic reconstruction developed without the help of sea-floor magnetic anomalies would be "necessarily speculative", the "correlation of Precambrian orogenic belts that were once continuous but are now truncated at modern or ancient continental margins provides a means of establishing former linkages between separated continents" (p. 1409). Currently there is

little opposition to the existence of the supercontinent Rodinia; however, “there is still no consensus regarding the number of participating cratons, their relative positions within the supercontinent, and the chronology and mode of assembly and [subsequent] break-up” (Li et al. 2008, p. 180). Amalgamation was likely complete by 900 Ma (Li et al. 2008), with the Laurentian craton occupying the centre in most models (eg. Hoffman 1991; Moores 1991) based on the presence of post-rift, passive margin sedimentation along its east and west margins. Currently, there is general agreement about the configuration of the eastern margin; but the identity of the conjugate block that rifted from western Laurentia remains a source of debate (Li et al. 2008).

Genetically related mafic dykes and sheets of Neoproterozoic age, such as those of the Gunbarrel mafic magmatic event (775-782 Ma)(Harlan et al., 2003) and the Franklin igneous event (723 Ma), features that crop out over several thousand kilometers, may be related to the rifting of Rodinia (Li et al, 2008). The amount of heat needed to produce such extensive melting is most readily provided by a mantle plume, which may have “been a precursor to, or may have caused, the initial Late Proterozoic rifting of North America” (Harlan et al. 2003, p. 1055). Currently there is some consensus that the onset of rifting in western Laurentia was at about 780 Ma, but that the main episode of rift magmatism occurred later between 750 and 720 Ma (Li et al. 2008).

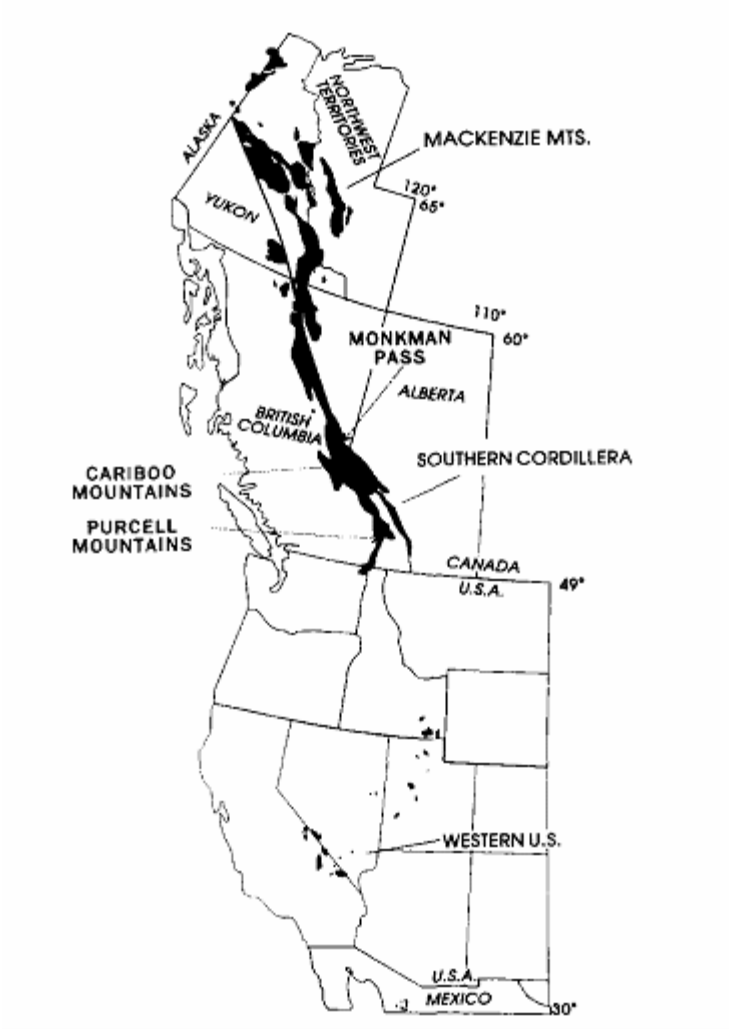

Figure 1.1 Distribution of strat from the Neoproterozoic Windermere Supergroup along western North America (Ross et al., 1995).

The continued evolution of the western margin of Laurentia up to the sub-Cambrian unconformity can be inferred from sedimentary rocks of the Neoproterozoic Windermere Supergroup, which crop out over a strike length of 4000km in western North America (fig 1.1). Exposures south of the U.S. Canadian border are discontinuous and consist mostly of shallow-marine and continental facies, whereas those in the Canadian Cordillera are more continuous and dominated by outer shelf, slope, and basin floor deposits (Link, 1993; Ross and Arnott, 2007). The scale and continuity of exposures suggests that deposition took place in a continuous basin (Eisbacher 1985). In the Southern Canadian Cordillera, rocks of the

WSG are up to 9 km thick and record a complex history of tectonism and two phases of deposition (fig 1.2). The first phase is represented by discontinuous syn-rift deposits, which then are overlain by a several km-thick upward-shoaling succession of the second phase of deposition that represents the progradation of the Laurentian passive margin under diminishing rates of thermal subsidence (Ross 1995). Intercalated mafic volcanics (Irene Formation) and coarse-grained rocks, including glacial diamictons of the Toby Formation, respectively represent flood basalt volcanism and rift basin sedimentation as an unknown conjugate block separated from Laurentia during the first phase. In the Cariboo Mountains, strata of the second phase are 5-7 km thick and comprise the Kaza Group conformably overlain by the Cariboo Group up to the sub-Cambrian unconformity. The Kaza Group is a 2-4 km thick assemblage composed primarily of metamorphosed sandstone interbedded with conglomerate, siltstone, and mudstone. The group is subdivided into lower, middle, and upper parts and is interpreted to represent deposition on the basin floor (Terlaky 2014, Ross et. al, 1995). The Middle and Upper Kaza groups are separated by a geochemically distinctive unit termed the Old Fort Point Formation, which forms an important regional marker (Smith et al., 2014). The Caribou Group is up to 5 km thick and comprises three formations, which stratigraphically upward are the Isaac, Cunningham, and Yankee Belle formations. The Isaac Formation is composed of metamorphosed mudstone and siltstone with subordinate sandstone, conglomerate, and carbonate interpreted to have been deposited on the slope and base-of-slope (Ross et. al, 1995), with carbonate intervals sourced from a local highstand shelf (Ross, 1991). Overlying the Isaac Formation is the Cunningham Formation consisting of a 550 m thick succession of oolitic-intraclastic limestones overlain

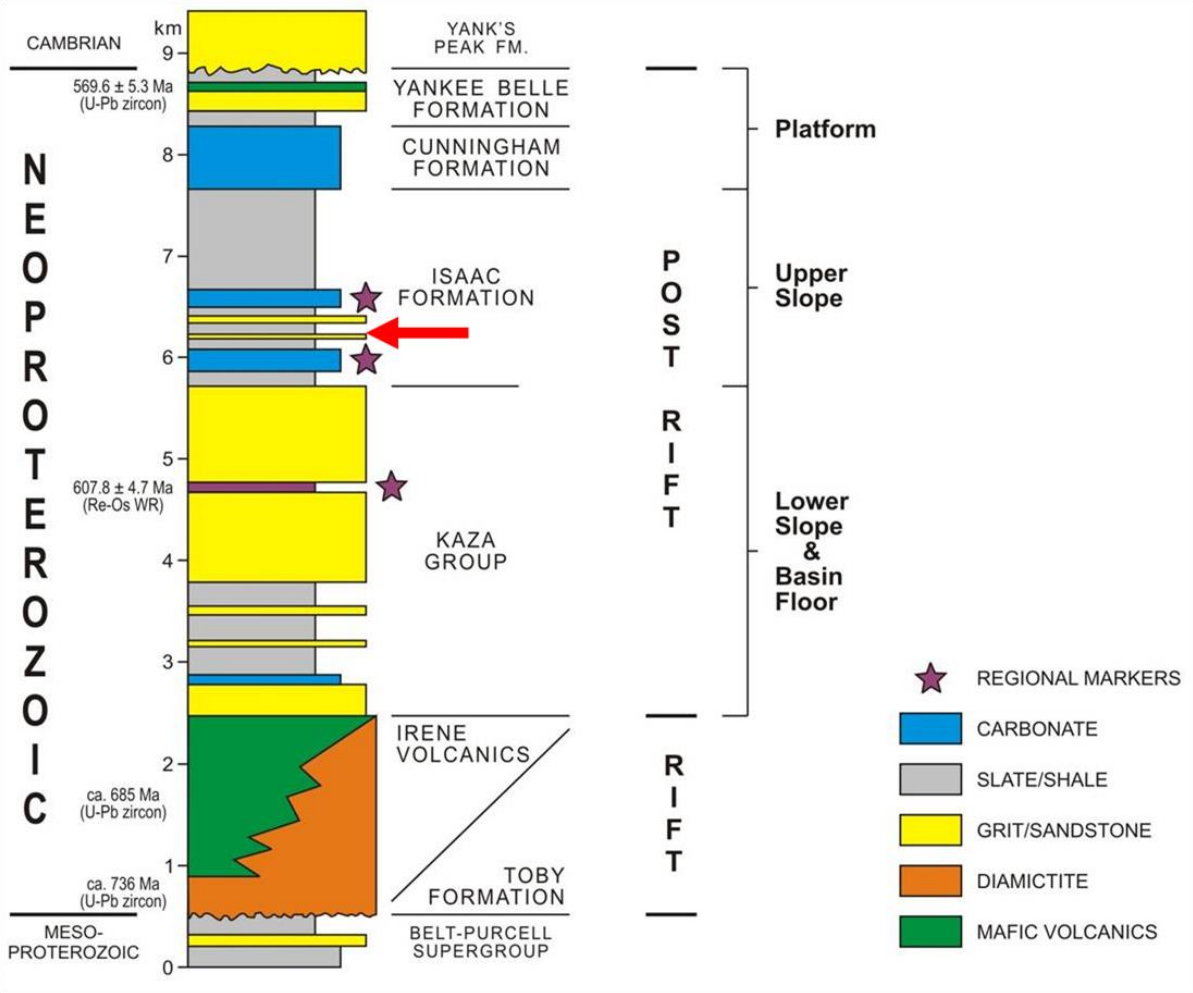

Figure 1.2: Schematic stratigraphy of the Windermere Supergroup in the southern Canadian Cordillera. Red arrow indicates the approximate location of the study area (Ross and Arnott, 2007).

conformably by a 900m thick succession of alternating limestone, siltstone, and shale of the Yankee Belle Formation (Gabrielse and Campbell, 1991). Both the Cunningham and Yankee Bell formations are interpreted to have been deposited on an upper-slope to shallow-marine, high-energy shelf (Ross et al., 1995). When palinspastically restored, exposed deep-marine rocks cover an area exceeding 80 000 km^2, and as a consequence is similar in size to modern deep-water turbidite systems like the Mississippi and Amazon fans (Ross 2000). Additionally, detrital zircons show a bimodal age distribution that consists of >2.66 Ga or 1.9-1.75 Ga (Ross & Bowring, 1990; Ross & Parrish, 1991) that likely were sourced from

the southern Canadian Shield and the northwestern United States (Ross et al. 1995; Ross & Arnott 2007). The scale of the system, combined with the likelihood of a single regional sediment source, argues strongly for deposition along an open, passive margin and necessitates the complete break-up of Rodinia (at least along its western margin) by this time.

While sparse, there is some geochronological control to constrain the timing of sedimentation of the WSG in the Southern Canadian Cordillera. Bedrock that unconformably underlies the Windermere, and therefore a maximum age for sedimentation, yields U-Pb zircon ages of ~735 Ma. Dates from igneous rocks that are interpreted to be correlative to the syn-rift Irene Formation range from 762-684 Ma (Smith 2010 and references therein). The Old Fort Point Formation, which separates the Middle and Upper Kaza in the Cariboo Mountains, has been dated by Re-Os dating of organic rich strata at 608 +/- 5 Ma (Kendall et al., 2004). Finally, rhyolites in the Cambrian section that unconformably overlies the WSG, and therefore a minimum age of sedimentation, have ages of 596 +/- 5 Ma (Colpron et al. 2002). Also, it is worth noting that shortening during the Late Jurassic to Early Tertiary caused by the accretion of allocthonous terranes along the margin of Laurentia (producing the Canadian Cordillera) (Price 2000) resulted in widespread deformation and metamorphism of all WSG strata; however, regions of relatively low metamorphic grade exist where primary sedimentary structures are preserved, particularly in the Southern Canadian Cordillera (Ross & Arnott 2007).

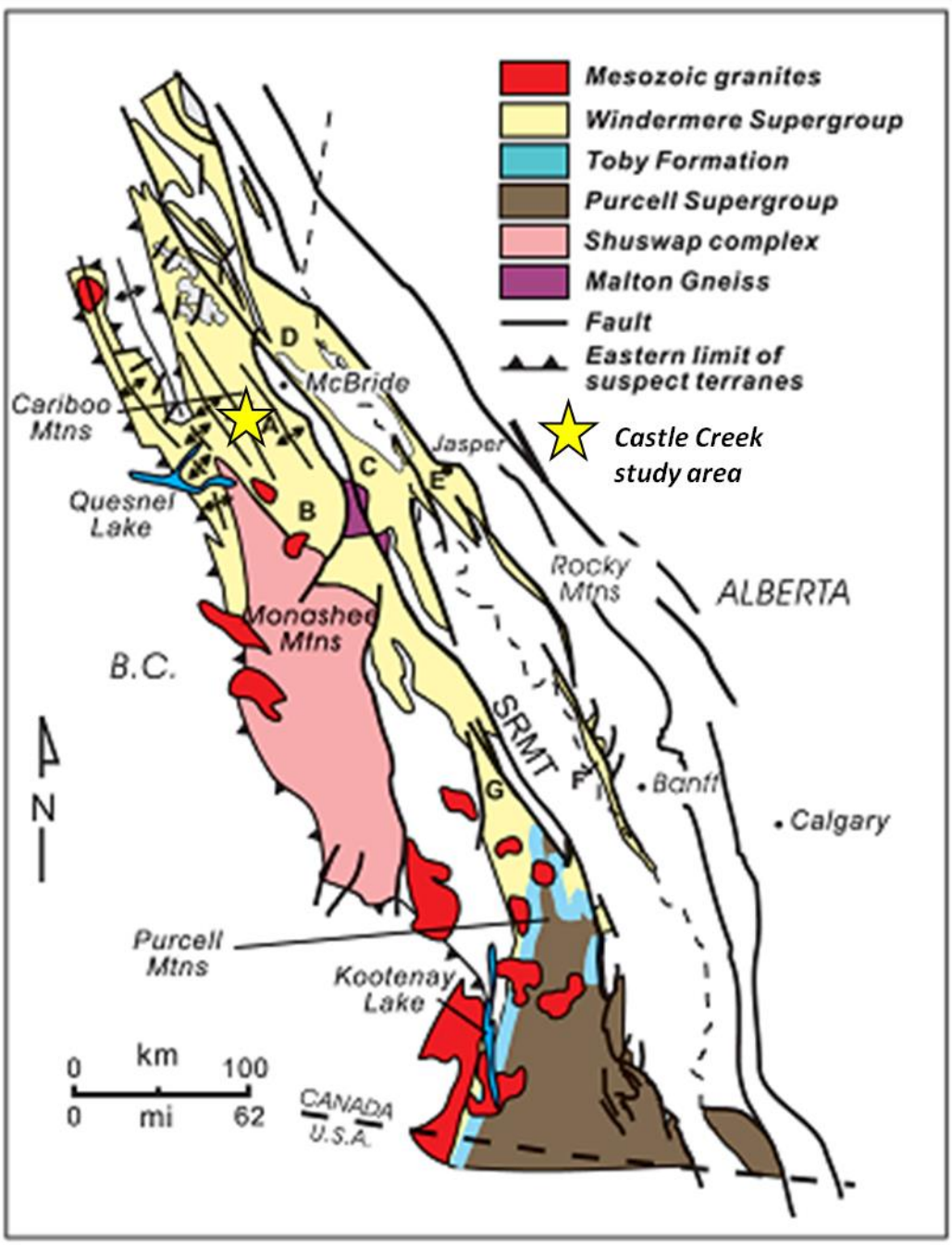

Figure 1.3: Geologic map of the southern Canadian Cordillera (modified from Young et al., 1973; Murphy and Ross, 1988; and Ross and Arnott, 2007) including the Castle Creek study area (yellow star).

1.3 Local Stratigraphy

The Castle Creek study area is located in the Cariboo Mountains, 35 km SSW of McBride B.C. (53° N 120° W)(fig 1.3). Here a superbly exposed succession of near-vertically dipping Windermere stratigraphy over 2 km thick has been uncovered by glacial retreat in the last 100 years. At the base of the section, a roughly 800 m thick unit of generally sheetlike basin floor deposits of the Upper Kaza Group crop out (Terlaky, 2014). The overall ratio of sand to mud/silt in the Upper Kaza is on the order of 75:25 (Meyer, 2004). The Kaza is then overlain by 1300 m of the lower Isaac Formation. The Isaac has a much lower sand to mud/silt ratio (25:75; Ross and Arnott, 2007) and is composed of six major, laterally discontinuous and coarse-grained channel fill successions encased in finer-grained levee or inter-channel deposits. These coarse-grained intervals, which are informally termed Isaac Channels 1-6, range in thickness from 15-100 m, and are interpreted to have been formed in a slope or base-of-slope setting. Mass movement deposits, like slumps or slides, while rare in the basin floor Kaza Group are common in the Isaac Formation.

1.4 Study Area and Methodology

This study documents the stratigraphy of three channel fill complexes in the low part of the Isaac Formation: Isaac Channel 2.3 on the south side of the glacier and Isaac units 14 and 21 on the north side of the glacier (fig 1.4). Data was collected during the months of July and August in 2012 and 2013 by measuring 32 detailed, cm-scale stratigraphic sections (fig 1.5), as well as mapping important stratal surfaces on 1:3800 aerial photomosaics taken in 2002. New 1:5000 aerial photomosaics of the study area were taken in September 2014 and

these higher resolution photos have been included where possible. Additionally, 47 samples were systematically collected and later cut into thin-sections for petrographic analysis on an Olympus BX-41 plane and polarizing light microscope.

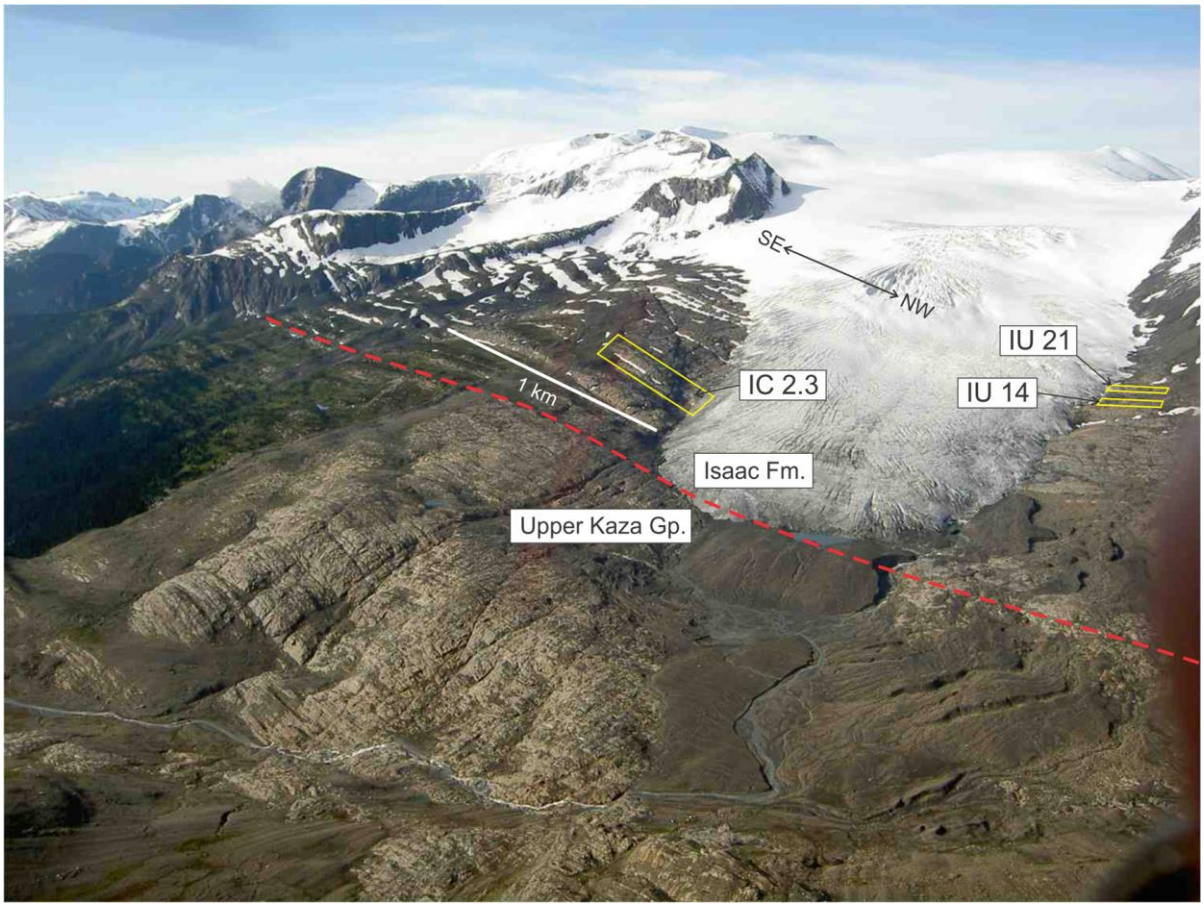

Figure 1.4: Photograph of the Castle Creek study area with the contact between the Upper Kaza Group and the Isaac Formation (dashed red line), Isaac Channel 2.3, Isaac Unit 14, and Isaac Unit 21 (yellow boxes).

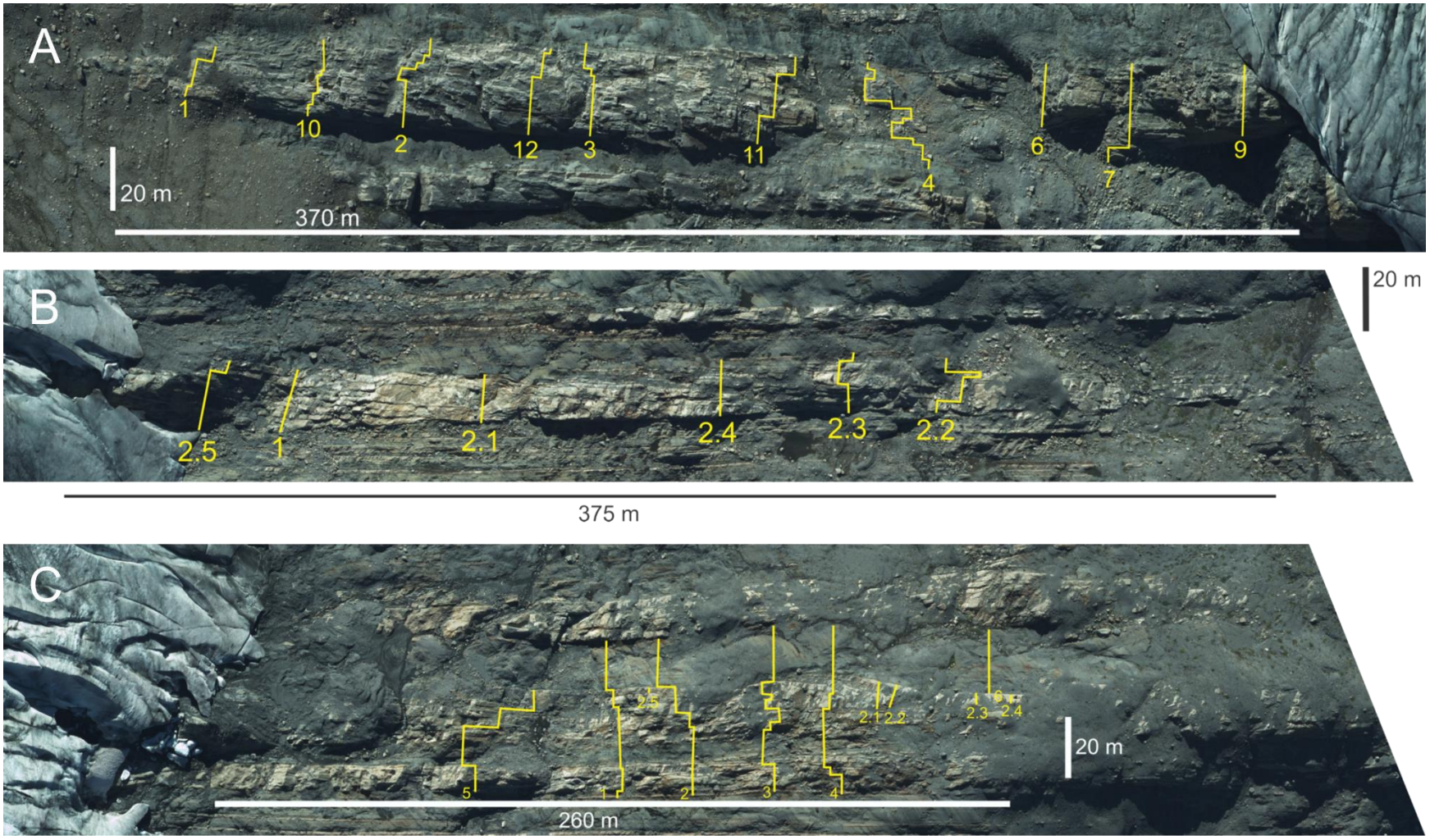

Figure 1.5: Aerial photographs of (A) Isaac Channel 2.3, (B) Isaac Unit 14, and (C) Isaac Unit 21 overlain with the locations of measured stratigraphic sections (presented in Chapter 3).

1.5 Previous Work

The regional stratigraphy of the Castle Creek study area was first described by Campbell et al. (1973). Numerous studies detailing the structural and regional geology of the region have since been performed, many of which were compiled and/or summarized by Aitken and McDonough (1990), Gabrielse and Campbell (1991), and Hein and McMechan (1994). More recently, attention has shifted towards detailed sedimentological, stratigraphic, and architectural analyses of these deep-marine deposits, and largely has been performed by the Windermere Consortium research group headed by R.W.C. Arnott at the University of Ottawa.

Gerald M. Ross was instrumental in recognising and establishing the Castle Creek study area, and who also made significant contributions on the subject (1988; 1991; 1995). This work draws heavily on material published by the Windermere Consortium, including work on Isaac Channel 2.2 and Isaac Unit 14 by R.W.C Arnott (2007a, b) and the postdoctoral research of Ernesto Schwarz (Schwarz and Arnott, 2007) on Isaac Channel 5 (on the north side of the glacier and to a lesser degree Isaac Unit 21 on the south side). Isaac Channel 2.2 was interpreted as the fill of a single migrating sinuous channel composed of coarse- and fine-grained inclined deposits, and prompted the introduction of the term lateral accretion deposits (LADs, discussed below) in the literature. Isaac Unit 14 was interpreted to be a channel fill complex composed of two laterally-accreting channel fills (Arnott, 2007b). Isaac Unit 14 was also studied by a team from Shell Corporation (O'Byrne et al., 2007). These authors interpreted it to be a series of four laterally-offset, poorly confined channel storeys with low to moderate rates of aggradation. Isaac Channel 5 was interpreted to contain three channel complexes composed primarily of aggradational channel fills – the uppermost

channel fill being capped by an inclined channel fill succession formed by a highly sinuous, laterally-accreting channel system (Schwarz and Arnott, 2007).

1.6 Theoretical Overview

1.6.1 Sediment Gravity Flows

1.6.1.1 Introduction

In contrast to fluvial systems where sediment is transported by a fluid moving down a slope (fluid-gravity flow), deep-marine sedimentation is dominated by sediment-gravity processes where gravity acts on particles suspended in a dense, particle-laden suspension, which then is pulled downslope through a less dense ambient fluid. Kuenen and Migliorini (1950) first theorized the existence of sediment-gravity flows after observing upward-fining trends in deep marine deposits. In 1962, Bouma described an ideal turbidite sequence comprising five divisions (fig 1.6) that now has been widely adopted in the literature. Stratigraphically upwards an idealized Bouma turbidite consists of: a) sharp-based, massive to normally graded structureless sandstone and/or conglomerate, b) planar-laminated sandstone, c) ripple cross-stratified sandstone d) diffuse, discontinuously laminated siltstone and mudstone, and e) structureless mudstone. Since then, numerous classification schemes for sediment gravity flows have been proposed and several, such as those by Lowe (1982) and Kneller and Buckee (2000), are also commonly used. While these schemes are helpful for the purposes of description, it is important to note that sediment-gravity flows exist along a mechanistic continuum, rather than as a set of discrete end-member kinds. As a result, this paper uses the physically-based scheme proposed of Mulder and Alexander (2001) (fig. 1.7), which is based

on flow behaviour, grain-size distributions, and grain support mechanisms. In their classification, two end-member types of sediment gravity flows are recognised: cohesive and frictional flows, where the latter is further subdivided into hyperconcentrated density flows, concentrated density flows, and turbidity currents.

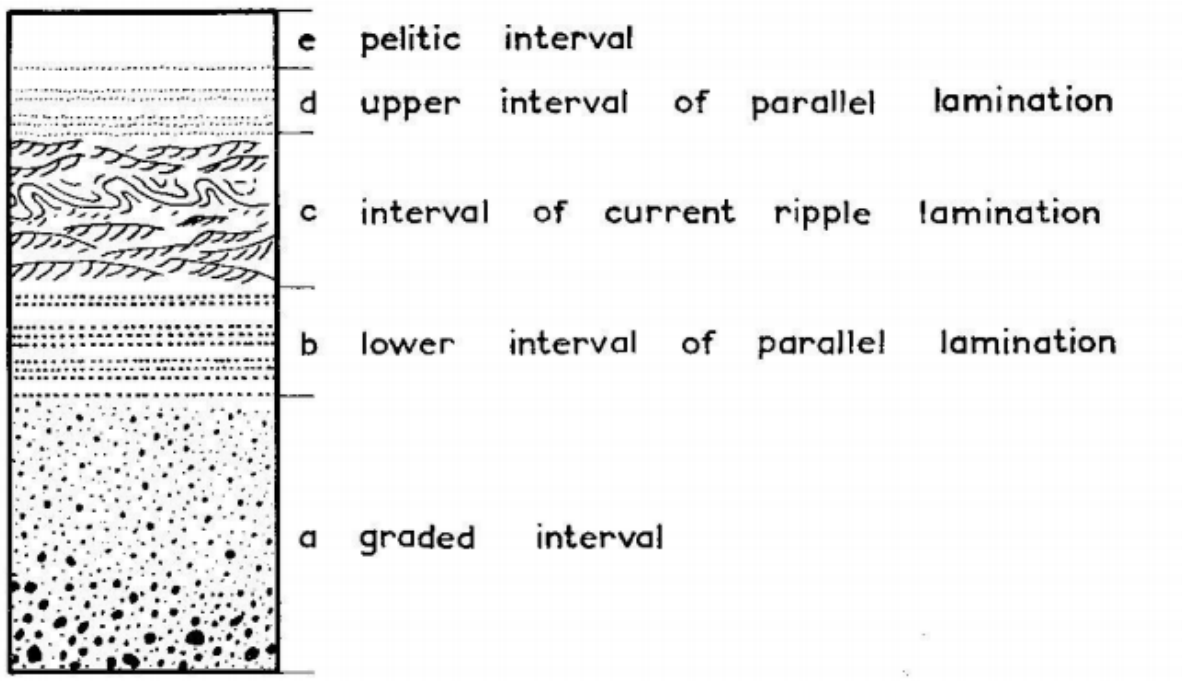

Figure 1.6: Schematic of the idealized Bouma turbidite sequence (Bouma and Brower, 1964).

1.6.1.2 Cohesive Flows

Cohesive flows, also termed debris flows, have a mud:sand ratio that exceeds 1:1.The abundance of clay-sized particles provides matrix strength (table 1.1) and also imparts a pseudoplastic rheology to the flow that together can maintain grains as large as coarse sand in suspension. Additionally, pore fluid pressure, buoyancy, and grain-to-grain interactions may also contribute to help maintain larger clasts in suspension. Moreover, the fine-grained

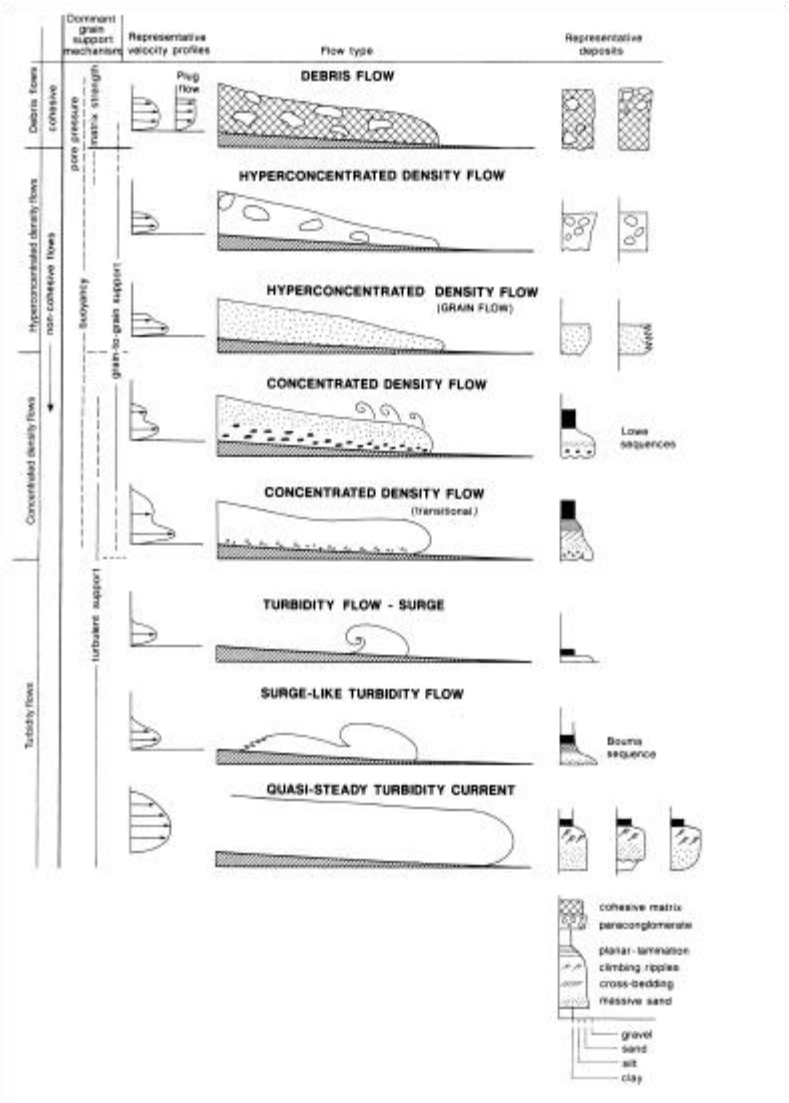

Figure 1.7: Physically-based classification scheme for subaqueous sedimentary density flows by Mulder and Alexander (2001). Indicated are the dominant grain-support mechanisms, idealized velocity profile, idealized flow shape, as well as a representative sedimentary log for each flow type.

matrix reduces particle settling velocity and as a consequence reduces the rate of deposition from the base of the flow, in addition to reducing the entrainment of ambient fluid and dilution of the flow. Debris flow deposits, or debrites, commonly have flat, non-erosional basal contacts. This is partly a consequence of turbulence damping by the cohesive matrix, but possibly also from hydroplaning, wherein a wedge of ambient fluid becomes trapped between the bed and the base of the flow (Mohrig et al., 1998; 1999). This fluid layer forms a

virtually frictionless surface on which the debris flow glides, and in many cases allows for long distance movement. Cohesive flows may undergo transformation to a non-cohesive flow during transport either through dilution at its head (Hampton, 1972), fluid entrainment along the upper boundary, or by passage through a hydraulic jump (Fisher, 1983; Weirich, 1988). Research by Hampton (1972; 1975) also indicates that this transformation is more likely to occur in flows that contain a high proportion of silt-sized or larger particles. Cohesive flows deposit sediment *en masse* through cohesive freezing when forces resisting shear become equal or exceed the driving force of gravity. Frictional freezing typically progresses from the top downward, and upon reaching the base of the flow causes it to be deposited *en masse.*

1.6.1.3 Frictional flows

1.6.1.3.1 Hyperconcentrated Density Flows

Hyperconcentrated density flows contain similar sediment:water ratios as cohesive flows but behave differently due to lower mud-sized particle content, although the boundary between cohesive and frictional behaviour is poorly defined. Grain-to-grain collisions, and to a lesser degree buoyancy, are important mechanisms for suspending sediment in hyperconcentrated density flows. Cohesive forces remain active and serve to sustain high pore fluid pressures, but are unable to prevent the progressive dilution of the flow due to the high degree of connectivity between pores. Hyperconcentrated density flows deposit sediment as increasing grain-to-grain interactions, and eventual grain interlocking, results in the vertical build up of successive layers related to flow surges (Mulder & Alexander, 2001).

Alternatively, hyperconcentrated density flows can also transform into concentrated density flows if they become sufficiently dilute and fluid turbulence (table 1.1) becomes involved in sediment suspension.

1.6.1.3.2 Concentrated Density Flows

Concentrated density flows are sufficiently dilute that they behave as Newtonian fluids (Lowe, 1982). Particle settling within the flow results in horizontal and vertical grain-size sorting, and the entire flow may be fully turbulent (Tilston et al., 2012). Towards the bed, grain-to-grain interactions and buoyancy become increasingly important in suspending sediment, although their contribution is less than in hyperconcentrated flows. Very coarse sand grains (and larger) are commonly transported as bed load in concentrated density flows and may produce traction transport structures (section 1.6.2.2). Concentrated flows may also possess erosive bases due to the interactions between sweeps (downward component of turbulent motion) and the bed and are more common if flows are accelerating. Eroded material is an important sediment source for maintaining the density gradient (the source of energy for sediment gravity flows) and, in many cases, may represent a large fraction of the total volume of sediment that is eventually deposited. Concentrated density flow deposits are typically coarse-tail graded, although massive and less commonly inversely graded beds are observed.

1.6.1.3.3 Turbidity Currents

According to Mulder and Alexander (2001), a turbidity current, *senso stricto,* is a sediment-gravity flow where all particles are fully supported by the upward component of fluid turbulence. The Bagnold limit (1962) of 9 sediment volume percent, or simply 9 vol%, is the maximum particle concentration that can be maintained by fluid turbulence alone**.** In reality, *senso stricto* turbidity currents are rare, so the term, *senso lato,* is used to describe flows where the near-bed sediment concentration exceeds the Bagnold limit, but much of the flow thickness is fully turbulent and more dilute. Both suspension and traction sedimentation play important roles in turbidite deposition, forming partial or complete classical (Bouma) turbidites (fig 1.6).

Name	**Mechanism**
Fluid Turbulence	Random motion of fluid to minimize a velocity gradient. The effects of turbulence increase with a steepening of the velocity gradient and is capable of suspending sediment when the magnitude of the upward component of turbulent motion exceeds the magnitude of particle settling (by gravity).
Hindered Settling	Forces that oppose the downward settling of a particle. Large contribution by the movement of displaced fluid past settling particles, which results in shear stress that increases in magnitude with increasing sediment concentration.
Buoyancy	Displacement of a dense fluid by a settling particle generates an upward force on the particle that is equal to the mass of the displaced fluid volume.
Dispersive Pressure	Collisions between individual particles generate dispersive forces that maintain particles in suspension. Importantly, this dilates the flow and therefore is self-limiting. Grain-to-grain interactions become significant at high sediment concentrations.
Matrix Strength	Large surface area:volume and unbalanced electrical charges on clay particle surfaces cause them to be bounded by electrostatic (Van der Waal's) forces. At significant concentrations, the attraction between clay minerals is sufficient to impart 'strength' to the matrix, which is capable of supporting larger grains.

Table 1.1: List of sediment support mechanisms in sediment-gravity flows.

1.6.2 Sedimentation Mechanisms

1.6.2.1 Suspension Sedimentation

Volumetrically, direct suspension sedimentation is the dominant mode of deposition from sediment-gravity flows. Two different modes of suspension sedimentation exist within flows, driven either by capacity or competence, and their contribution to deposition is largely controlled by rates of sediment fallout. Under capacity driven sedimentation, particle concentrations are sufficiently high that grain-grain interactions result in hindered settling and finer particles are carried downward by the voluminous downward flux of settling coarse particles (Sylvester & Lowe, 2004). Under these conditions, instantaneous sedimentation rates are high and vertical grading in the aggrading beds is poorly developed. Capacity driven deposits are characteristically matrix-rich (Kuenen, 1966), poorly sorted, and massive or coarse-tail graded (Arnott & Hand, 1989). Postma et al. (2009) and Postma and Cartigny (2014) related the deposition of coarse-tail graded structureless sandstone facies to processes associated with a hydraulic jump. In this model stratified flows undergo explosive expansion within the jump, which then is followed immediately downflow by rapid sediment fallout in a zone of minimal horizontal shear. In contrast, competence driven sedimentation occurs when particle concentrations within a flow are sufficiently dilute and grains are independently mobile. This results in much slower, highly selective (mostly by grain size) grain-by-grain settling and the deposition of well-sorted, distribution graded deposits.

1.6.2.2 Traction Sedimentation

Traction sedimentation occurs as sediment becomes disentrained after being moved for some distance along the top of the bed. Bedload transport has been recognized as playing a role in deep-marine sedimentation, for example the Bouma Tb and Tc divisions, which are typically attributed to transport and deposition under upper-plane bed and current ripple conditions (Postma et al., 2014). Noticeably absent, however, is dunes, which in a waning unidirectional flow and in sediment coarser than middle fine sand and finer than coarse sand, should be sandwiched in between the Tb and Tc divisions, yet is rarely observed (Arnott, 2012). Previous explanations focused on the requisite bed configuration and hydraulic conditions needed for dune development, including insufficient time for growth (Walker, 1965), (negative) influence of suspended sediment-fallout on the development of incipient bed features (Lowe, 1988), (negative) impact of turbulence suppression associated with higher suspended sediment concentrations (Allen and Leeder, 1980; Lowe, 1988), and the (negative) effect of increasing clay content on flow structure and bed rheology (Baas and Best, 2002). However Arnott (2012) argued that based on the typical textural and geometric attributes of the cross-stratified part of most turbidites, in addition to the much longer duration of natural turbidity currents compared to the time needed to form angular bed forms like ripples and dunes, these earlier explanations are questionable. More recently, attention has turned towards the mechanisms by which angular bedforms are created. Dunes, as well as current ripples, are known to become initiated and evolve from an initial bed defect. Eventually, fluid flow over the defect induces flow separation, which then amplifies the defect and leads to the eventual growth of equilibrium angular bedforms. Several different theories have attempted to explain the formation of defects through turbulent behaviour,

either in single sweeps (Williams & Kemp, 1971) or larger aggregate vortex structures (Best, 1992). These theories have been questioned on the basis of the small scale of sweep-induced defects (Allen, 1982), and the more recent work of Coleman and Eling (2000) who formed angular bedforms in laminar flows. Recent experimental work by Venditti et al. (2005, 2006) showed that low-amplitude waveforms, commonly only several grains in height, form very quickly and spontaneously from a plane bed under conditions of general bed-surface traction transport. These waves organize themselves into regularly spaced, sharp crested bedforms in as little as several tens of seconds, and influenced local hydraulic and sediment transport patterns. Venditti et al. theorized that the waveform is the result of a hydrodynamic instability between the bed surface bed load layer and the overlying moving fluid. The model proposed by Arnott (2012) suggests that the paucity of dunes in the deep-marine sedimentary record is related to the maintenance of high sediment concentration in the lower part of most turbidity currents until they are flowing at speeds where sediment fallout rates are negligible and ripples are the stable bedform. In the absence of the hydrodynamic instability, defects do not form, flow separation is inhibited, and plane bed remains stable. In the case where sediment concentrations never falls to the requisite levels during traction transport, the planar laminated Tb division is overlain directly by the Td and Te divisions.

1.6.3 Sinuous Channels and Lateral Accretion

It is widely known and easily demonstrated that continental fluvial channels commonly exhibit a sinuous planform. The principal depositional unit in these systems is the point bar with its well-known upward-fining succession of lithofacies separated by

erosional surfaces (Allen, 1964; 1970). Bridge and Jarvis (1982) showed that point-bar deposition was associated with bedload transport at near-bankfull stages. During these high-energy episodes inertial (fluid) forces cause flow super-elevation along the outer bank (cut bank), which results in a barotropic pressure gradient and subsequent return current, termed the secondary flow, that travels down the cut bank and up the point bar. The vector resultant of the primary and secondary flow components results in the oblique-upward migration of increasingly finer sediment along the point bar surface, and hence and typical upward-fining succession of lithofacies (Allen, 1970; Bridge and Jarvis, 1982). Much more recently it has been shown that many deep-marine channels are similarly sinuous (e.g. Posamentier and Kolla, 2003; Babonneau et al, 2002; Redbourn et al., 1993; Damuth et al., 1988, Kastens and Shor, 1985), and in the case of a number of ancient systems form important hydrocarbon reservoirs, including offshore west Africa (e.g. Abreu et al., 2003; Wynn et al., 2007) and the Gulf of Mexico (Wynn et al., 2007). Nevertheless, despite similarities in morphological features such as bend cut-offs or the relationship between channel width and sinuosity (Kolla et al., 2007), deep-marine sinuous channels differ in many other respects to those in the fluvial realm, which most probably relates to fundamental differences in the nature of the flows that pass through them, specifically sediment-gravity versus fluid-gravity flows. For example, sediment-gravity flows exhibit greater super-elevation and flow stripping at channel bends, resulting in more significant overbank processes (Wynn et al., 2007). Accordingly, the levees of deep-marine sinuous channels are typically much higher, thicker and wider than those in fluvial systems, and also with a characteristic 'gull-wing' geometry in seismic cross-sections (Wynn et al., 2007) and have good reservoir potential (e.g. Clemenceau et al., 2000). Deepwater channels also commonly exhibit high rates of aggradation, a condition not observed in fluvial channels (Wynn et al., 2007). Additionally,

channel width and depth generally decreases downflow in deepwater systems (Normark et al., 1985) with much lower channel bank angles (Babonneau et al., 2002). Comparisons between fluvial and deepwater seismic data sets by Kolla et al. (2007) noted that fluvial channels show continuous lateral migration often with significant downflow translation and rarely exceed a single seismic loop in thickness. In contrast, deepwater channel migration may be continuous or episodic, with negligible downflow translation. In addition, channels commonly aggrade steeply.

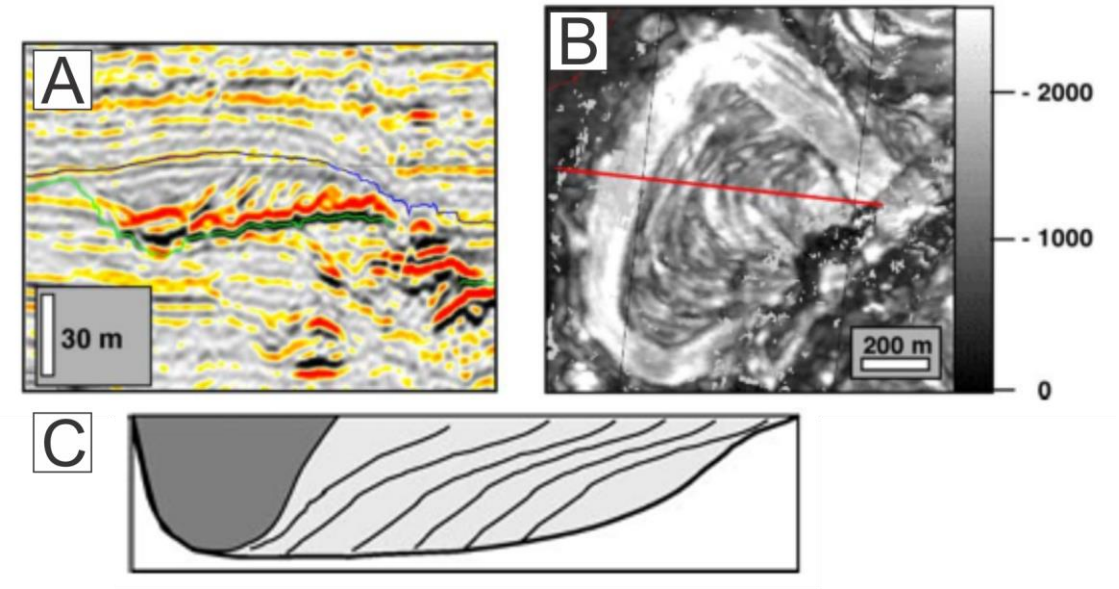

Figure 1.8: High-resolution (65 Hz) (A) seismic cross-section of the Green Channel Complex (along red transect) showing shingled reflections, (B) amplitude map extracted from the green horizon at the base of the channel depicting characteristic 'scroll-bar pattern', and (C) cartoon of a laterally-migrating channel (Abreu et al., 2003).

Abreu et al. (2003) observed that deposits from the highly-sinuous subsurface Green Channel Complex (Lower Miocene, offshore Angola) contained shingled reflectors along the margins of channel fills (fig 1.8). These reflectors paralleled the inner channel bend, dipped towards the last-stage channel fill, and were interpreted to have formed from the lateral migration of the channels. Based on these characteristics, the term lateral accretion packages (LAPs) was introduced to describe these features. In the same study, the authors suggested that (ancient) outcrop analogues could be used to better understand the facies architecture of LAPs and cited several examples to populate a lithological model (their fig.13). The term LAP has since been used to describe a variety of deposits in outcrop where lateral channel accretion and associated lateral accretion deposition is interpreted to have occurred (e.g. Dysktra and Kneller, 2009; Janocko, 2011). Importantly, the thickness of ancient laterally accreting channel fills is typically of the order of about 10 m, and therein close to the minimum resolution of industry seismic. More profoundly, the width of individual (inclined) lateral accretion "packages" in outcrop are measured in meters to at most several meters, and therefore well below seismic resolution (e.g. Janocko, 2011). In recognition of this problem Arnott (2007a) introduced the term lateral accretion deposit (LAD), which is used in this thesis, to describe the several-meter wide lateral accretion deposits visible in outcrop and their composite beds (fig 1.9) . By extension, the term LAP may be used to describe deposits in outcrop, but should be restricted to instances where the observed features are on a scale similar to those on seismic, and in fact may describe a channel-belt composed of discrete and laterally-offset channels.

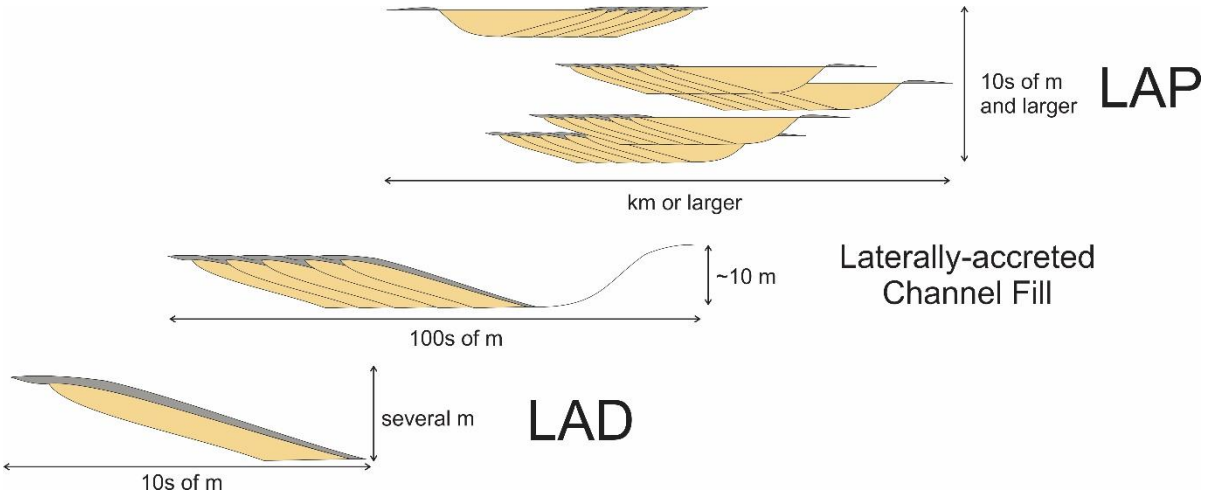

Figure 1.9: Cartoon illustrating the differences in scale between an individual lateral accretion deposit (LAD), a laterally-accreted channel fill composed of lateral accretion deposits, and a lateral accretion package (LAP) composed of laterally-accreted channel fills.

In the current sedimentological literature there are a number of documented examples of inclined stratal surfaces bounding strata in deep-marine channel fills. Although these could potentially represent LADs (see Janocko, 2011), sufficiently detailed stratigraphic descriptions are typically missing, although exceptions exist (see Chapter 4). The good exposure and vertical dip of strata in the Castle Creek study area afford an excellent opportunity to examine the vertical and lateral facies characteristics of this type of channel in detail.

1.6.4 Secondary Flow in Deep-Marine Sinuous Channels

Currently, there is much debate regarding the nature of secondary flow in deep-marine sinuous channels. Due to the inaccessibility, destructiveness, and sporadic timing of natural turbidity currents, laboratory channels, computer simulations, and outcrops have been used in lieu of direct observation. Results from currents produced in the laboratory have been contradictory, with secondary currents along the channel floor oriented toward (e.g. Imran et

al., 2007; Islam et al., 2008; Abad et al., 2011) and away from (e.g. Corney et al., 2006; Keevil et al., 2006; Peakall et al., 2007; Amos et al., 2010) the channel's inner bank. In each case, there are numerical models that support the laboratory results (e.g. Corney et al., 2008; Imran et al., 2008). Similarly, there are examples of LADs with paleoflow measurements oriented obliquely down (Pyles et al., 2010; 2012) as well as up (Dysktra and Kneller, 2009; Janocko, 2011) inclined lateral accretion surfaces. Collectively these differences highlight the need for further research to better understand the fluid and sediment transport conditions in sinuous deep-marine channel bends, but such an undertaking is beyond the scope of this thesis.

1.6.5 Effects of Relative Sea-Level Change on Deep-Marine Sedimentation

1.6.5.1 Introduction

Deep-marine sedimentary systems with a wide shelf and well-developed shelf-slope break, such as the one thought to have existed on the northern margin of Laurentia during the Neoproterozoic (see section 1.2 above), possess a sediment supply, and by extension, depositional environment, that is significantly influence by the position of relative sea-level. Different schemes exist to interpret these sedimentary sequences and their boundaries (e.g. Catuneanu et al., 2009), this paper will utilize the four stage systems tract model composed of falling-stage, lowstand, transgressive, and highstand (sensu Hunt and Tucker, 1992), as well as the model proposed by Arnott (2010, fig. 1.10) detailing the specific sequences present in a point-sourced deep-marine system.

1.6.5.2 Falling-Stage Systems Tract (FSST)

The fall of relative sea-level following a local maximum results in the progradation of the shoreline towards the shelf-slope break, reintroducing the supply of fluvially transported sediment into the deep-marine. Sediment-gravity flows initially contain a high mud:sand ratio and are out of the grade with the existing slope gradient, resulting in extensive erosion. Submarine canyons and channels are excavated along the upper- and mid-slope, primarily bypassing the base-of-slope zone and depositing along the basin floor (Arnott, 2010). Additionally, mass wasting processes (i.e. downslope movement of coherent or semi-coherent sediment) are a common occurrence during falling sea-level due to gravitational instabilities generated along the shelf-edge and upper slope.

1.6.5.3 Lowstand Systems Tract (LST)

The ratio of sand:mud in the sediment supply increases steadily as shelf deltas prograde and approach the shelf-slope break. The relative increase of coarse sediment in the system serves to decrease overall flow efficiency as well as increase the slope of the equilibrium graded profile. Channels in the mid- and lower-slope regions undergo systematic deposition and aggradation in order to bring channel profiles into equilibrium, temporarily starving the basin floor of sediment and causing local retrogradation. As equilibrium is re-established, the active center of deposition shifts back to the basin floor and depositional lobes resume progradation.

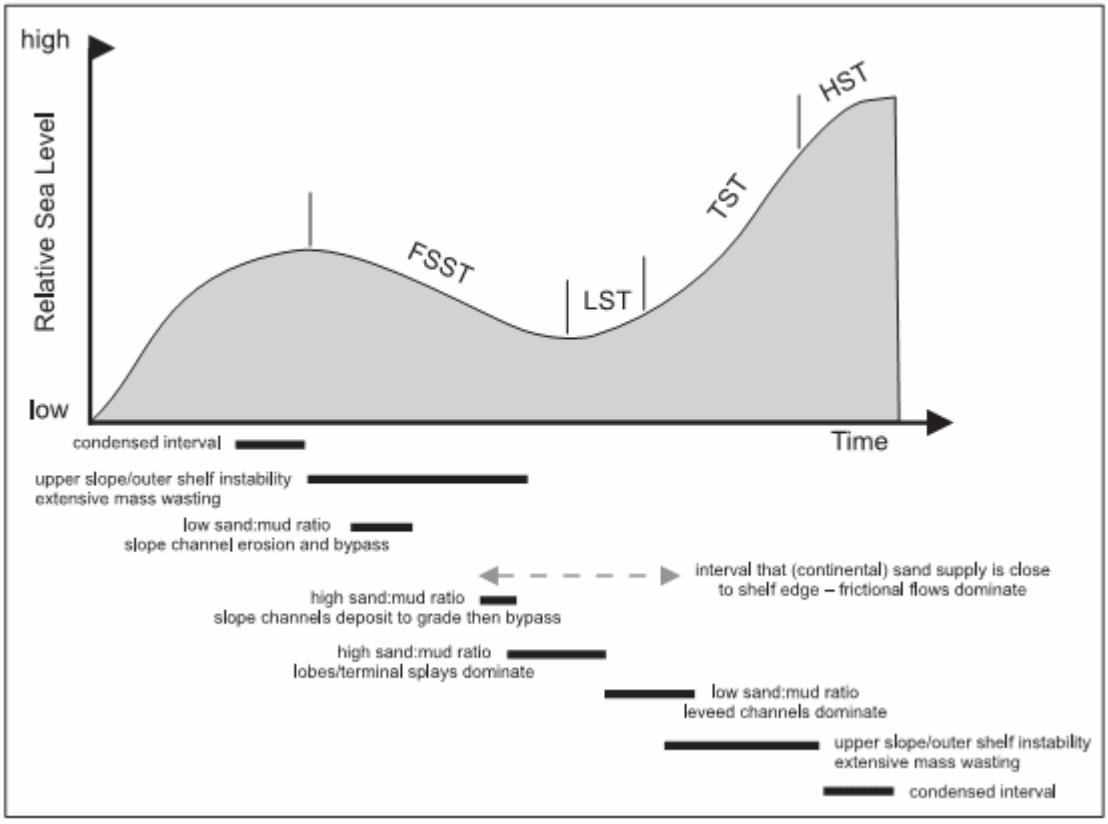

Figure 1.10: Idealized model relating characteristics of sediment transport and deposition to positions of relative sea level on a passive continental margin with a single point-sourced sediment supply (Arnott, 2010; modified after Posamentier and Walker, 2006).

1.6.5.4 Transgressive Systems Tract (TST)

As sea level begins to rise sediment sourced from continental erosion becomes increasingly sequestered in aggrading coastal plains and deltas (Posamentier and Walker, 2006), causing the deep marine to become increasingly starved of clastic sediment input. Gravitational instability along the shelf-edge and upper slope increases as the equilibrium profile (slope) changes, causing an increase in the frequency of mass-transport events and related mass-transport deposits (MTDs) (Posamentier and Kolla, 2003). Flows that succeed

in transporting sediment along the shelf contain lower sand:mud ratios and are typically highly stratified. These channel systems have high confinement and sinuosity, well-developed erosional levee, and are commonly highly aggradational (Arnott, 2010)

1.6.5.5 Highstand Systems Tract (HST)

As sea-level approaches its next local maximum, the supply of sand and gravel to the deep-marine becomes severely restricted, if not entirely eliminated. The continental shelf is commonly flooded and, if conditions are appropriate, may initiate the growth of a carbonate platform. If present, carbonate sediment is frequently shed from the platform and transported downslope where it deposits along with relict siliciclastic and biogenic suspension sediment (Arnott, 2010).

2 FACIES DESCRIPTIONS AND INTERPRETATIONS

2.1 LF1: Thin to very-thick bedded, ungraded and normally-graded sandstone and conglomerate

2.1.1 Description

Facies LF1 is the most common lithofacies in the study and consists of ungraded or coarse-tail normally-graded sandstone or conglomerate. Beds range from 0.08 to 2.4 m thick, but typically are between 0.35-1.25 m. At the base of beds, grain size ranges from matrix-supported (medium to coarse sand) pebble conglomerate to medium sandstone, with coarse and very-coarse sandstone the most common. At the top of graded beds, grain size ranges from fine to very-coarse sandstone but typically is between coarse to very-coarse sandstone. Beds bases are usually planar or shallowly scoured with common more deeply scoured (>20 cm) and welded contacts (fig 2.1) and uncommon loaded or undulatory contacts. Beds are typically amalgamated but locally can be traced laterally for several tens of meters. Beds are less commonly interstratified with LF3 strata. Mineralogically LF1 beds are framework-supported quartz arenites with low matrix content (fig 2.2).

Figure 2.1: Welded contact between two Ta beds.

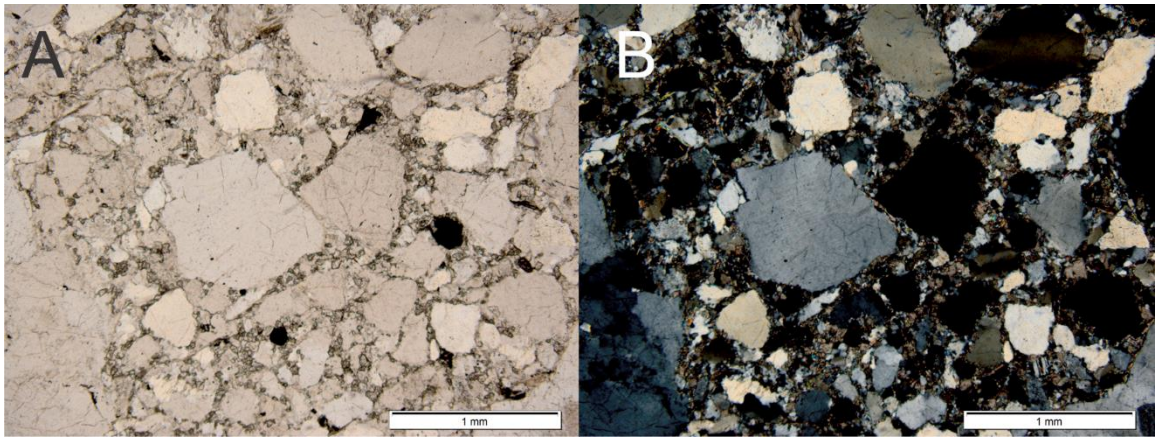

Figure 2.2: Photomicrograph of LF1 strata in plane (A) and cross (B) polarized light.

2.1.2 Interpretation

LF1 strata are interpreted to have been deposited by concentrated density flows (Mulder and Alexander, 2001), and are analogous to the S3/R3 beds of Lowe (1982). Concentrated density flows are believed to be made up of two parts: an upper part where the flow is fully turbulent, and a high concentrated basal part that exceeds the Bagnold (1962) limit and where fluid turbulence is effectively damped (Li and Davies, 2001). High sediment concentration also reduced grain mobility causing flows to be poorly graded both vertically and longitudinally, and ultimately resulting in capacity-driven deposition with minimal horizontal shear (Postma and Cartigny, 2014). Such rapid deposition may have been the result of locally developed hydraulic jumps that resulted in vigorous flow expansion and subsequent deposition immediately downflow (Postma et al., 2009; Postma and Cartigny, 2014). Deposition of coarse-tail graded versus massive strata are attributed to changes in the relative thickness of the basal, high concentration part of the flow. Work by Russell and Arnott (2003) indicates that concentrated flows with relatively thin basal sections (and thick turbulent upper sections) tend to deposit coarse-tail graded beds with differential, albeit limited, grain settling (Mulder and Alexander, 2001). In contrast, flows with thick basal sections are thought to result in higher rates of instantaneous sedimentation during flow collapse and deposit massive beds (Middleton and Hampton, 1973; Arnott and Hand, 1989).

2.2 LF2: Medium to very-thick bedded, ungraded and normally-graded sandstone and conglomerate with mudstone clasts

2.2.1 Description

LF2 consists of very-coarse sandstone or a matrix-supported granule conglomerate with a coarse sandstone matrix with dispersed mudstone clasts (fig. 2.3). Beds range in thickness from 0.32-2.0m and commonly are between 0.75-1.10 m. Beds are typically ungraded, but rare coarse-tail grading is observed with coarse sandstone at the top of the bed. Dispersed mudstone clasts are common and vary from 4-105 cm in length and 2-21 cm wide, and are oriented sub-parallel to the base of the bed. Clasts are typically composed of massive mudstone, although some clasts have planar or deformed pin-stripe siltstone laminae. Bed bases are subtly to deeply scoured (up to 50 cm), although loaded contacts are observed. Strata of LF2 are generally discontinuous beyond several meters laterally, although rarely extend laterally over several tens of meters.

Figure 2.3: LF2 bed with dispersed, elongated mudstone clasts and a slightly undulatory basal contact. Red lines indicate bedding contacts.

2.2.2 Interpretation

LF2 strata are interpreted to have been deposited by hyperconcentrated density flows (Mulder and Alexander, 2001) that underwent frictional freezing because of a dramatic increase in cohesion and grain-grain interlocking. Mudstone clasts, likely sourced from erosion of the local seabed, quite possibly related to scouring within hydraulic jumps (Postma and Cartigny, 2009), became partially disintegrated and increased the dispersed mud content, and accordingly the strength of the flow's fluid phase. Increased fluid strength would also have increased the flows ability to resist shear, and eventually helping it to

frictionally freeze. Additionally, grain-grain interlocking significantly reduced internal shear, which similarly enhanced frictional freezing (Mulder and Alexander, 2001). It is important to note that unlike cohesive flows, which freeze progressively downward and then deposit *en masse*, hyperconcentrated flows deposit by the successive addition of layers of "frozen" sediment from the base of the flow onto the aggrading bed. Deposition by frictional freezing (see section 1.6.1.2) involves negligible suspended sediment deposition and commonly forms massive beds (Mulder and Alexander, 2001). Sylvester and Lowe (2004) described deep-marine sandstones that showed evidence of cohesive freezing in the form of mud-rich banding possessing a chaotic grain arrangement that were interpreted to have been transported by a turbidity current *sensu lato* prior to deposition. The abundance of scoured basal contacts suggests that initially flows were not hyperconcentrated, as such flows exert minimal shear stresses on the bed due to hydroplaning (Mulder and Alexander, 2001).

2.3 LF3: Thin- and very-thinly bedded sandstone, siltstone, and mudstone

2.3.1 Description

Facies LF3 is separated into two subfacies that are differentiated based on the presence of sandstone and Bouma Tabc intervals. Very thinly-bedded strata of LF3a consist of fine to very fine grained, ripple cross-stratified sandstone commonly several sets thick (Bouma Tc) or medium to fine grained planar-laminated sandstone (Tb) that in most cases is abruptly overlain by fine to very fine-grained ripple cross-stratified sandstone (Bouma Tbc). Thin beds have a basal structureless layer of medium sandstone overlain by medium to fine grained planar-laminated sandstone overlain by fine to very-fine grained ripple cross-

stratified sandstone (Bouma Tabc)(fig. 2.4). Beds are well-sorted and have sharp planar basal contacts, although scoured, undulatory and loaded contacts are also observed. LF3a strata form bedsets that range in thickness from 0.14 – 4.12m.

Subfacies LF3b consists of mudstone and siltstone that range from very thin laminae up to planar-based very thin beds and form bedsets that range in thickness from 2-30 cm thick. LF3b strata are most commonly interbedded with semi-amalgamated LF1 strata. Surface cover and weathering prevent LF3 strata from being traced laterally for more than several tens of meters.

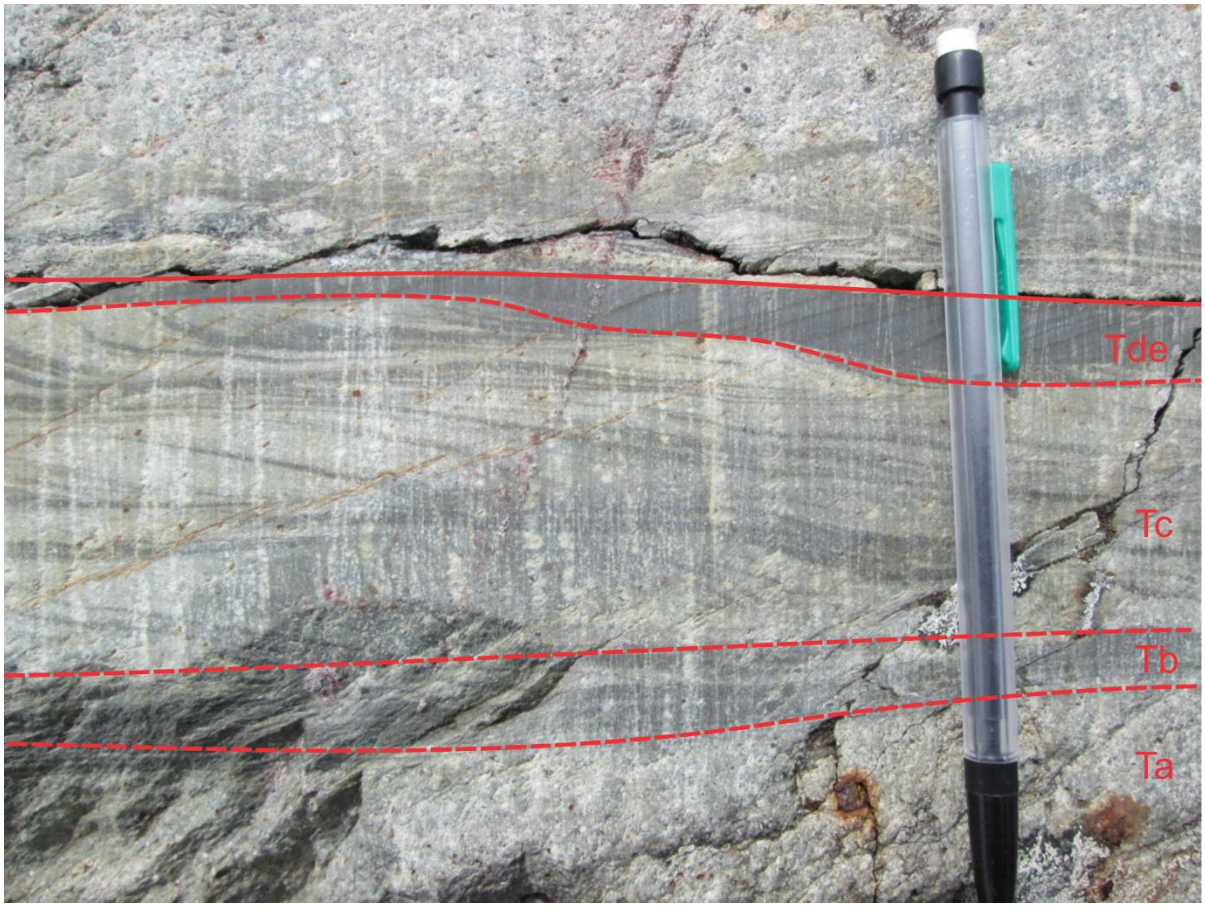

Figure 2.4: LF3a bed with Bouma Tabcd divisions. Solid red line indicates bedding contact and dashed lines are contacts between divisions.

2.3.2 Interpretation

LF3 is interpreted to have been deposited from waning, potentially surge-like turbidity currents (*senso stricto,* Mulder and Alexander, 2001). Density flows with low particle concentrations (see fig 1.7) are typically formed by the progressive dilution of an initially more concentrated flow (see section 1.6.1.3.3), and likely exhibit well developed longitudinal and vertical (grain size) grading. Deceleration of the flow allows suspended sediment to settle to the bed and then be moved as bedload. The planar laminated Tb division is commonly interpreted to represent upper-plane-bed transport (i.e. high speed) conditions. Alternatively, planar lamination may have formed at lower speeds where high near-bed sediment concentrations prevented the formation and amplification of bed-surface defects from which ripples and/or dunes would have otherwise grown (Arnott, 2012). Eventually suspended sediment concentrations became sufficiently reduced that defects formed, and because of low flow speeds, ripples developed (Tc division). In the study area ripples are commonly several-sets-thick and show no discernible angle of climb, indicating that the rate of suspended sediment fallout was extremely low (Khan, 2012). With further deceleration deposition of planar stratified mudstone/siltstone (Td division) primarily through alternating suspension settling and episodic bedload transport takes place. Lastly, pure suspension sedimentation of the finest particles results in deposition of a massive mudstone (Te division) layer (for a complete summary and discussion of the various layers, see Lowe, 1982). Although uncommon, structureless sandstones (Ta) at the base of LF3a beds represent direct suspension sedimentation with negligible bed-surface transport (e.g. Arnott and Hand, 1989). This layer is then overlain by planar-laminated succeeded by ripple cross-stratified sandstone indicating reduced rates of suspension fallout and more prolonged bedload transport. Very

thinly-bedded turbidites of LF3b are likely the distal equivalents of larger, coarser flows that deposited most of their coarser sediment further upflow.

2.4 LF4: Medium-scale cross-bedded sandstone

2.4.1 Description

Strata of LF4 are uncommon in the study area and consist of high-angle cross-bedded, coarse to very coarse, well-sorted sandstone that occur as discrete beds or sharply overlie strata of LF1 (fig. 2.6). Cross-bed sets range from 7-18 cm thick and are easily distinguished in outcrop by their distinctive alternating bands of light and dark colours that parallel the cross-stratification. LF4 are typically not laterally continuous beyond several meters.

2.4.2 Interpretation

Cross-stratified LF4 strata are interpreted to have formed from sediment reworked from the underlying bed by migrating subaqueous dunes. Dunes were formed by sediment-gravity flows with exponentially decaying near-bed sediment concentration profiles and whose speed was within the dune stability field. These conditions allowed the flow to form the requisite hydrodynamic instability at the top of the bed-load layer to generate bed-surface defects, which then evolved into dunes (see section 1.6.2.2; Arnott, 2012; Venditti *et al.*, 2005; 2006). The 3-dimensional stability field diagram published by Postma and Cartigny (2009, fig 2) shows dunes forming under subcritical conditions.

Figure 2.5: LF4 bed abruptly overlying Ta bed, thick dashed line indicating basal contact and thin dashed line paralleling cross-bedding.

2.5 LF5: Very-thick bedded poorly-sorted silty granular mudstone

2.5.1 Description

LF5 strata forms a single bed and is only observed at one locality. Here it ranges from 8 to 12 m thick and is laterally continuous over the width of the outcrop (several hundred m). It is composed of silty and sandy mudstone with dispersed very coarse sand grains and granules as well as rare carbonate cemented sandstone clasts that range in size from cobbles to small boulders. The matrix is dominated by mud and silt with dispersed very fine sand grains. The basal contact of LF5 strata is commonly planar or loaded (fig 2.6).

2.5.2 Interpretation

LF5 is interpreted to be a debrite, the result of *en masse* deposition through cohesive freezing (Mulder and Alexander, 2001). High matrix strength imparted by a network of clay particles impeded particle settling and resulted in a somewhat chaotic arrangement of clasts within the debrite. Large carbonate-cemented sandstone clasts are interpreted to be fragments eroded from the upper slope or continental shelf where early diagenetic carbonate cement partly lithified siliciclastic sand. These clasts, in addition to siliciclastic clay and silt, were then remobilized downslope as a debris flow initiated by instabilities along the shelf-edge or high on the continental slope (see sections 1.6.1.2, 1.6.5.2, 1.6.5.4; Posamentier and Kolla, 2003).

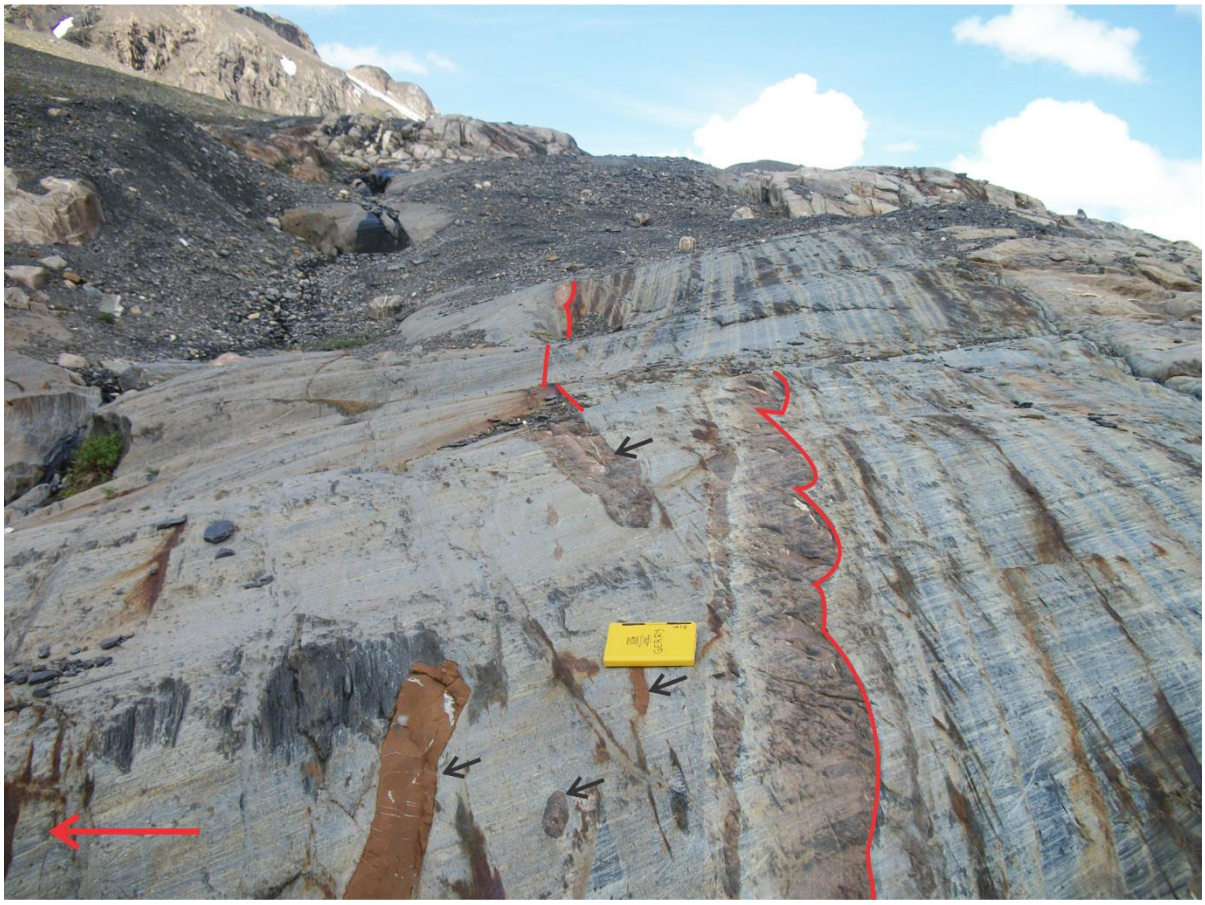

Figure 2.6: Debrite bed with large clasts (black arrows) and loaded contact with LF3 strata below (red line, broken at the top of photograph due to perspective).

3 CHANNEL FILL DESCRIPTIONS

3.1 Classification Hierarchy

In order to organize and classify strata in this study the organizational hierarchy of McHargue et al. (2011) is used. The fundamental unit in that hierarchy is the channel element, which is on the order of a decameter thick and several hundred meters wide and delineated by a channel-form basal surface overlain by a sedimentary fill. In many cases this fill consists of smaller-scale channel fills termed channel storeys, which in this study are the LADs described in chapter 1, and are several meters thick and extend laterally for several tens of meters. Individual channel elements are distinguished on the basis of abrupt lateral shifts or changes in their orientations and then in turn stack to form larger features termed a channel complex that is several tens of meters thick and extends laterally for hundreds of meters.

3.2 Channel 2.3

Cropping out immediately adjacent to the Castle Creek Glacier, Isaac Channel 2.3 (IC 2.3) is up to 33 m thick and currently is exposed over a strike length of 370 m. The top of IC 2.3 is subhorizontal but the unit thickens toward the northwest as a result of erosion along its basal surface. IC 2.3 is interpreted to be a channel complex comprising at least 5 channel elements, herein termed CE 2.3-1 to 5 (fig. 3.1 and 3.2). The cryptic nature of the contacts that separate most channel elements and the typically amalgamated nature of the sandstone fills makes them difficult to differentiate in the field, but also on aerial photos. The basal

surfaces of channel elements in IC 2.3 dip at about 8-12º and are commonly erosive with strata that are subparallel to the dipping basal surface. Elements are typically filled with medium to very-thick bedded coarse and very-coarse grained sandstone and conglomerate (LF1) that is occasionally interbedded with medium to very-thick bedded very-coarse grained sandstone and conglomerate with mudstone clasts (LF2). Interbeds of thinly to very-thinly bedded medium to very fine grained sandstone, siltstone, and mudstone (LF3) are present at the tops of the fills (fig. 3.3). CE 2.3-1 is up to 5 m thick but thins progressively over 98 m laterally until it becomes truncated by CE2 (fig 3.1. Lateral thickening is a consequence of erosional relief along the base of the channel, which angles downward at about 10º and close to where CE 2.3-1 is truncated by CE 2.3-2 is about 12 m deep. CE1 is then filled mostly with LF1 with rare interbeds of LF2 and LF3.

CE 2.3-2 erosively overlies CE 2.3-1 and incises downward by 23 m over its strike length of 195 m (maximum inclination of 10°). On the aerial photographs the base of CE 2.3-2 can be identified as a consistent linear trend that also coincides with the appearance of 2 thickly-bedded granule conglomerates in log 1. CE 2.3-2 is up to 11 m thick and is dominated by LF1 strata with common LF2 beds and rare LF4 (cross-bedded coarse to very-coarse sandstone) beds.

CE 2.3-3 has an inclined basal surface that dips by 22 m over its strike length of 330 m at a maximum angle of 9° relative to the horizontal. The upper bounding surface is identified on aerial photographs by the terraced 'step' in the base of IC 2.3. CE 2.3-3 has a maximum thickness of 14 m and is filled with strata that subparallel the base of the channel element and consist primarily of LF1, though LF2, LF3, and LF4 strata are also observed.

Interbeds of LF3 strata occur towards the top of the channel element (in log 1 and log 10) where several LF1 beds thin obliquely upwards.

The base of CE 2.3-4 scours continuously downward by 25 m over a strike length of 290 m with a maximum inclination of 9° relative to horizontal. The base of CE 2.3-4 is marked by a medium-grained sandstone bedset (see logs 4 and 11) that is finer than typical LF1 strata and is laterally continuous over several tens of meters before being eroded. The bedset is up to 3.5 m thick and can be readily identified in the field by its green colour on weathered surfaces resulting from more abundant chlorite compared to other LF1 strata (fig 3.5). The channel element fill has a maximum thickness of 15 m and is composed mostly of LF1 strata. Like CE 2.3-3, coarse amalgamated strata (LF1) thin obliquely upwards and then become interbedded with LF3. In the best exposed example (fig 3.4) a fine granule conglomerate thins abruptly from 1 m to 0.07 m over 3.5 m before terminating. The granule conglomerate scours underlying LF3 strata obliquely downward until truncating them completely where the conglomerate amalgamates with other LF1 strata. Beyond the updip terminus of the granule conglomerate LF3 strata that underlie and overlie the conglomerate are continuous with no evidence of erosion.

The basal contact of CE 2.3-5 scours down 13 m over an exposed strike length of 205 m at a maximum angle of 8° relative to horizontal. The base of CE5 sharply overlies an interval of LF3 strata at the top of CE 2.3-4 (see log 11) and coincides with a consistent linear trend on the aerial photographs. Like the other elements, CE5 thickens towards the northwest and reaches a maximum thickness of approximately 11 m immediately adjacent to the glacier.

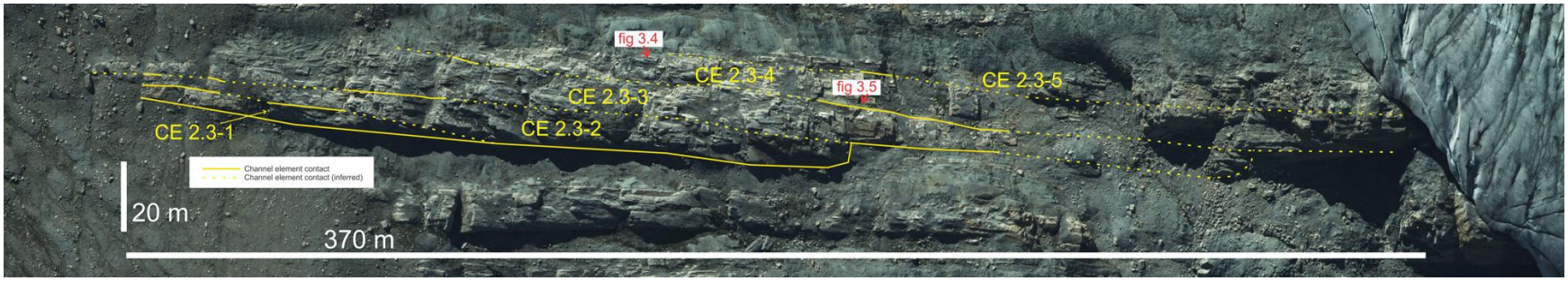

Figure 3.1: Isaac Channel 2.3 channel element boundaries overlain on an aerial photomosaic.

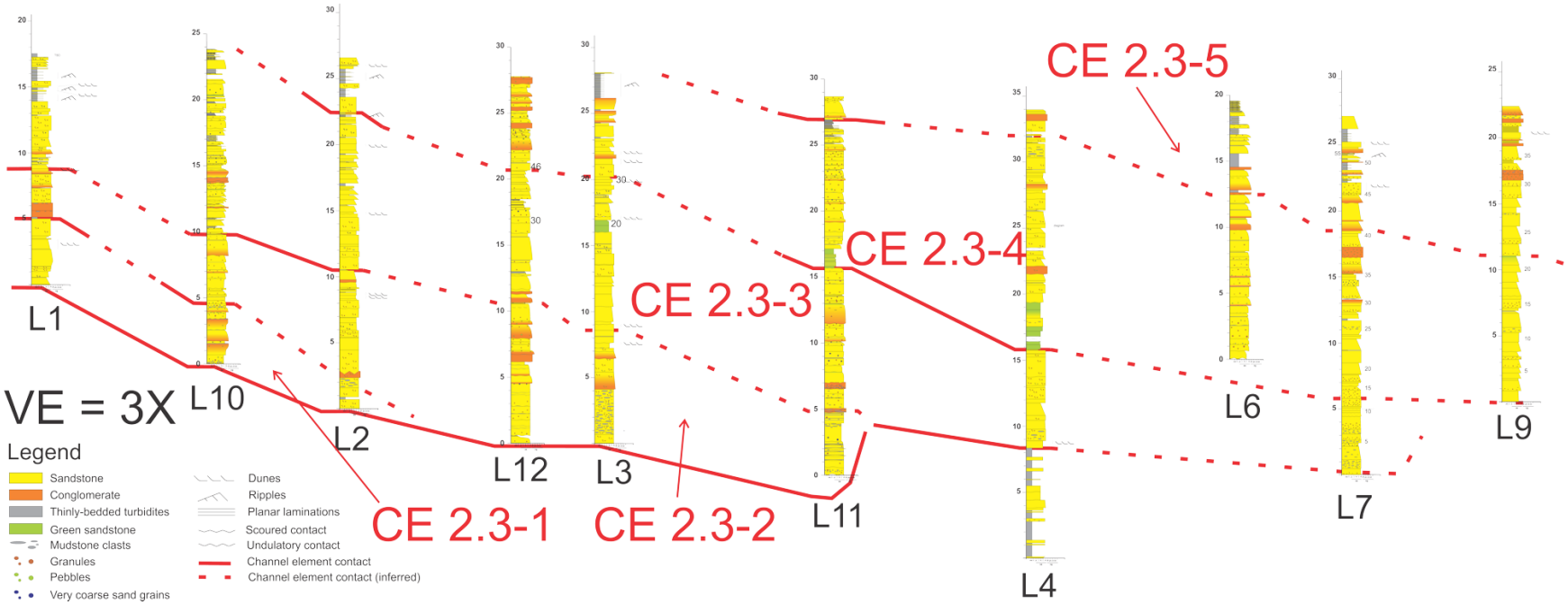

Figure 3.2: Isaac Channel 2.3 channel element boundaries overlain on stratigraphic logs.

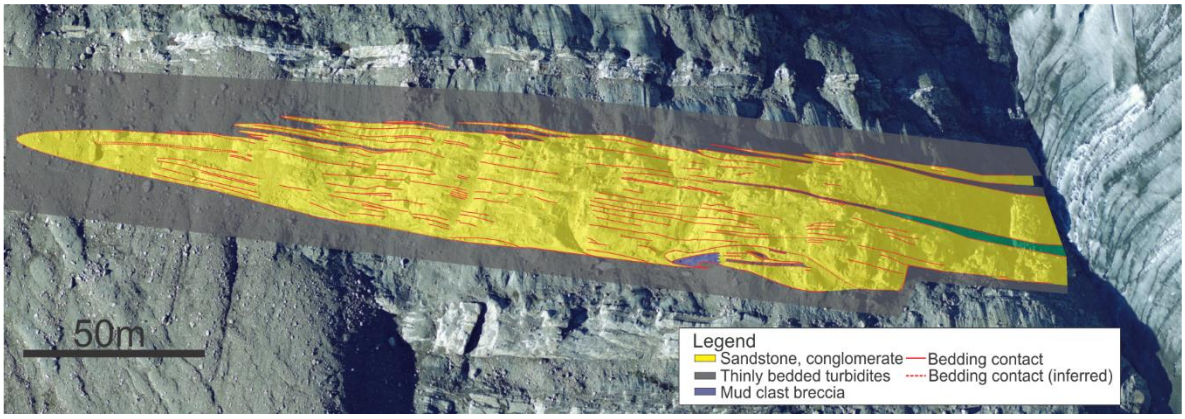

Figure 3.3: Isaac Channel 2.3 lithologies overlain on aerial photomosaic.

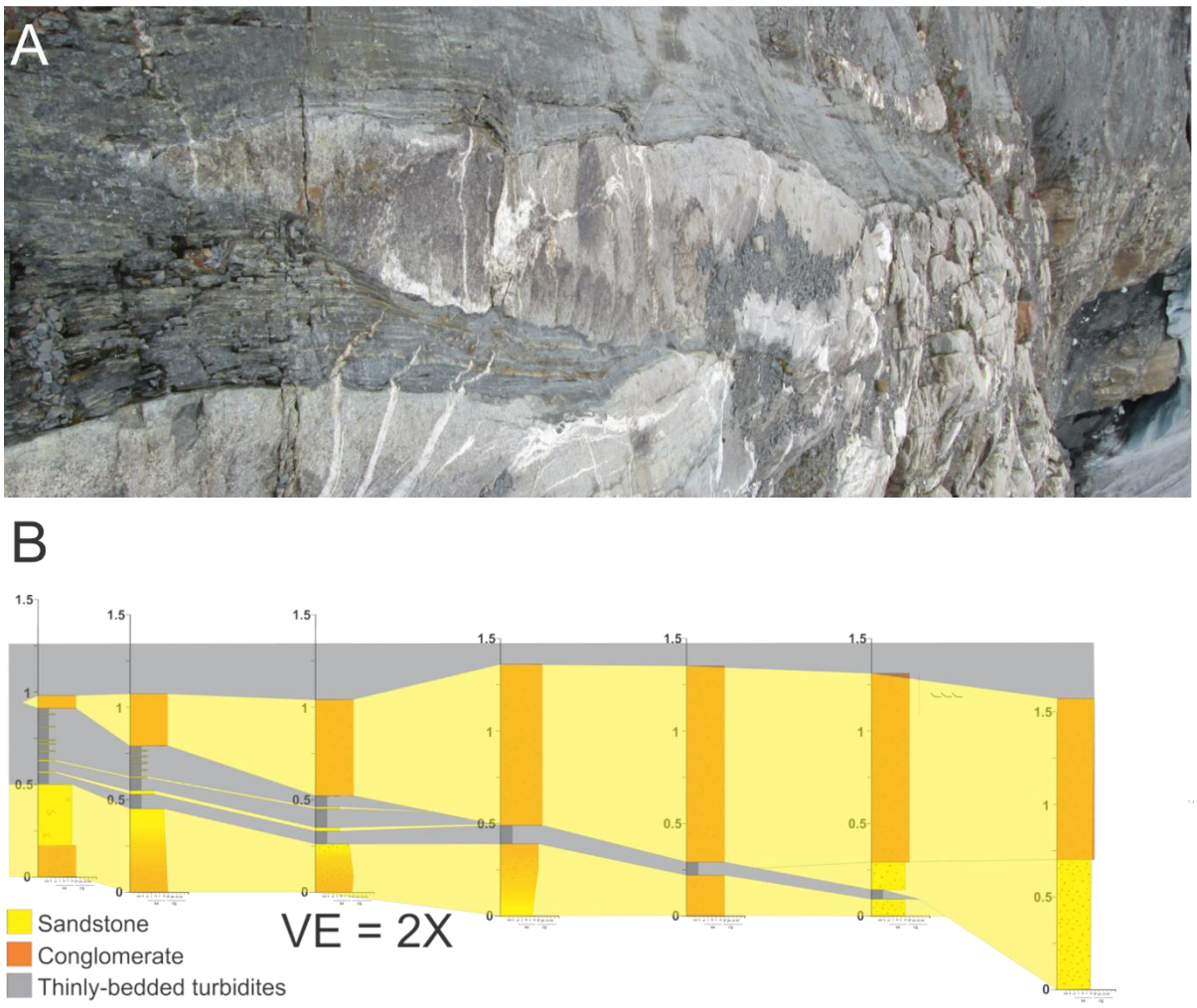

Figure 3.4: (A) photograph and (B) correlated stratigraphic logs of a lateral accretion deposit depicting an abrupt termination of the conglomerate on the updip terminus and amalgamation with underlying coarse strata obliquely downdip.

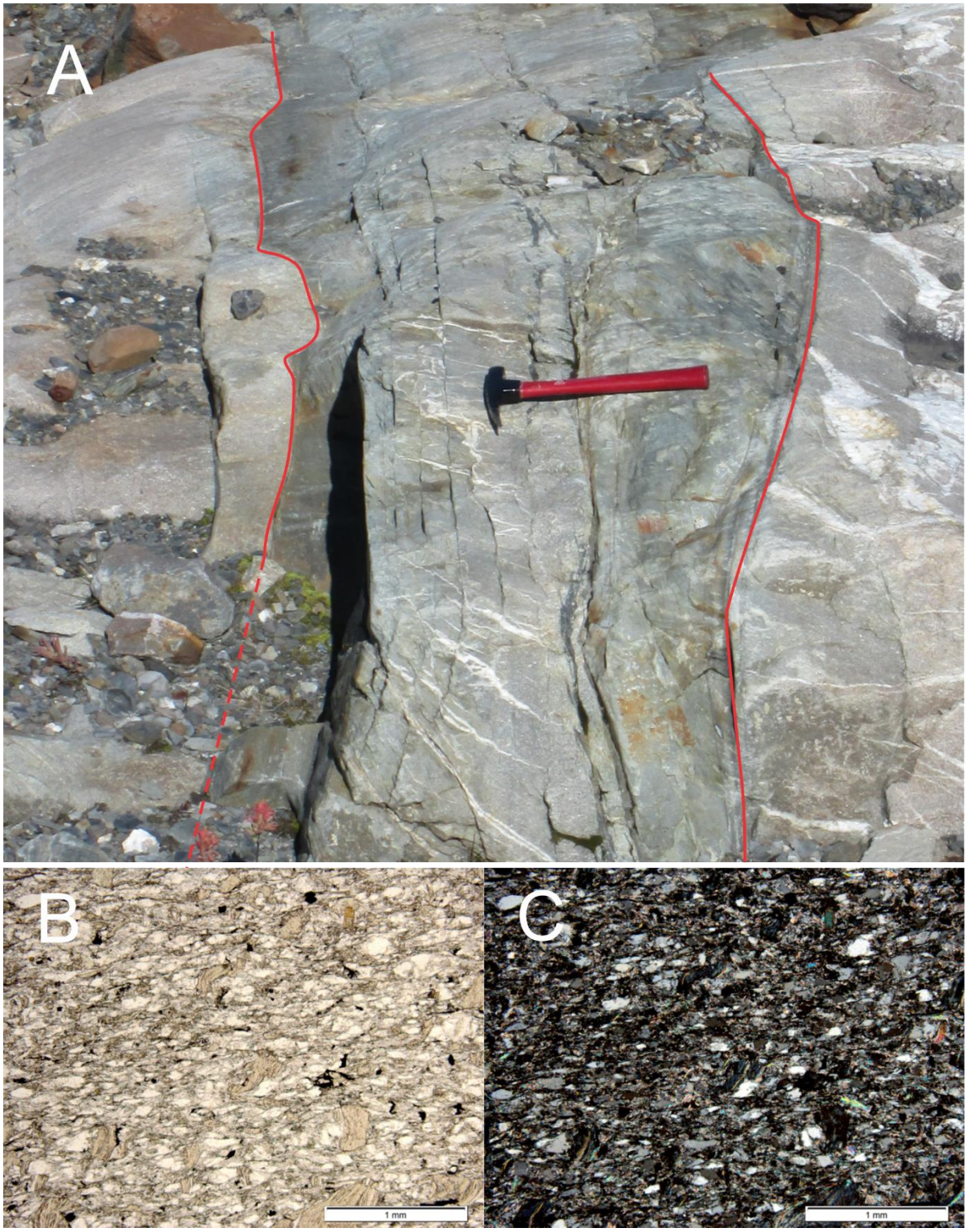

Figure 3.5: (A) Photograph and photomicrographs (B = PPL, C = XPL) from medium-bedded green sandstone interval with high chlorite content.

3.3 Unit 14

Currently Isaac Unit 14 has a maximum exposed thickness of 22 m and width of 375 m. It is a channel complex composed of at least two channel elements, termed CE 14-1 & CE 14-2 (fig. 3.7 and 3.8). CE 14-1 has a maximum thickness and width of 22 m and 285 m, respectively. The base of the channel is shallowly scoured towards the glacier (average dip of 1.6 degrees over 245 m) and overlies a succession of matrix-rich sandstones, sandstones, and thinly-bedded turbidites. It is thickest next to the glacier and thins towards the NW where it is sharply overlain by CF 14-2. Most of the channel is filled with amalgamated (LF1) beds that at the top of the fill are uncommonly interbedded with LF3 bedsets (fig 3.6). No discernible upward change in grain size and only negligible change in bed thickness were noted. Beds are consistently inclined up to about 10° relative to the base of the channel. Where exposed, several LF1 beds at the top of the channel fill are observed to thin abruptly obliquely upwards where they scour into, and in turn, are draped by LF3 strata.

CE 14-2 has a maximum thickness of 12 m and a maximum exposed width of 225 m. The basal contact of the channel fill is sharp and inclined at about 4º (average) where it erosively overlies CE 14-1, but further laterally becomes subhorizontal where it forms the base of the channel complex. A several-meter-thick unit of mudstone breccia (LF2) interbedded with medium-bedded LF1 strata separates CE 14-1 and CE 14-2 but thins and then terminates down dip along the erosive channel contact. The channel fill is dominated by amalgamated LF1 strata that subparallel the base of the channel complex (fig 3.4). Like CE 14-1, there is no discernible upward fining trend but near the top there is a noticeable thinning where LF1 strata become progressively interbedded and eventually overlain by LF3 strata (fig 3.6).

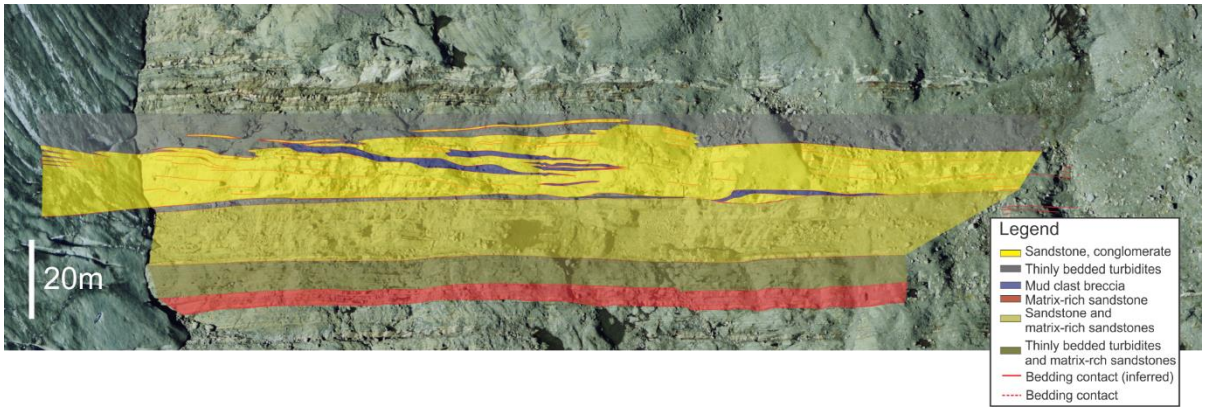

Figure 3.6: Isaac Unit 14 lithologies overlain on an aerial photomosaic.

3.4 Unit 21

Isaac Unit 21 is a channel complex composed of four channel elements, CE 21-1 to 4 (fig 3.10 and 3.11), that has a maximum thickness of 37 m and is currently exposed over a length of 260 m. It crops out about 150 m above Isaac Unit 14. The intervening section consists of a paired slide-debrite unit overlain by a thick succession of carbonate-cemented, thinly- and lesser medium-bedded turbidites. CE 21-1 has a planar basal contact, is up to 8 m thick, and is composed largely of LF1 strata uncommonly interbedded with LF2 strata (fig 3.9). At the top of the fill, LF1 strata become interbedded with LF3 strata. All strata in CE 21-1 are subhorizontal and parallel the channel base. There is no discernible upward fining or thinning trend in CE 21-1, and it is overlain by a 9 m thick interval of LF3 strata intercalated with long, laterally tapering lenses of sediments intruded from the base of CE 21-2.

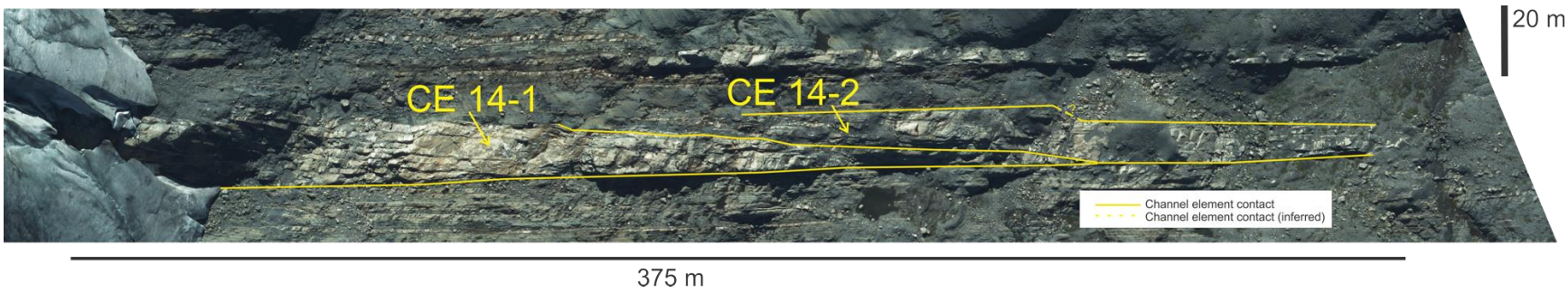

Figure 3.7: Isaac Unit 14 channel element boundaries overlain on an aerial photomosaic.

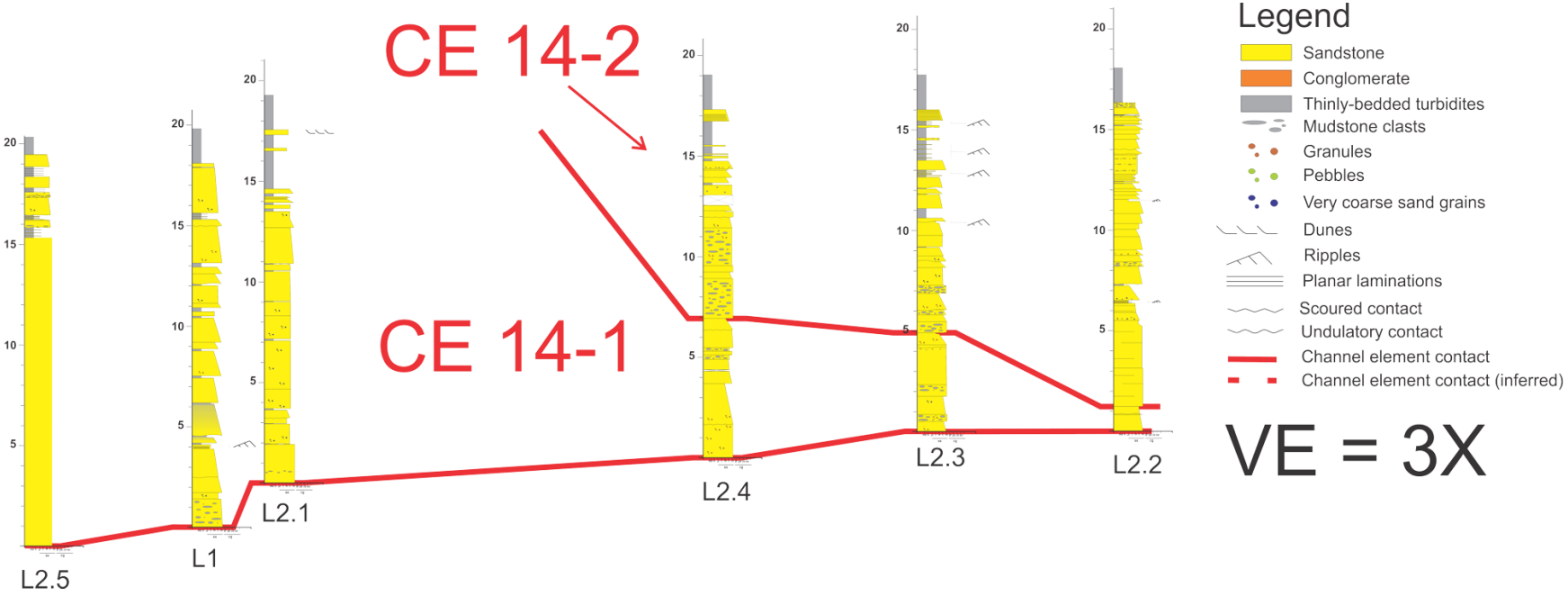

Figure 3.8: Isaac Unit 14 channel element boundaries overlain on stratigraphic logs.

Next to the glacier the base of CE 21-2 is planar but laterally towards the northwest becomes obscured by injected sandstone and mudclast breccia lenses. Laterally tapering lenses subparallel bedding (i.e. sills) and consist of coarse sandstone to fine granule conglomerate that are up to 2 m thick and extend laterally for several tens of meters. Dikes are rare. CE 21-2 has a maximum thickness of 15 m on the southeast side of the outcrop but thins to 5 m toward the northwest. The channel is filled mostly with LF1 strata, but LF2 beds and LF3 intervals are not uncommon. All beds are subhorizontal and parallel the planar basal contact. In addition, strata thin upward but show little change in grain size.

CE 21-2 is overlain by CE 21-3; the contact is planar at the southeast end of the outcrop but becomes erosive towards the northwest, scouring down 6 m over a length of 80 m at a maximum angle of 8° before becoming subhorizontal relative to the base of the channel complex. CE 21-3 thickens from about 1 m in the southeast to a maximum of 7 m. The fill is composed almost entirely of LF1 strata with rare LF2 beds and shows little to no upward fining or thinning. Beds are oriented subparallel to the scoured basal contact.

CE 21-4 erosively overlies CE 21-3 with a contact that scours down 7m towards the northwest over a length of 30 m and at a maximum angle of 24°. The channel fill is dominated by LF1 strata that interfinger with LF3 strata towards the top of the fill. Most of the fill shows negligible upward fining or thinning, but clustered at the top of the section, although exposure is poor, are several beds that taper and grade laterally from coarse to medium-grained sandstones. Strata in CE 21-4 subparallel the channel base. CE 21-4 is overlain by an interval of LF3 strata that is up to 7 m thick, which, in turn, is abruptly overlain by a 12 m thick mudstone-rich debrite (LF5).

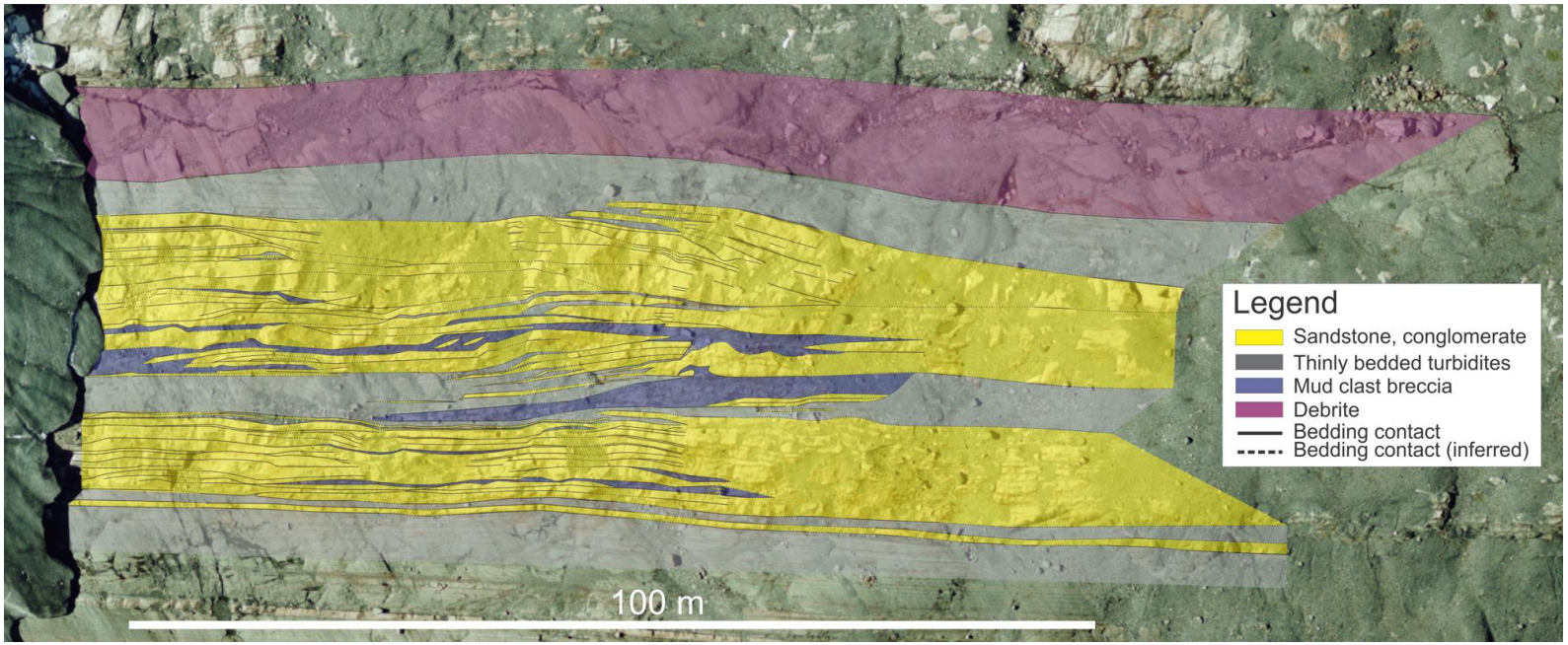

Figure 3.9: Isaac Unit 21 lithologies overlain on an aerial photomosaic.

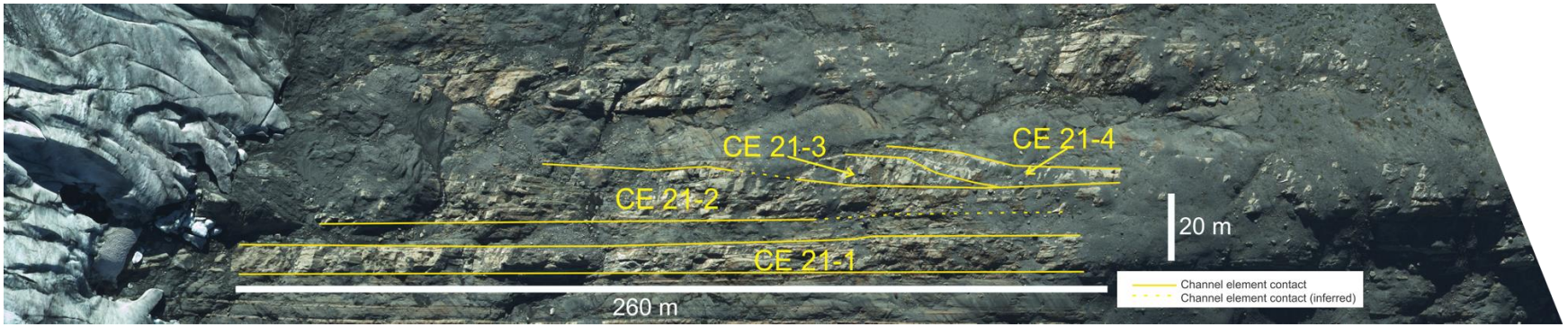

Figure 3.10: Isaac Unit 21 channel element boundaries overlain on an aerial photomosaic.

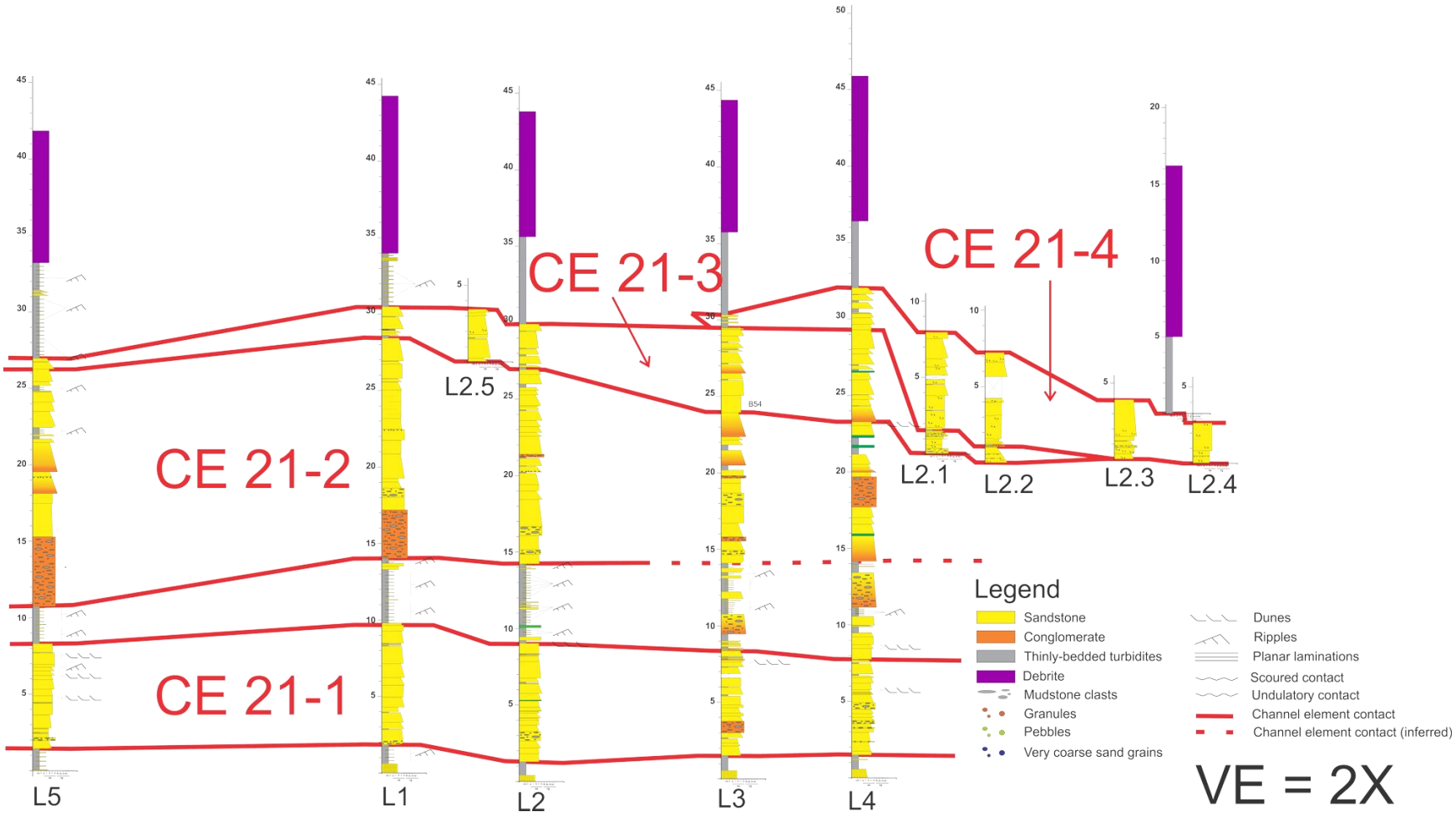

Figure 3.11: Isaac Unit 21 channel element boundaries overlain on stratigraphic logs.

4 REVIEW OF LATERALLY-ACCRETED CHANNEL FILL OUTCROPS

4.1 Introduction

As discussed earlier in Chapter 1, there are a number of reported examples of inclined surfaces bounding strata in ancient deep-marine channel fills. Isaac Channel 2.3, Isaac Unit 14, and Isaac Unit 21, described in Chapter 3, are interpreted to have been deposited as the result of lateral accretion during channel migration. This section summarizes a number of other examples from the geological record in order to identify any trends or similarities (see table 2.1) to serve as a basis for later comparison. Of primary interest is the morphology and sedimentological characteristics of the LADs that make up the channel fills as well as the channel fills themselves; however, their distribution within the overall system and the geological setting are also discussed.

4.2 Examples

4.2.1 Rosario Formation, San Fernando Canyon, Mexico

One of the best described examples of deep-marine lateral accretion deposits is from the Rosario Formation in the San Fernando Canyon located approximately 40 km southwest of the town of El Aguajito in northern Mexico. The Rosario Formation is the youngest unit in the Late Cretaceous Peninsular Ranges forearc basin, a package of discontinuously exposed sedimentary rocks stretching for 500 km between southern California and Baja California Norte (Morris and Busby-Spera, 1990; Dykstra and Kneller 2007; 2009). Sediments were deposited along the western side of an arc complex that existed from the Upper Jurassic to the Upper Cretaceous (Morris and Busby-Spera, 1990). The Rosario Formation is up to 5 km

thick and consists of continental to deep-marine rocks depending on location (Dykstra and Kneller, 2009 and references therein). In the San Fernando Canyon, the Rosario Formation comprises a deep-water valley fill and is overlain by a succession of leveed channels (Dykstra and Kneller, 2007) that unconformably overlies continental deposits of the El Gallo Formation. Flows were confined to the submarine valley and then the levee-bounded channels (Dysktra and Kneller, 2009). Canyon and leveed-channel deposits comprise interbedded conglomerates and sandstones bounded by thinly interbedded siltstones and sandstones that thin laterally (Dysktra and Kneller, 2007).

Channels containing lateral accretion sets are exposed throughout the succession (Dysktra and Kneller, 2009); however accessible and documented examples crop out at the base and middle of the canyon-fill (Dykstra and Kneller, 2009; Janocko, 2011). Those at the base of the succession and described by Dykstra and Kneller (2009) are located along the coast at a locality informally named Pelican Point, which is further divided into North and South outcrops. The channel containing the LADs in the North Outcrop (fig 4.1) is between 2 and 5 m thick, 60 m wide, and situated stratigraphically below those in the South Outcrop (described below). It overlies, and in the case of the youngest beds, erodes into horizontal conglomerate and sandstone beds interpreted to be the deposits of an aggradationally-filled channel (Dykstra and Kneller, 2007). The channel-fill is composed of at least twenty-nine medium- to very thickly-bedded, normally graded sandstone and conglomerate beds that on average dip at 10° relative to the aggradational beds below (Dykstra and Kneller, 2009). Some of the inclined beds (beds c-e in Dykstra and Kneller 2009, fig. 12) exhibit minor fining down-dip, whereas the youngest beds (beds f-i) show pronounced fining up-dip. There is an overall fining upward trend through the laterally accreting channel fills which is

attributed to a change in sediment supply (Dysktra and Kneller, 2009). The lateral accretion set is interpreted to represent deposition by a single laterally accreting channel, and the systematic change in strike of the beds (over 100°) is attributed to channel sweep (Dysktra and Kneller, 2009).

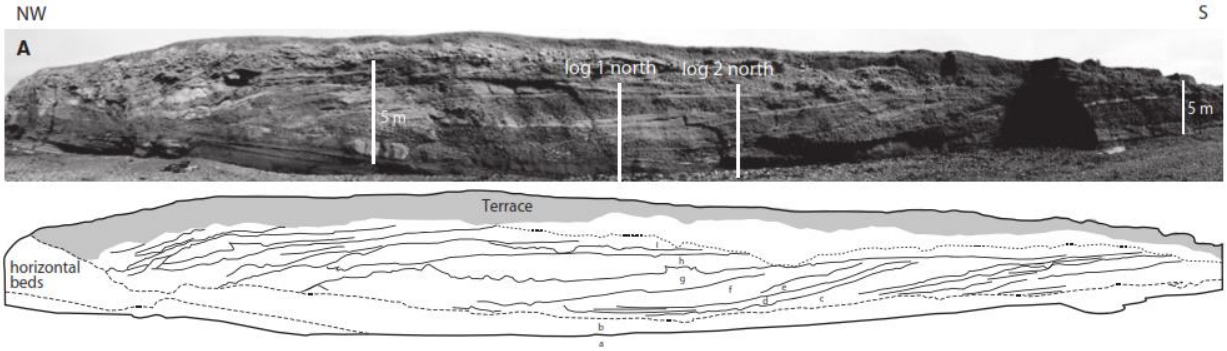

Figure 4.1: Photomosaic and line drawing of the Pelican Point North Outcrop in the Rosario Formation showing inclined beds which accreted from right to left (Dykstra and Kneller, 2009, fig 12).

Four lateral accretion sets crop out in the South Outcrop (fig 4.2); however, only the lowermost (LAP I in Dysktra and Kneller, 2009; fig 8) is accessible and complete with measured sections. The deposit is between 2.5 and 3 m thick and is composed of at least 15 beds that are mostly amalgamated toward the top and bottom of the lateral accretion surfaces. The laterally-accreted beds overlie thinly-bedded sandstone, siltstone, and mudstone that commonly are normally-graded with ripple cross-lamination (Dykstra and Kneller, 2009). LADs are composed of conglomerate and sandstone couplets that are normally graded and inclined at up to 10° relative to the thin beds below. Conglomerates grade upward to medium sandstone with floating pebbles and mudstone clasts and finally to fine to very fine-grained sandstone with faint parallel laminations (Dykstra and Kneller, 2009). The majority of beds display fining and thinning both up and down dip from the center. In addition, there is a mean grain-size decrease stratigraphically upwards through the lateral accretion set (Dykstra

and Kneller, 2009). This trend is interpreted to represent enhanced bypass in the channel thalweg, and is similar to observations in fluvial and tidal point bars and attributed to the early waning stages of flow (Dysktra and Kneller, 2009; Thomas et al., 1987; Miall, 1996). The youngest beds also erode into a mass-transport deposit that is interpreted to represent a local failure of the cut bank (Dykstra and Kneller, 2009). Erosional surfaces between the first and subsequent lateral accretion sets, as well as changes in the orientations of the beds, have been interpreted to represent different channels undergoing lateral migration or as reactivation surfaces of the same point bar (Dykstra and Kneller, 2009).

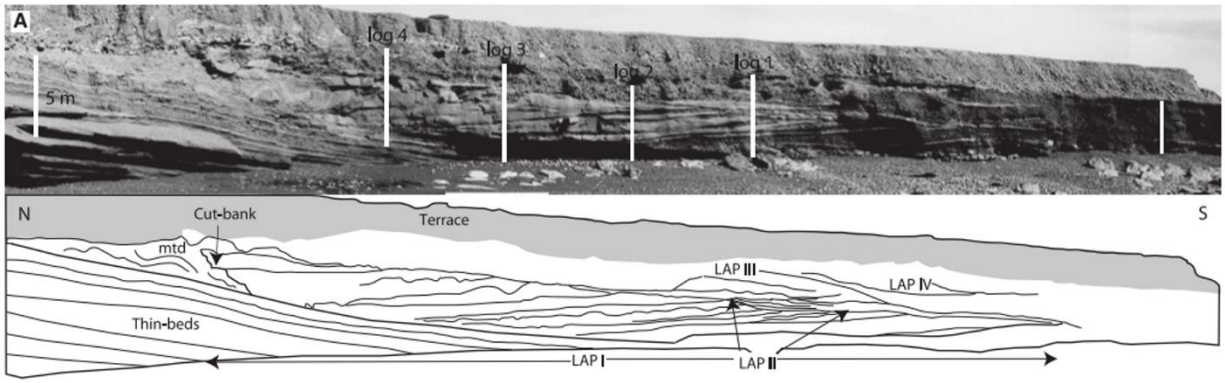

Figure 4.2: Photomosaic and line drawing fo the Pelican Point South Outcrop showing four laterally-accreted channel fills and one associated cut-bank in the Rosario Formation. Underlying thin beds used for paleo-horizontal (Dykstra and Kneller, 2009, fig 8).

Three other examples of laterally accreted channel fills in the Rosario Formation were described by Janocko (2011). The first two crop out at the base of the valley-fill succession and the third is located mid-way up the valley-form. The first example crops out on two connected outcrop faces (Janocko, 2011; fig 4.11 & 4.10b) and has been partially eroded by an overlying channel-belt complex. At its thickest it is 4.3 m thick and 10 and 15 m wide. The inclined channel fill overlies fine to very-fine, planar laminated and ripple cross laminated sandstone with siltstone and mudstone caps that are either massive or sporadically laminated (Janocko, 2011). The LADs are bipartite beds with a sigmoidal shape and consist

of normally-graded and planar stratified pebble conglomerate with a matrix of medium sand abruptly overlain by normally-graded and planar-stratified sandstone that are much less laterally continuous (Janocko, 2011). The contact between the two divisions is commonly sharp and beds show little change in grain size obliquely upward along each LAD. (Janocko, 2011). Along each set there is a progressive increase in the inclination of the lateral accretion surfaces from 3 to 12° (Janocko, 2011).

The second laterally-accreted channel fill is approximately 12 m thick and is well-exposed for over 80 m along a mountain side, although the width of the channel is estimated to be over 200 m (fig 4.3). The channel fill has an erosional and slightly aggradational contact that overlies slope mudstones with rare thinly-bedded sandstones and siltstones that also confine the LAD on the cut-bank side (Janocko, 2011). The LADs are sigmoidal in shape, with a maximum thickness of 1.5 m, and a typical bipartite texture. Normally-graded or weakly planar-stratified pebble to coarse cobble conglomerate with a coarse to medium-grained sandstone matrix is overlain sharply by a layer of sandstone that is normally-graded, massive, and/or planar-stratified (Janocko, 2011). Up-dip fining is observed chiefly within the gravel divisions (Janocko, 2011).

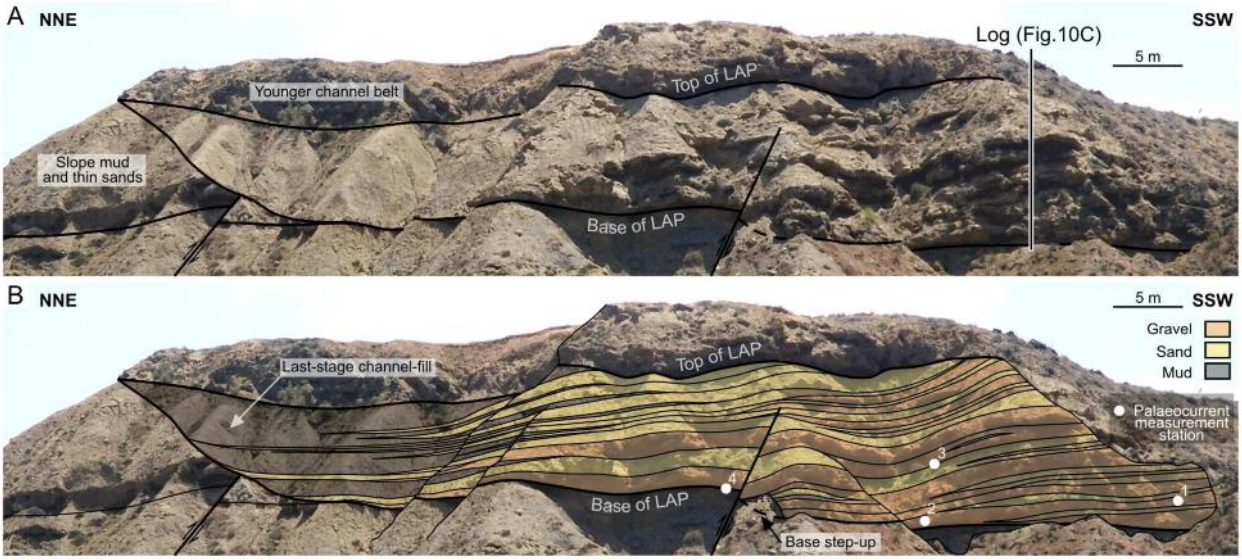

Figure 4.3: Outcrop photograph and overlay drawing for a laterally-accreted channel fill in the Rosario Formation (Janocko, 2011, fig 4.12)

The uppermost example is a channel complex composed of three separate channel fills, the lower two exhibiting features indicative of lateral accretion. The erosively-based channel fills are approximately 50 m wide with preserved thicknesses ranging between 1-3 m (fig 4.4). The LADs are made up mostly of tabular, commonly planar-stratified, grain-supported, cobble conglomerate beds with a fine to medium-grained sandstone matrix. Individual LADs range from 20-50 cm in thickness and are inclined up to 12° relative to the channel base (Janocko, 2011). The beds in the first laterally-accreted channel fill fine slightly up-dip, and there is a stepped basal contact at the last-stage channel fill that has horizontal injections of coarser-grained strata into muddy outer-bank deposits (Janocko, 2011). The second channel fill possesses thin sand lenses that locally separate the gravel beds, and the last-stage channel fill is composed of a massive, medium-grained sandstone bed with large floating mudclasts.

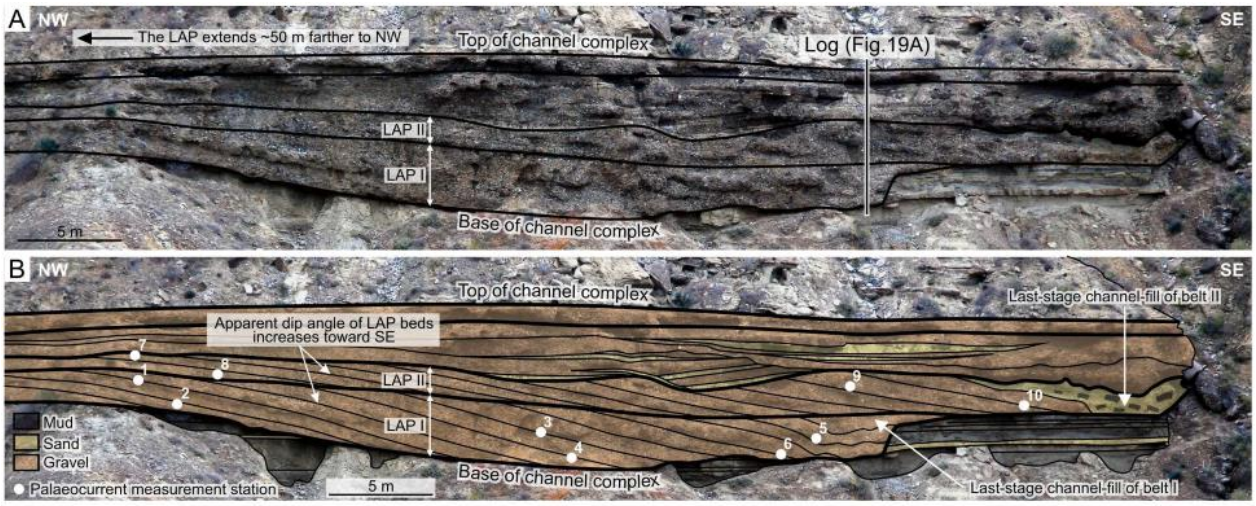

Figure 4.4: Photograph and overlay drawing for two laterally-accreted channel fills in the Rosario Formation (Janocko, 2011, fig 4.18).

4.2.2 Solitary Channel, Tabernas Basin, Spain

The Tabernas Basin in Spain is a small, elongate feature that was formed as a result of folding and faulting of basement rocks due to compressive forces between the European and North African plates (Kleverlaan, 1989; Cronin, 1995). The basin is situated between the Sierra de los Filabres and the Sierra Alhamilla and stretches for 30 km east-west with a maximum width of 15 km (Kleverlaan. 1989). The basin fill is Neocene in age and 1500 m thick, 900 m of which is marine in origin (Kleverlaan, 1989). The marine fill is dominated by a deep-marine sequence, with the upper and lower 50 m of the section consisting of shallow marine deposits (Kleverlaan, 1989; Cronin, 1995). The basin was tectonically active during the Neocene and episodically received large volumes of coarse-grained detritus (Kleverlaan, 1989). Three distinct channel-lobe systems were identified by Kleverlaan (1989) with the youngest, the Solitary Channel, containing LADs (Wynn et al., 2007; Cronin, 1995). The Solitary Channel is slightly sinuous and measures 8 km in length with a maximum width of 150 m and an average depth of 25 m (Wynn et al., 2007; Kleverlaan, 1989). The planform shape of the channel is interpreted to be the result of intrabasinal faulting (Kleverlaan, 1989).

The Solitary Channel fill is described as a mix of lenticular and sheet-like sandstone and conglomerate in packages up to 25 m thick (Cronin, 1995). Cronin (1995) recognized four different stages of channel fill, the oldest, Unit A, being about 5.5 m thick and containing LADs. Massive beds of medium- to coarse-grained sandstone between 1.4 - 2 m thick with sharp or erosive basal contacts and local lenses of conglomerate form lateral accretion surfaces that extend for up to several tens of meters and are draped by shale beds up to 25 cm thick (Cronin, 1995; Wynn et al., 2007). Abreu et al. (2003) documented a laterally-accreted channel fill in the uppermost part of the Solitary Channel (their Channel Complex Set 4; fig 17) with several LADs composed of normally-graded, very coarse- to coarse-grained, thickly-bedded sandstones interbedded with medium- to thinly-bedded, massive, medium- to fine-grained sandstones and very thinly-bedded mudstones. The channel fill has a maximum thickness of about 10 m with inclined lateral accretion surfaces that extend for several tens of meters at 8° relative to the base of the channel fill.

4.2.3 Beacon Channel Complex, Brushy Canyon Formation, Delaware Basin, Texas

The Upper Permian Brushy Canyon Formation is a submarine fan deposited within the Delaware Basin of west Texas when the region was covered by an epicontinental sea and represents the easternmost extent of the Basin and Range Province (Pyles et al., 2010). The Brushy Canyon Formation is up to 450 m thick and unconformably overlies the calcareous Cutuff Formation and siliciclastic Pipeline Shale Member. In turn it is overlain by a regionally correlatable package of siltstones interpreted to represent the abandonment of the submarine fan system (Pyles et al., 2010 and references therein). High slope-to-basin relief

was created by platform carbonates that formed the margin of the basin. Sediment for the Brushy Canyon Formation came from a western source that shifted progressively southward and is interpreted to be related to a network of 6-8 different submarine canyons (Gardner and Borer, 2000). Two laterally extensive organic-rich siltstone layers, which divide the Brushy Canyon Formation into lower, middle, and upper members, can be detected on geophysical logs throughout the Delaware Basin and have been interpreted to represent fourth-order stratigraphic cycles (Zelt and Rossen, 1995; Gardner et al., 2003; Romans, 2003).

The Beacon Channel Complex is located in the middle of the upper Brushy Canyon Formation and is interpreted to have been located on the mid-slope of the ancient submarine fan system (Pyles et al., 2010). Beaubouef et al. (2007) first described the Beacon Channel Complex and divided it into three main channelform units. Strata were exposed on five cliff faces and based on facies associations was argued to have a sinuous planform. Pyles et al. (2010) revisited the outcrop and based on detailed 3D mapping suggested that five different channelized units were exposed. The channel complex is about 15-20 m thick with a width of several hundred meters. The bulk of the fill consists of medium- to thick-bedded, tabular or lenticular, fine-grained sandstone. Beaubouef et al. (2007) documented inclined surfaces (their Unit 2; fig 4 & 6) in a package that is 5 m thick, up to 100 m wide and composed of thickly-bedded, cross-bedded or planar laminated, medium-grained sandstones that downlap onto the base of the Beacon Channel Complex. The beds are interpreted to be the result of the lateral accretion of a channel. These lateral accretion surfaces dip at 10° relative to the channel base and extend for several tens of meters laterally. The sandstone beds also appear to interfinger obliquely upwards with very fine-grained, thinly-bedded sandstone and siltstone. Pyles et al. (2010; Unit 3) described the LAD as being up to 10 m thick and

composed of sigmoidal-shaped beds that transitioned upward from thick-bedded, large-scale cross- and planar-stratified sandstone, and fine- to medium-grained, planar-stratified sandstones at the base to fusilinid conglomerates with a fine-grained matrix and then to siltstone and ripple- and cross-laminated, fine-grained sandstone in the upper part. Adjacent to the inclined beds are coeval levee deposits composed of thinly-bedded, fine-grained sandstones and siltstones that dip and fine and thin away from the channel deposits.

4.2.4 Makarska Flysch, Croatia

There is general agreement that the eastern coast of the Adriatic Sea consists of one or more authocthonous carbonate platforms overthrust by nappes. During the early Eocene, the Adriatic Carbonate Platform developed on what had been a passive-margin in the Cretaceous before it became drowned and dominated by deep-marine sedimentation. In central and southern Dalmatia, Paleogene limestones typically unconformably overlie Mesozoic strata and then are overlain by transitional marls and up to 1.8 km of deep-marine sediments, of which turbidites occur in the upper 850 m (McCann, 2008 and references therein).

Janocko (2011) documented a laterally-accreted channel fill that crops out along a road-cut northwest of the city of Makarska. The channel fill is roughly 6 m thick and 40 m wide. The fill is surrounded by muddy slope strata interbedded with thinly-bedded turbidites and the channel base is slightly aggradational in the last-stage part of the fill. The LADs comprise sigmoidal beds that are normally-graded and composed of faintly-stratified pebble conglomerate that thin updip and pass abruptly into planar-stratified, medium- to fine-

grained sandstone. The wide-angle photograph published in Janocko (2011, here fig 4.5) has distortion, though bedding surfaces are indicated and appear to dip at around 10° relative to the channel base.

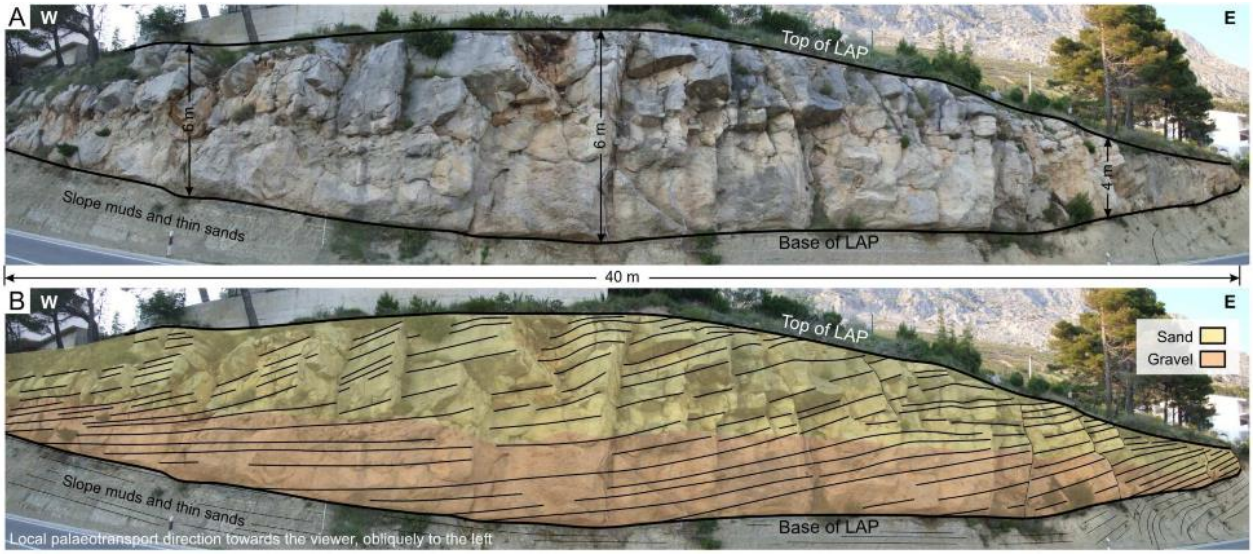

Figure 4.5: Wide-angle photograph and overlay drawing for a laterally accreted channel fill in the Makarska Flysch (Janocko, 2011, fig 4.17).

4.2.5 Ross and Gull Island Formations, Shannon Basin, Ireland

The intracratonic Shannon Basin of western Ireland was formed by crustal extension in the Late Devonian to the Early Carboniferous. The basin is filled with sedimentary rocks of the Shannon Group, which at its base comprises 180 m of basinal shale of the Clare Formation overlain by 930 m of basin floor and slope turbidites of the Ross and Gull Island formations, and then 900 m of deep- and shallow-water deltaic deposits of the Central Clare Group (Martinsen and Collison, 2002).

The Ross Formation is 380 m thick and dominated by fine- to medium-grained turbidites (70:20 sandstone: siltstone/mudstone ratio) that range from 5 cm to over 5 m, but on average are <30 cm thick, (Martinsen et al., 2000), and were deposited during rapid

subsidence of an area surrounding the present-day Shannon Estuary (Elliott, 2000). Channels are the dominant architectural style in the middle to upper parts of the formation (Elliott, 2000) and channels filled with lateral accretion deposits are interpreted to crop out at Rehy Cliff (Elliott, 2000, fig. 16; Abreu et al., 2003, fig 22; Wynn et al., 2007, fig 10, here fig 4.6) and Rinevella Point (Sullivan, 2000, fig 4; Abreu et al., 2003, fig 19). The Rehy Cliff outcrop is situated on a steep, high seaside cliff, and as a consequence no detailed stratigraphic studies have been conducted to date. Photographic images suggest that the channel is about 7 m thick and filled with apparently heterolithic strata that are inclined up to 7° to horizontal strata in the underlying aggradationally-filled channel. Abreu et al (2003) infers that the resistant portions of the outcrop are made up of Ta beds, whereas recessive/covered parts are underlain by mud clast conglomerates or mudstones. The Rinevella Point outcrop is less steep and more easily accessed. The inclined surfaces illustrated in Sullivan (2000, fig 4) are interpreted to be part of a channel that is about 15 m deep and which migrated laterally over 100 m. Unfortunately, descriptive details are generally lacking and photographic images do not show that part of the outcrop in detail. Later, Abreu et al (2003, fig 19) published a photo of the same outcrop showing apparently inclined surfaces in a succession of massive sandstones, although no horizontal datum was provided.

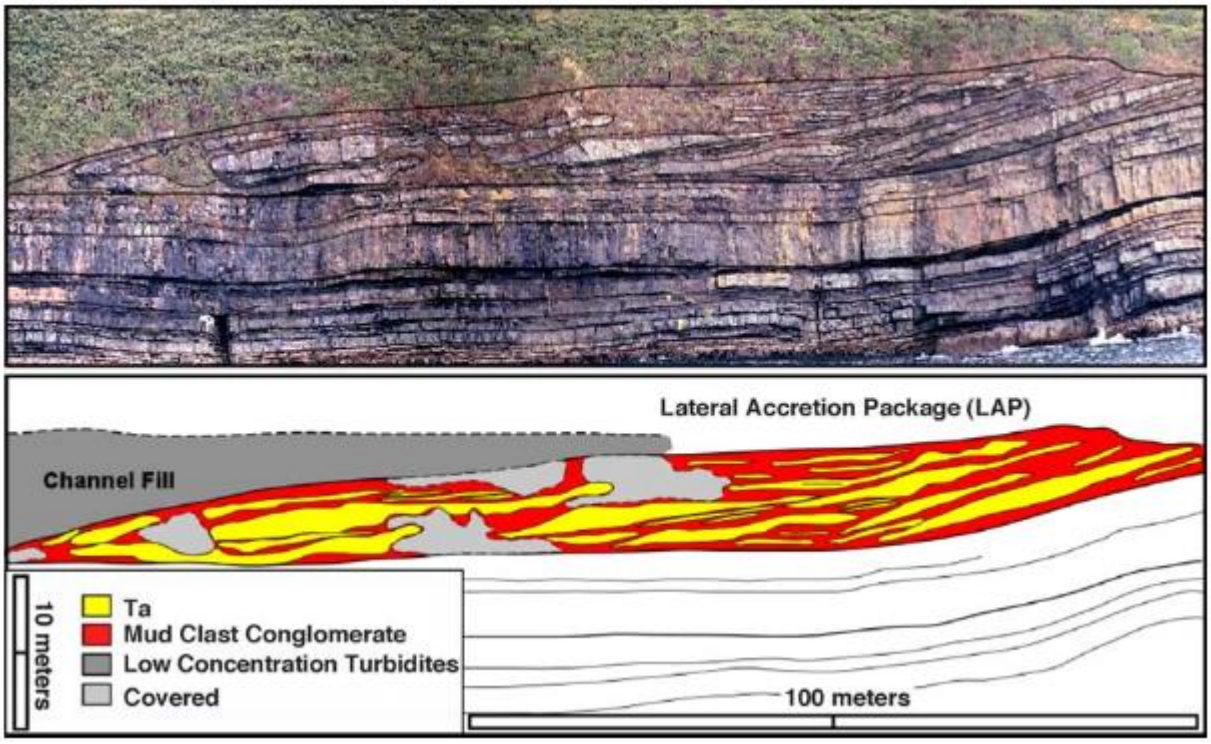

Figure 4.6: Photograph and line diagram of interpreted lithologies for the Rehy Cliffs outcrop of the Ross Formation (Abreu et al., 2003, fig 22).

The Gull Island Formation has a maximum thickness of 550 m and is dominated (up to 70%) by structures suggesting syn-sedimentary deformation (Martinsen and Bakken, 1990). Undeformed strata includes channels composed of very fine to fine-grained sandstones and shale (Martinsen et al., 2000). A photograph of a cliff-side exposure near the town of Ballybunion published in Martinsen et al. (2000, fig 14) shows an outcrop that is 15 m high and contains a unit interpreted to be made up of sandy turbidites and possessing inclined surfaces that dip at approximately 6° relative to its base. Unfortunately, the inaccessibility of the outcrop has prevented any detailed sedimentological studies to date and hence it is unclear if the inclined surfaces are related to lateral channel migration or some other process.

4.2.6 Jackfork Group, Ouachita Basin, Arkansas

Sediments of the Ouachita Basin were deposited during subsidence of a foreland basin in the Late Carboniferous, and currently are exposed in the Ouachita Mountain fold and thrust belt in Arkansas that was formed by the collision of the North and South American plates (Coleman et al., 2000; Sprague, 1985 [unpublished Ph.D., taken from Abreu et al. and Zou et al. 2012]). Big Rock Quarry, located near the city of North Little Rock, features an exposure of sandstone, shale, and conglomerate that is 60 m high and nearly a kilometre long. Partly exposed is a much larger channel complex that is about 10 m wide and up to 24 m long. The quarry is believed to be almost 800 m from the top of the Jackfork Group, which in central Arkansas is approximately 2 km thick (Coleman et al., 2000).

The interpreted laterally accreting channel deposit crop out near the top of the quarry wall, though due to its inaccesibility has not been described in detail (photographic interpretation only). A photograph of the deposit in Abreu et al. (2003, here fig 4.7) is vertically exaggerated and the actual angle of the dipping surfaces is estimated to be approximately 10°. In outcrop the channel fill appears to be about 8 m thick and almost 200 m long. Resistive portions of the outcrop have been interpreted to be Ta beds, in both the laterally-accreted channel fill as well as the aggradationally-filled last-stage channel fill, and the recessive portions are interpreted to be mud-clast conglomerates.

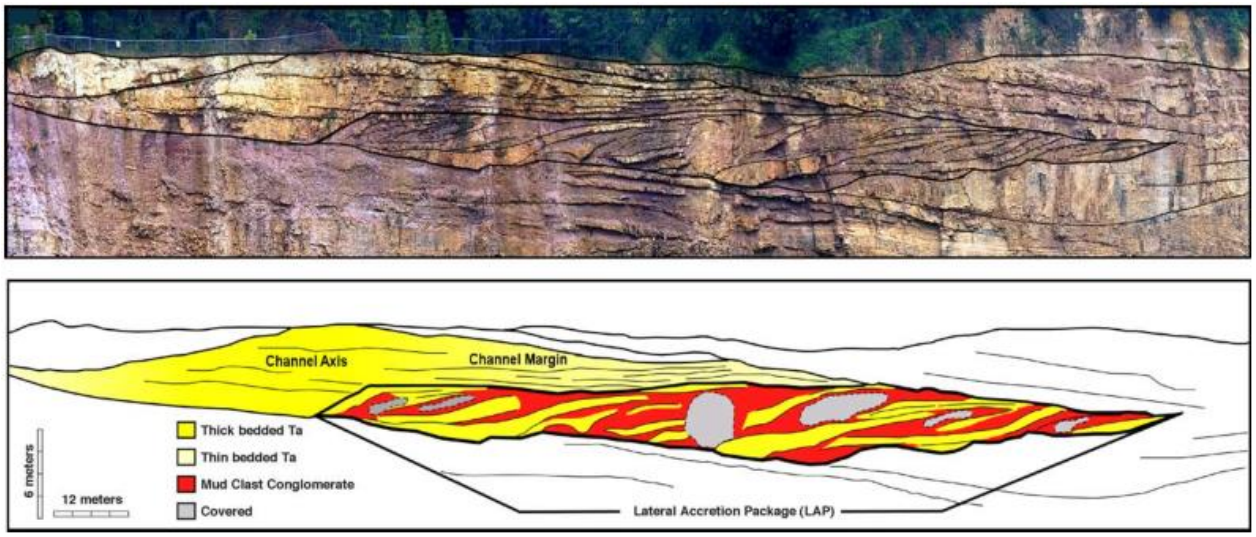

Figure 4.7: Photograph and line drawing of interpreted lithologies for the Big Rock Quarry outcrop of the Jackfork Group (Abreu et al., 2003, fig 23).

4.3 Summary

Currently there is a paucity of well-documented and accessible examples of laterally-accreting, deep-marine channel fills in the sedimentological literature. Outcrops in the San Fernando Canyon, the Solitary Channel, the Beacon Channel Complex, and the Makarska Flysch are cases where detailed sedimentological studies have been conducted and the inclined surfaces and associated strata were likely deposited by laterally accreting channels. The Rehy Cliffs, Ballybunion, and Big Rock Quarry outcrops are morphologically similar to the previous examples and could potentially be laterally-accreted channel fills; however they lack sedimentological details to be considered unequivocal.

As summarized in Table 2.1, these studies suggest that laterally-accreting channels form in a variety of different kinds of sedimentary basins and at various stratigraphic positions within a channel-complex or channel-complex set. Channel fills are typically on the order of 10 m thick and although the exposures are often less than 100 m wide, the actual lateral extent of the channels may be larger. LADs are commonly composed of thickly-

bedded, tabular or sigmoidal beds. Grain size is commonly coarse, with common granular or pebble conglomerates that may grade or transition abruptly upwards into sandstone. An exception to this is the laterally accreting unit in the Beacon Channel Complex, which is composed of medium-grained sandstone. It is, however, coarser grained than the other, aggradationally-filled channels in the Brushy Canyon that are dominated by fine- or very fine-grained sandstone. The degree to which LADs dip in relation to the channel base is somewhat variable but on average appears to be of the order of 10^{o} – note that the true angle of dip is higher if the inclined lateral accretion surfaces intersected the face of the outcrop obliquely (see discussion in Chapter 5), a probable outcome given the interpreted high sinuosity of the channels.

Outcrop	Location	Basin Type	Channel Fill Dimensions	Position	LADs		
					Morphology	Grain-Size	Dip
San Fernando Canyon	Mexico	Forearc	1 – 12 m thick; 50 – 80 m wide	Base to middle of valley-fill complex	Sigmoidal and tabular	Conglomerate, conglomerate grading upwards into medium- to fine-grained sandstone, and abruptly graded bipartite conglomerate and medium-grained sandstone beds	7-12°
Solitary Channel	Spain	Intracratonic (compressional)	5 – 10 m thick;	Base and top of channel fill complex, uppermost of three channel-lobe systems	Tabular	Conglomerate normally grading upwards into sandstone interbedded with fine-grained sandstone and mudstone	8°
Beacon Channel Complex	U.S.A.	Intracratonic (extensional)	5 – 10 m thick; 100 m wide	Base or near base of channel fill complex	Sigmoidal	Medium-grained sandstone; medium- and fine-grained sandstone transitioning obliquely upwards into fine-grained sandstone	10°
Makarska Flysch	Croatia	Continental margin	6 m thick; 40 m wide	Upper half of deep-marine deposit; position within architectural system unknown	Sigmoidal	Pebble conglomerate grading abruptly into medium- to fine-grained sandstone	10°
Rehy Cliffs	Ireland	Intracratonic (extensional)	8 m thick; 165 m wide	Middle of the formation	Sigmoidal	Sandstone-rich Ta beds interbedded with mudclast-rich conglomerate (based on weathering profile)	7°
Ballybunion			8 m thick; 100 m wide	Base of the formation	Unknown	Sandy turbidites (based on photograph)	6°
Big Rock Quarry	U.S.A.	Intracratonic (compressional)	8 m thick; 200 m wide	1.6 km from the base of 2 km thick group	Sigmoidal	Sandstone-rich Ta beds interbedded with mudclast-rich conglomerate (based on weathering profile)	10°

Table 4.1: Summary of outcrop examples of interpreted laterally accreting deep-marine channel fills.

5 DISCUSSION

5.1 Characteristic Attributes of Laterally-Accreted Channels at Castle Creek

5.1.1 Abundance of coarse-grained sediments

As described in Chapter 3, strata of Isaac Channel 2.3 and Isaac Units 14 & 21 are predominantly upper coarse and very coarse sandstone (LF1) that show little to no upward or lateral fining or thinning (figs 3.2, 3.4, 3.6, and 3.9). In contrast, channel fills of Isaac Channels 1 and 3, although similar in thickness, typically exhibit well-developed upward and in many cases lateral fining and thinning trends in what is interpreted to be aggradationally filled channels (Navarro, 2005; Schwarz & Arnott, 2007). Notably, many other examples of laterally-accreted channels that have been reported from the ancient geological record are similarly coarse-grained, with strata usually consisting of coarse sandstone to pebble conglomerate or, in the case of the Beacon Channel Complex (Beaubouef et al., 2007; Pyles et al., 2010), are distinctively coarser-grained compared to other channel fills.

The uniquely coarse-grained nature, and potentially also non-normally distributed grain-size distribution in the laterally-accreted channels in Castle Creek, is interpreted to be the product of differences in the sediment supply compared to what formed aggradationally-filled channels; specifically a reduction in the relative proportion of medium and fine sand but relative increase in coarse sand and larger grains. As discussed in Section 1.6.5, changes in relative sea level are one possible mechanism that can account for systematic changes in sediment supply to the deep marine. During a rise in relative sea level, sediment deposited on the continental shelf during lowstand experiences erosion and reworking by shelf processes during transgression (Plint, 2010). Easily transported grains, like medium to fine sand and

finer, follow the shoreline and eventually build up barrier islands. As a consequence the residuum of stranded sediment coarsens, and similarly the supply of sediment into the deep marine (Arnott, 2010). In addition, resedimented carbonate material is observed overlying all three studied intervals. Carbonate occurs as cement in thinly bedded turbidites and as carbonate cemented mudstone and sandstone clasts in mass transport deposits. This is interpreted to be the result of transgressive flooding of a shallow-water platform that shed a mixture of siliciclastic and carbonate sediment downslope.

5.1.2 Abrupt transition to fine-grained upper division turbidites

Isaac Channel 2.3 (CE 2.3-4) contains the best LAD exposures (see fig 3.4) that highlight the abrupt transition between coarse-grained sandstone and conglomerate (LF1) and fine-grained, upper-division turbidites (LF3). Cartoons of more poorly exposed laterally-accreting channels in the literature, for example the Beacon Channel Complex (Beaubouef et al., 2007) and Rosario Formation (Janocko, 2015), show similar transitions. At Castle Creek, the bases of the coarse-grained LF1 beds are commonly shallowly scoured and thin abruptly obliquely upwards before being overlain by LF3 strata. The scour does not extend beyond the updip terminus of the LF1 bed, indicating that the LADs caused local erosion of the channel during their deposition and do not simply onlap a larger-scale surface. This abrupt transition is attributed to the development of a strong density interface (high gradient Richardson number) that separates a dense basal part of the flow from a much finer and more dilute upper part.

5.1.3 Channel filled with inclined strata

Bedding planes in channel fills of the Isaac Formation vary from subhorizontal up to a maximum inclination of 12° (see sections 3.2, 3.3, and 3.4). As noted in Chapter 4, other documented examples of laterally-accreted channels in the literature commonly dip at approximately 10° relative to the channel base (table 4.1). The presence of channels filled with inclined strata is only common at discrete stratigraphic horizons in the Isaac Formation. Elsewhere, such as Isaac Channel 1 and 3, channels are filled with subhorizontal, aggradationally-stacked strata (Navarro, 2005). The inclined character of strata in some channel fills is interpreted to be the result of deposition on the dipping, inner bend surface of a laterally migrating sinuous channel. Importantly, not all strata in these channel complexes are inclined, and channel element fills within the same complex commonly have angular discordances. These discrepancies are interpreted to be the result of differences in the exposed position along the sinuous channel (e.g. apex of the bend, entrance or crossover point) and/or differences in the orientation of the various laterally juxtaposed channels as they intersect the outcrop face.

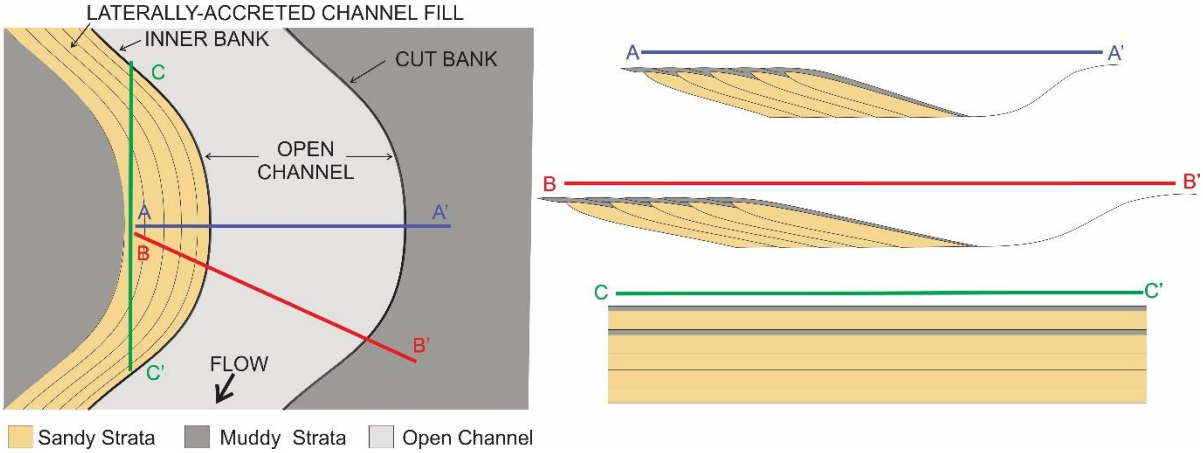

Figure 5.1: Cartoon illustrating the difference in the dip of laterally-accreted strata as a function of the orientation of the outcrop face versus dip direction of the LADs.

Figure 5.1 illustrates an idealized laterally-accreted channel element with variably oriented transects and their associated cross-sections. Note that the true dip of a LAD is only observed if the cross-section is oriented parallel to the direction of channel accretion. In exposures oriented oblique to this direction, the observed dip of a LAD and its associated beds is less than the true dip:

$$\tan(truedip) = \frac{\tan(appdip)}{\cos\beta}$$

where β is the angle separating the apparent dip from the true dip

Where the cross-section is oriented perpendicular to the direction of accretion, strata are horizontal. Further, the inherently 2-dimensional nature of the Castle Creek outcrop, the vertical (tectonic) dip of the entire exposure, and interpreted high sinuosity of the laterally-migrating channels makes it quite probable that many of the channel elements, if not all, are intersecting the outcrop face at a variety of oblique angles.

5.1.4 Relatively Flat Basal Contacts

The base of Isaac Unit 14 and Isaac Unit 21 is subhorizontal (figs 3.5 and 3.8). Line diagrams of lateral accretion deposits in the Rosario Formation (Dysktra and Kneller 2009; their figs 6,8, and 12, here figs 4.1 and 4.2) exhibit similar low-relief surfaces. The base of Isaac Channel 2.3 (fig 3.1) is unique in that it is erosive and also contains two 'steps' or terraces that are interpreted to have formed by erosion along the outer-bend margin of the channel prior to an abrupt lateral shift of the channel-form between channel elements. In

contrast, the base of aggradationally-filled channels in Isaac Channel 3 possess angled, higher relief contacts with their adjacent levee deposits (e.g. Navarro, 2007). In the context of laterally accreting channels, these basal surfaces are not interpreted to represent a single master cut that subsequently was filled, but rather is a composite surface resulting from the continuous lateral migration of an open channel form. Channel elements with erosive bases within a flat-based channel complex, such as CE 14-2, CE 21-3 and CE 21-4, commonly possess an angled contact with underlying channel elements that is consistent with the inner bank of a channel form.

5.1.5 Presence of injection complexes

Clastic injections, although not uniquely, are most commonly observed along the margins of laterally-accreting channel fills. Injection complexes are present in the fine-grained units that sharply bound Unit 21 (fig 5.2) and IC 2.3 (fig 5.3) (this study), as well as Isaac Contact Channel (Navarro, pers comm 2015).

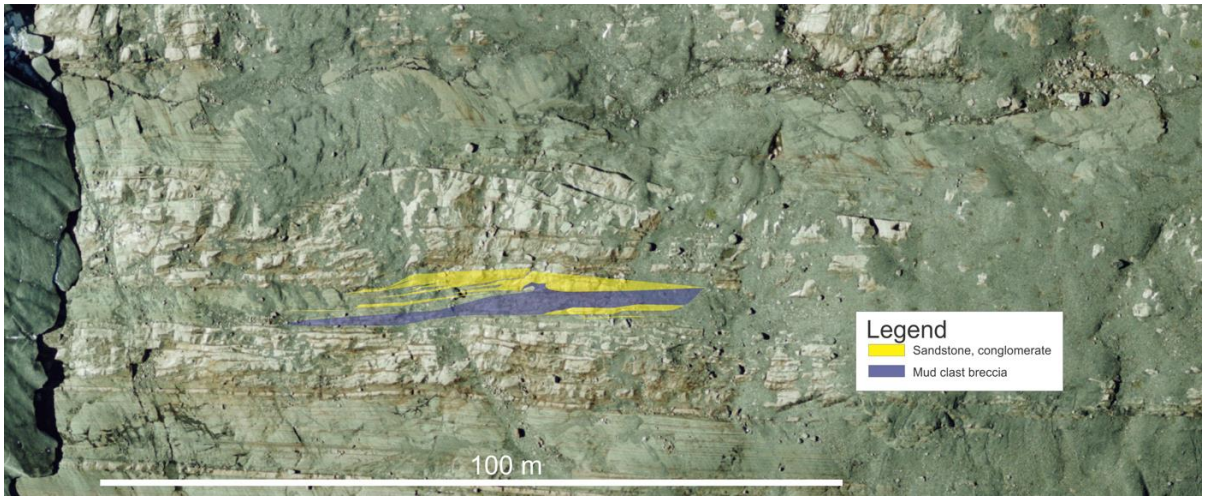

Figure 5.2: Aerial photomosaic of CE 21-1 overlain by injected sandstone, conglomerate, and mudclast breccia originating from CE 21-2.

Figure 5.3: Aerial photomosaic of Isaac Channel 2.2 overlain by thinly-bedded turbidites that along the step at the base of CE 2.3-2 were injected by coarse-grained sand and mudclast breccia originating from CE 2.3-2.

Clastic injections form in a wide variety of geological settings, but are most common in deep-marine deposits (Jolly and Lonergan, 2002). These features are the result of highly pressurized and mobilized pore fluids with entrained sand grains that are forcibly injected into surrounding stratigraphy (Jolly and Lonergan, 2002). In order for fracturing to initiate and then propagate, the surrounding sediments must have a degree of tensile strength that allows the pore pressure to build. Some to much of this increase is related to fluids expelled from compacting adjacent mud-rich sediments that seeped into the sand-rich channel fills, eventually resulting in overpressure conditions (i.e. pore-fluid pressure deviating from hydrostatic). In order for the lateral seal to fail and injection to initiate, pore fluid pressure must exceed the tensile strength of the enveloping mud-rich sediments. Failure was probably instantaneous and resulted in fluid movement that was sufficient to entrain grains as large as granules (fluidization). Fluidization, and propagation of the fractures, will continue so long as an adequate pressure gradient is maintained, after which the intrusion stops and the intrusion 'freezes' (Jolly and Lonergan, 2002).

At Castle Creek, clastic injections are characterized by sills with only few dikes. This observation is consistent with injections following only shallow depths of burial and the axis of minimum stress ($\sigma 3$) being oriented normal to bedding (i.e. sills). The abundance of sills in accretion deposits compared to aggradationally-filled channels may be largely the result of

differences in the sand content of channel margin strata, respectively mud-rich versus sand-rich. In addition, the interpreted highly density stratified nature and the coarseness of the sediment in the lower parts of the flows that form laterally-accreted channels at Castle Creek would preferentially deposit muddy levees along the outer margin of sinuous channels, thereby forming an effective seal. In addition, instantaneous deposition of mass transport deposits, which directly overlie Channel 2.3 and Isaac Unit 21, could have provided the impetus for seal failure and subsequent intrusion. Injected sediments are described from one channel unit in the Rosario Formation (Janocko, 2011), but the channel margins are sandy (Dykstra & Kneller, 2007), and as a consequence form a poor lateral seal thereby inhibiting the build up of overpressure.

5.2 Lateral accretion model

Different forces are exerted on fluids as they round a channel bend. The first is the inertial (centrifugal) force that draws a moving body away from the centre of rotation and, in the case of channelized flows, towards the outer-bank,

$$F_I = \frac{\rho v^2}{R}$$

where ρ is the density of the fluid, v is the velocity, and R is the radius of curvature

The second is the pressure force that forces fluids to move along a gradient from a region of high fluid pressure to one of low fluid pressure.

$$F_P = \rho g h$$

where g is the acceleration due to gravity and h is the thickness of the overlying fluid column.

In the case of open-channel flows, spatial differences in fluid density are negligible. Upon entering a bend, fluid motion is directed towards the outer-bank by the outward-directed centrifugal force. This motion results in an elevated cross-stream water surface slope. This, in turn, increases fluid pressure along the outer-bank at the base of the flow and instigates fluid movement in the lower part of the flow to move toward the inner-bank. Together their opposing motions: outward at the surface and inward at the bed, creates a circulation cell, or secondary flow, that becomes superimposed on the streamwise primary flow (fig 5.4). Fluid and particle motions, then, are controlled by the vector resultant of these two forces. Through the bend the centrifugal force at any given height above the bed remains constant, however, the secondary flow component progressively strengthens toward the bend apex and then weakens toward the exit. At the bend apex these two forces are at their maximum. Here fluid particles, and if basal shear is sufficiently high, bed load sediments are moved obliquely up the inner-bank where the fluid then turns over and returns to the outer-bank along the surface. At the bend exit the outward-directed inertial force ceases to exist but the still diminishing pressure gradient diverts bottom fluid motion towards the outer bank of the next channel bend downstream, whereafter the process repeats.

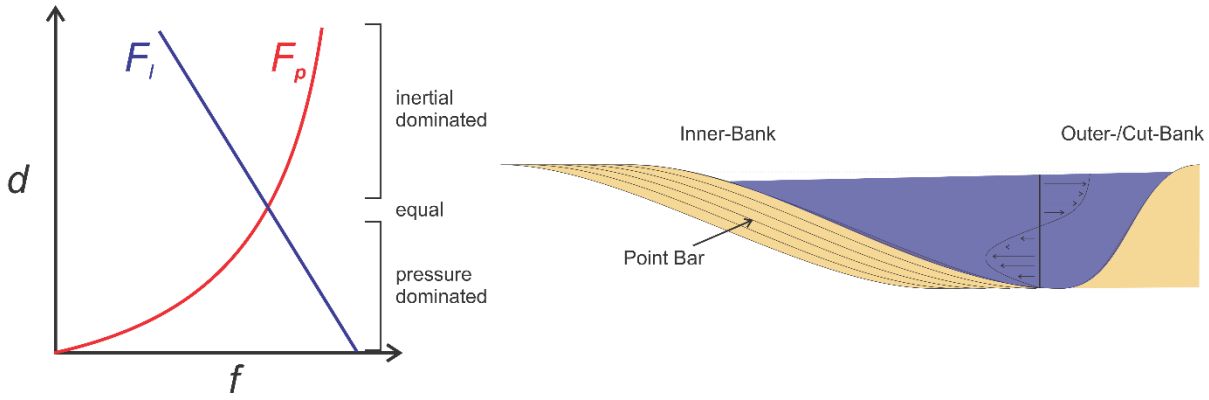

Figure 5.4: Cartoon illustrating the forces present in an open channel flow meander bend and the resultant secondary circulation.

In the case of sediment gravity flows travelling through sinuous deep-marine channels, fluid density is not always uniformly distributed within the flow, but instead is usually a diminishing function with height above the bed. Laterally-accreted channels investigated in this study are unique in their grain size make-up, being enriched in coarse and very coarse sand, and seemingly depleted in finer sand grain sizes. Such a grain size distribution would likely have caused the flows to become highly density stratified, with a dense, coarse-grained basal layer overlain by a much more dilute and finer grained upper layer. In the coarse, dense lower layer density (i.e. sediment concentration) is mostly uniformly distributed (i.e. plug-like) (fig 5.5). Coupled with a velocity structure in which U_{max} is elevated above the bed (fig 5.5), causes the high momentum, upper part of the basal layer to be diverted toward the outer bank, thereby enhancing channel bank erosion (fig 5.6A). As fluid becomes increasingly more concentrated the cross-channel density gradient steepens, which in turn strengthens the secondary current towards the inner bend. Theoretically bed load and suspended load transport would be directed obliquely up the inner bend margin. However, the inability of the flow to lift the coarse suspended sediment grains in order to complete the circulation cell would result in a reservoir of progressively more concentrated suspended sediment laden fluid to build up along the inner bend (fig 5.6B).

Eventually this too would create a cross-stream density gradient, but in this case directed towards the outer bend. This second circulation cell would be superimposed on the basal inner-bend rotating cell (fig 5.6C). Coarse sediment in the upper cell would most probably settle into the lower cell during transport towards the outer bank. Finer, more easily suspended sediment, however, would continue to circulate within the upper cell. A similar circulation has been reported in estuaries (e.g. Nidzieko et al., 2009) where flow in the dense (saline) lower part of the flow is directed towards the inner bend which then builds up a volume of dense fluid that then flows towards the outer bank forming a second but counter-rotating circulation cell (fig 5.7). Recent measurements in the saline underflow north of the Strait of Bosphorus by Sumner et al. (2014) suggest a similar circulation pattern wherein a basal inward-directed (i.e. normal) secondary circulation shifts dense bottom fluid towards the channel margin where it becomes trapped because the secondary current cannot lift it up to complete the circulation. This fluid then flows toward the outer bank thereby forming an outwardly counter-rotating circulation cell.

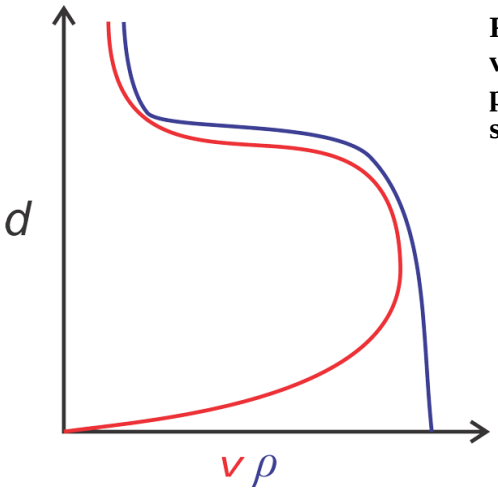

Figure 5.5: Cartoon illustrating the velocity (red) and density (blue) profiles through a highly stratified sediment gravity flow.

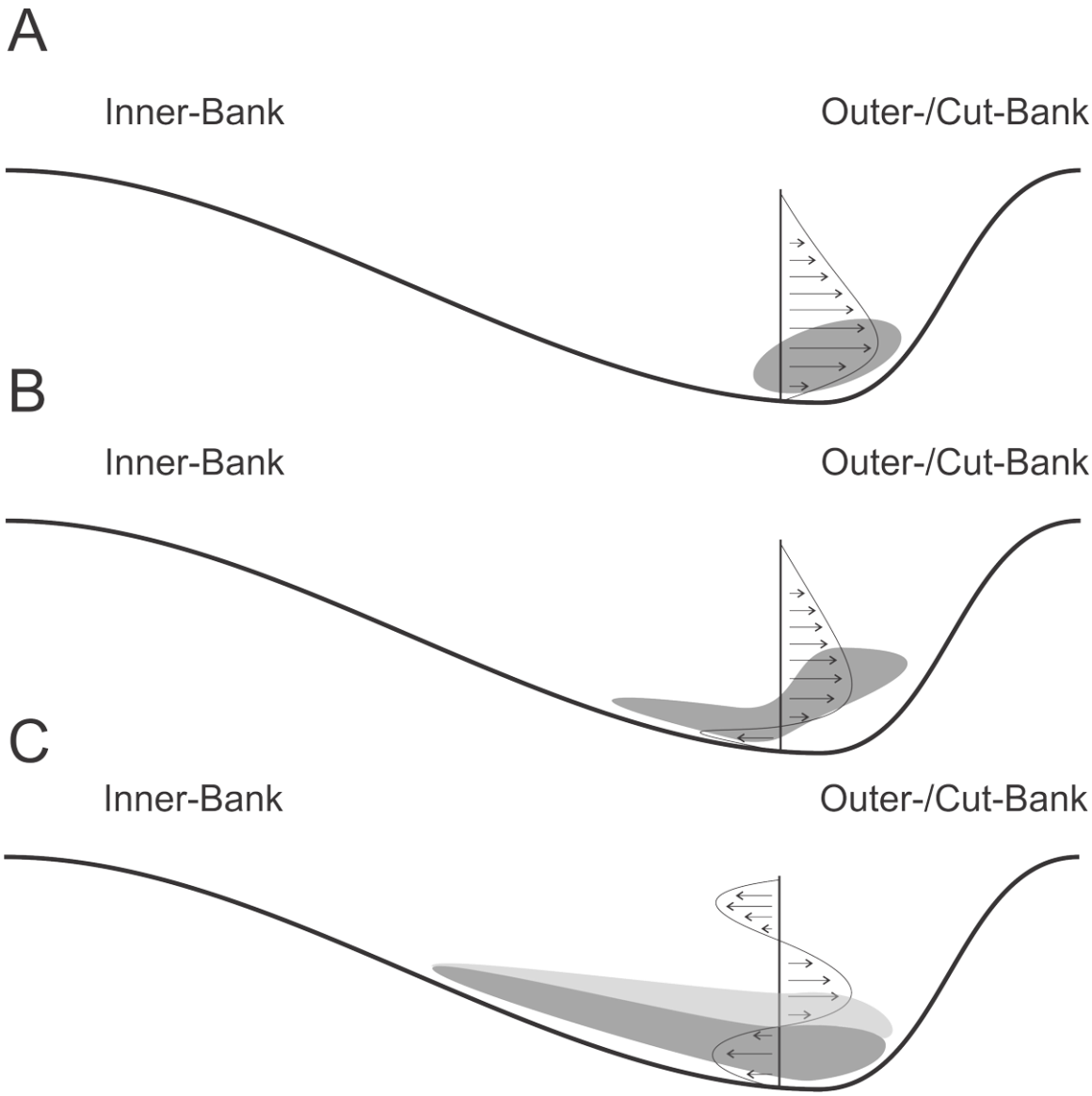

Figure 5.6: Sequence of cartoons depicting cross-stream fluid flow in a deep-marine channel as a highly stratified sediment gravity flow (A) enters the bend, (B) develops a reservoir of coarse suspended sediment along the inner-bend, and (C) two superimposed circulation cells. Dark grey areas indicate density maxima due to high suspended sediment concentrations.

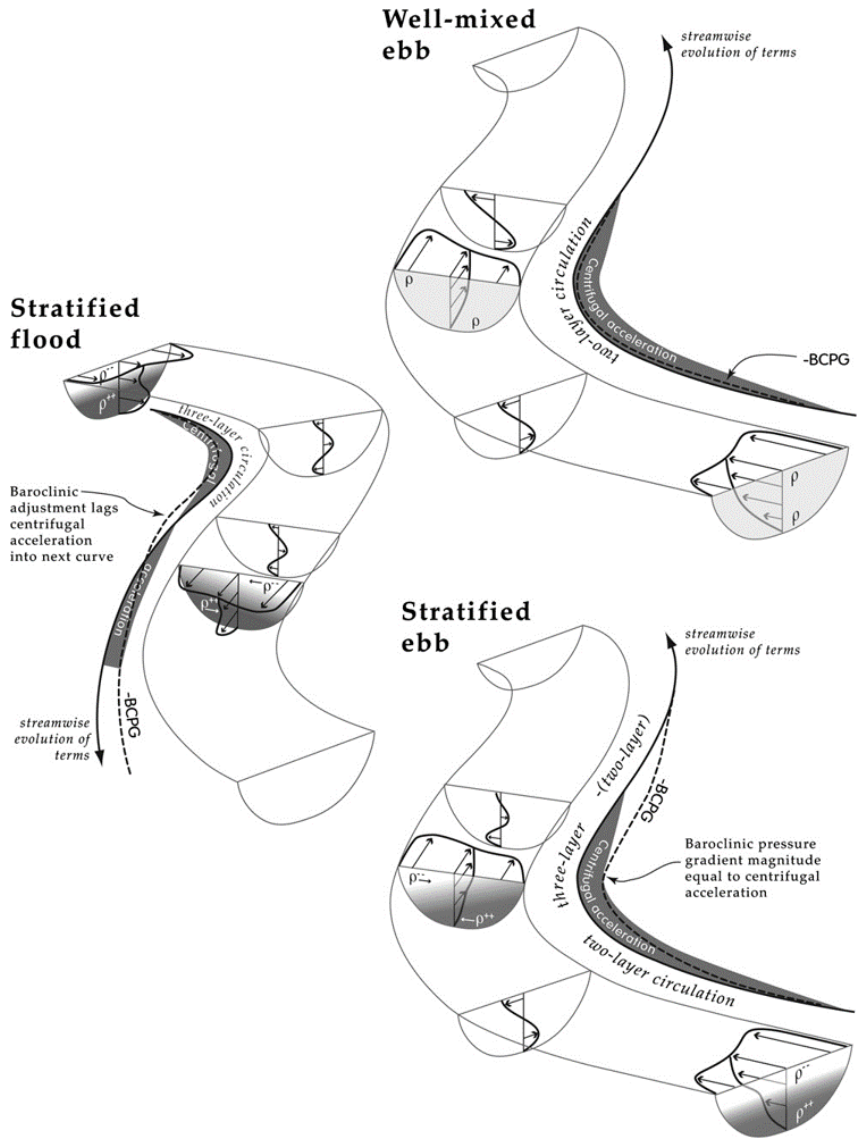

Figure 5.7: Conceptual diagram of interaction between stratification (shaded areas in cross-sections), centrifugal acceleration (grey areas along streamwise axis), and adjustment of baroclinic pressure gradient (dashed line along streamwise axis). Representative lateral velocity profiles are shown in each cross-sections (Niedzieko et al., 2009, fig 12).

The alternation between coarse and fine-grained sediments of the LADs in Isaac Channel 2.2 was interpreted by Arnott (2007) to represent systematic, recurring changes in flow conditions related to channel dimensions. Outer-bank erosion and failure caused by outward-directed inertial forces would lead to an increase in the cross-sectional area of the channel, decrease the local efficiency of subsequent flows, and promote local sedimentation. Once equilibrium channel dimensions were restored the system returned to bypass (transport)

conditions. Alternatively, Janocko (2015) interpreted the beds in Isaac Channel 2.2 to represent changes in the nature of the flows passing through the channel, with collapses of the shelf edge leading to the sporadic influx of coarser-grained sediment. These coarser-grained, highly energetic flows caused increased erosion on the cut-bank side, enlarging the channel and encouraging deposition on the inner-bank before lower energy, finer-grained flows would resume and drape the new deposits. The rhythmic nature of the LADs observed in Castle Creek suggests that the mechanism responsible for their deposition operates in a consistent and reproducible manner, and therein inconsistent with a process that relies on changes in the sediment source area which would be expected to operate with temporal and volumetric variability (Arnott, 2007).

5.3 Depositional History

5.3.1 Channel 2.3

IC 2.3 is interpreted to be a channel complex composed of five channel elements resulting from the lateral offset stacking of laterally-accreting channel fills (see section 5.2 above for the proposed mechanism). Due to the subparallel orientation of the strata and their bounding surfaces throughout the channel complex, individual channel elements are interpreted to be separated by a lateral offset of channel-forms but with little change in channel orientation. In addition, the lack of any systematic change in the orientation of successive channel fills suggests that the outcrop face is oriented subparallel to the direction of offset migration. CE 2.3-1 is interpreted to have been scoured and truncated by CE 2.3-2 (fig 5.8B). The angled contact between CE 2.3-2 and CE 2.3-3, in addition to being erosive,

was marked by a more significant lateral offset that resulted in at least partial preservation of the outer bank of CE 2.3-2 (fig 5.8C). This is also interpreted to be the case with the contact between CE 2.3-3 and CE 2.3-4 (fig 5.8D). CE 2.3-4 and CE 2.3-5 extend laterally beneath the glacier and as a consequence the nature of the surface that separates them is unknown (fig 5.8E).

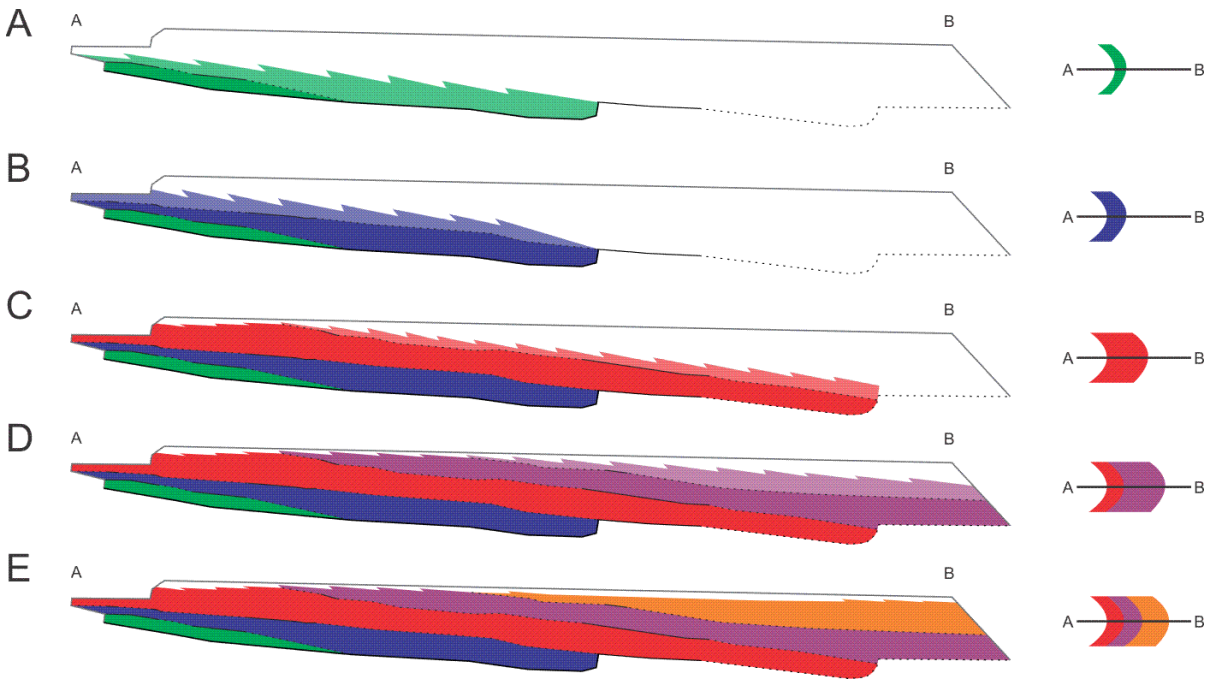

Figure 5.8: Cartoon illustrating the proposed depositional history of Isaac Channel 2.3 in both cross-section and plan view.

5.3.2 Unit 14

IU 14 is interpreted to be a channel complex comprising two offset-stacked, laterally-accreted channel elements, but significantly with different orientations. CE 14-1 was deposited with a channel profile oriented subparallel to the outcrop face, as evidenced by the high-angle of the dipping stratigraphic surfaces within the fill (fig 5.9A). Subsequent erosion by CE 14-2 formed a mudclast breccia along the contact which then filled with strata oriented subperpendicular to the outcrop face (fig 5.9B).

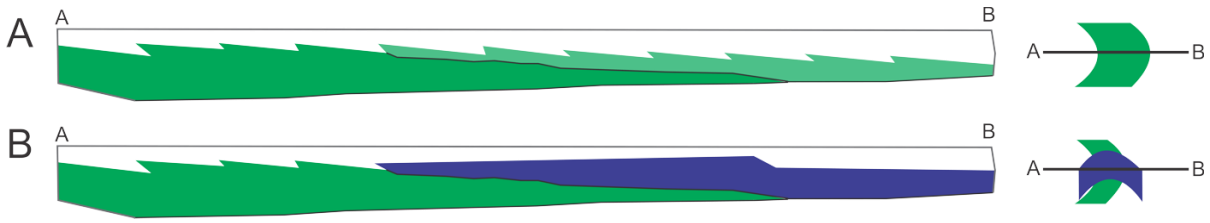

Figure 5.9: Cartoon illustrating the proposed depositional history of Isaac Unit 14 in both cross-section and plan view.

5.3.3 Unit 21

IU 21 is interpreted to be a channel complex consisting of four laterally accreted channel elements. CE 21-1 and CE 21-2 were deposited by channels with a profile oriented subperpendicular to the outcrop face and separated by an interval of thinly bedded turbidites indicative of a period of local(?) quiescence and channel deactivation (fig 5.10A and B). Inclined contacts and stratal surfaces observed in CE 21-3 and CE 21-4 are interpreted to be of two laterally offset channel elements with profiles that are oriented subparallel to the outcrop face (fig 5.10C and D). This, then, is followed by another period of channel deactivation and deposition of thinly bedded turbidites prior to the emplacement of a mud-rich debrite.

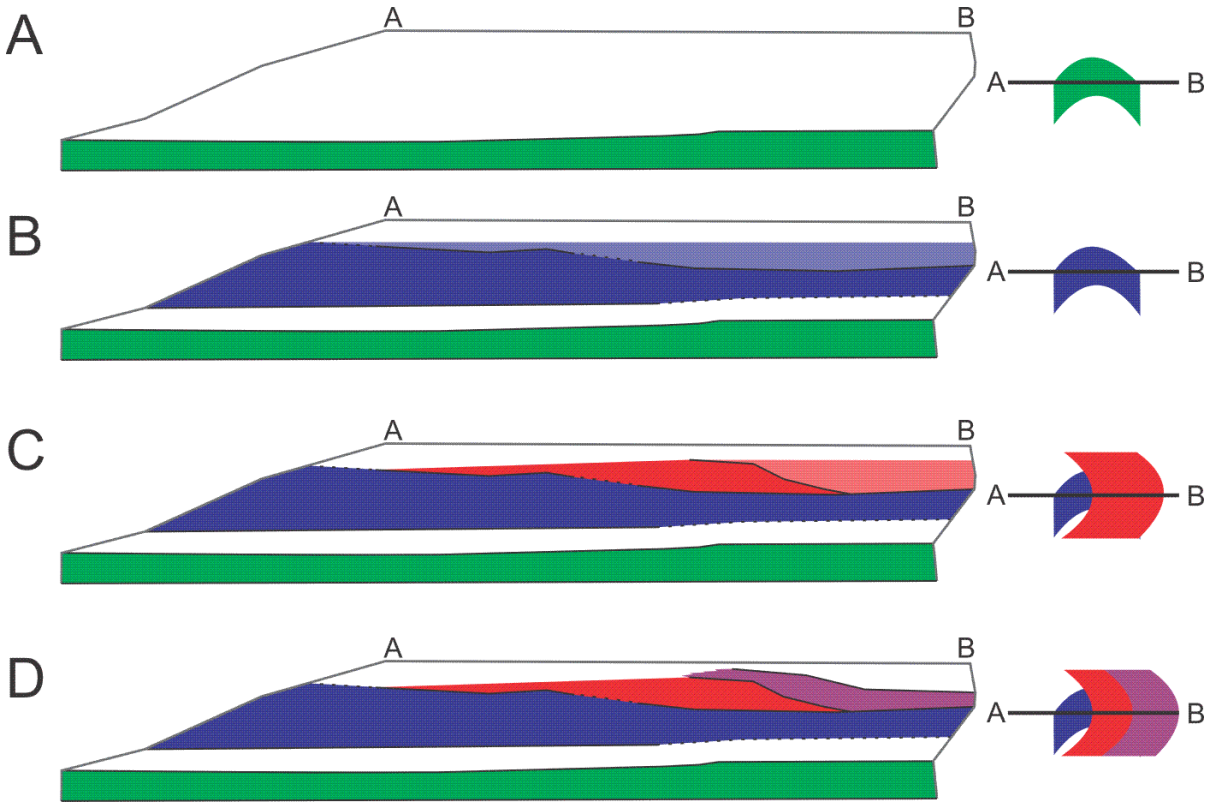

Figure 5.10: Cartoon illustrating the proposed depositional history of Isaac Unit 21 in both cross-section and plan view.

6 CONCLUSIONS

Continental slope channels are the primary conduits for transporting sediments from the continental shelf to the basin floor and when filled with sediment often form important hydrocarbon reservoirs. Recently, high resolution seismic surveys of highly-sinuous slope channels (e.g. Abreu et al., 2003) have documented shingled reflectors on the inner margin of channel bends, which are interpreted to have formed by the lateral migration of the channel. These reflectors appear to closely resemble well known lateral accretion deposits observed in modern and ancient fluvial systems, however, because of the paucity of accessible and well-documented cases of meter- to several-meter-scale lateral accretion deposits (LADs, figure) in sinuous deep-marine channels, this correlation remains equivocal. Examples of inclined deep-marine channel fills in the geological record are typically of the order of 10 m thick and whose width is constrained by the outcrop, which typically is less than 100 m. As a consequence the width of individual channels or the distance of their lateral migration, is currently poorly understood. Notwithstanding, channels are commonly filled with thickly-bedded, tabular or sigmoidal beds and grain size is commonly coarse with common granular or pebble conglomerates that may grade or transition abruptly upwards into sandstone. Bedding surfaces are typically inclined at 10º relative to horizontal.

At Castle Creek, Isaac Channel 2.2 (Arnott, 2007), Isaac Channel 2.3, Isaac Unit 14, and Isaac Unit 21 (this study) are interpreted to be the depositional product of laterally migrating, coarse-grained deep-marine sinuous channels. Each of these “channels” is in fact a channel complex composed of multiple channel elements that range from 5 to 15 m in thickness and commonly extend laterally for several hundreds of meters. Each channel element is typically filled with LADs, which in their lower part consist of amalgamated

upper coarse to very coarse sandstone, but obliquely upwards become distinctively interbedded and interfinger with thinly-bedded turbidites before terminating abruptly. Individual LADs are laterally offset stacked to form channel elements. Bedding inclination within the channel elements varies from around 10º to subhorizontal and is interpreted to reflect differences in the position of the exposure along the length of the sinuous channel and/or differences in the orientation of the various laterally juxtaposed channels as they intersect the outcrop face. Individual channel elements are separated on the basis of abrupt lateral offsets or changes in stratal inclination.

Based on textural attributes in outcrop, the flows that filled the channels are interpreted to have been enriched in coarse and very-coarse sand and comparatively depleted in finer sand, which likely is the result of winnowing of shallow-marine deposits during marine transgression. This resulted in highly density-stratified flows composed of a highly concentrated, coarse-grained basal part overlain abruptly by a finer, more dilute part (fig 5.5). The concentrated basal part of the flow is interpreted to be responsible for deposition of the coarse-grained part of the LADs in this study and also Arnott (2007), whereas the thinly-bedded turbidites, which interfinger with the sandstone and conglomerate, are interpreted to the product of deposition by the dilute upper part. Systematic lateral accretion of the channel is accomplished by recurring changes in flow conditions passing through the bend (Arnott, 2007). Upon entering a bend, the high-momentum core of the flow is diverted toward the outer-bank by inertial forces, enhancing erosion and increasing the cross-sectional profile. The continual accumulation of sediment-laden fluid along the outer bend would progressively steepen the cross-stream momentum imbalance (gradient) and accordingly the cross-channel secondary current toward the inner bend (a combination of baroclinic and barotropic flow components). At the same time, but along the inner bend, the near-bed

transport of coarse sediment would lead to a progressively more dense volume of coarse-grained sediment due to the inability of the current to lift these grains and complete the circulation cell. The continual accumulation of dense sediment-laden fluid on the inner bend would result in a second baroclinic pressure gradient, but this one directed toward the outer bank. These conditions would form a second circulation cell superimposed on the lower one, and also with the opposite sense of rotation -- toward the outer bank at its base and toward the inner bank at its top, and therein similar to flow patterns in modern stratified estuaries (e.g. Niedziko et al., 2009). Flows entering an enlarged cross-sectional profile (i.e. non equilibrium (bypass) dimensions) would expand and preferentially deposit sediment along the inner-bank, thereby returning the channel to equilibrium dimensions while continuously migrating laterally.

The channel elements in IC 2.3, IU 14, and IU 21 are interpreted to have formed by lateral migration of the channel and accretion along the inner bank largely controlled by the abnormally coarse sediment calibre of the flows. Contacts between channel elements are the result of either vertical offsets, such as the contact between CE21-1 and CE 21-2, or lateral offsets, for example between CE 2.3-2 and CE 2.3-3, and are likely controlled by differences between the equilibrium channel slope profile and the continental slope profile at the time of deposition. In cases where the difference is negligible, the tendency is for the channel to migrate laterally with little to no aggradation, such as IU 14. In contrast, when the equilibrium channel slope is higher than the physical slope the system aggrades and successive channel elements are vertically offset.

In conclusion, laterally-accreted channel fills described in this study and filled with lateral accretion deposits (LADs) differ by an order of magnitude (see fig 1.9) from lateral accretion packages (LAPs) resolved on seismic surveys (e.g. Abreu et al., 2003). While possibly

related, laterally accreted channel fills composed of LADs should not be considered equivalent to LAPs for the purposes of predicting their stratigraphic architecture. Shingled seismic reflectors, which are interpreted to be the result of lateral channel migration (e.g. Abreu et al., 2003), are more consistent with the notion of multiple offset-stacked channels, since intra-channel stratal architecture is most probably below seismic detection, and further compromised by its amalgamated sandstone (i.e. acoustically uniform) make-up. Future studies of laterally-accreted channel fills in the ancient sedimentary record should be performed to improve upon existing knowledge and create more robust models of these enigmatic channel types while simultaneously working to merge these observations with high-resolution seismic datasets.

BIBLIOGRAPHY

Abad, J.D., Sequeiros, O.E., Spinewine, B., Pirmez, C., Garcia, M.H., & Parker, G. (2011). Secondary current of saline underflow in a highly meandering channel: Experiments and theory. *Journal of Sedimentary Research*, 81, 787-813.

Abreu, V., Sullivan, M., Pirmez, C., & Mohrig, D. (2003). Lateral accretion packages (LAPs): an important reservoir element in deep water sinuous channels. *Marine and Petroleum Geology, 20*, 631-648.

Aitken, J.R., & McDonough, D.M.R. (1990). *Late Proterozoic glaciation, rifting, and eustasy, as illustrated by the Windermere Supergroup*. Geologic Association of Canada, NUNA Research Conference, Invermere and Valemount, British Columbia, 27 p.

Allen, J.R.L. (1964). Studies in fluviatile sedimentation. Six cyclothems in the Lower Old Red Sandstone, Anglo-Welsh Basin. *Sedimentology,* 3, 163-198.

Allen, J.R.L. (1970). Studies in fluviatile sedimentation. A comparison of fining-upwards cyclothems, with special reference to coarse-member composition and interpretation. *Journal of Sedimentary Petrology*, 40, 298-323.

Allen, J.R.L. (1982). *Sedimentary structures; their character and physical basis v1* (593 p.). New York, USA: Elsevier.

Allen, J.R.L., & Leeder, M.R. (1980). Criteria for the instability of upper-stage plane beds. *Sedimentology,* 27, 209-217.

Amos, K.J., Peakall, J., Bradbury, P.W., Roberts, M., Keevil, G., & Gupta, S. (2010). The influence of bend amplitude and planform morphology on flow and sedimentation in submarine channels. *Marine and Petroleum Geology*, 27, 1431-1447.

Arnott, R.W.C. (2007). Stratal architecture and origin of lateral accretion deposits (LADs) and counterminous inner-bank levee deposits in a base-of-slope sinuous channel, lower Isaac Formation (Neoproterozoic), East-Central British Columbia, Canada. *Marine and Petroleum Geology*, 24, 515-528.

Arnott, R.W.C. (2007). Stratigraphic architecture and depositional evolution of a levee to proximal crevasse-splay to channel fill succession: Units 13 and 14, Castle Creek North, Isaac Formation, Windermere Supergroup, British Columbia, Canada i*n* T.H. Nilson, R.D. Shew, G.S. Steffens and J.R.J. Studlick (Eds.), *Atlas of deep-water outcrops* (pp. 111-114). AAPG studies in Geology 56.

Arnott, R.W.C. (2010). Deep-marine sediments and sedimentary systems, Ch. 12, *in* N.P. James and R.W. Dalrymple (Eds.), *Facies Models* 4 (pp. 295-321), Geological

Association of Canada.

Arnott, R.W.C. (2012). Turbidites and the case of the missing dunes. *Journal of Sedimentary Research*, 82, 379-384.

Arnott, R.W.C., & Hand, B.M. (1989). Bedforms, primary structures, and grain fabric in the presence of suspended sediment rain. *Journal of Sedimentary Petrology*, 59, 1062-1069.

Baas, J.H., & Best, J.L. (2002) Turbulence modulation in clay-rich sediment-laden flows and some implications for sediment deposition. *Journal of Sedimentary Research*, 72, 89-103.

Babonneau, N., Savoye, B., Cremer, M., & Klein, B. (2002) Morphology and architecture of the present canyon and channel system of the Zaire deep-sea fan. *Marine and Petroleum Geology*, 19, 445-467.

Bagnold, R.A. (1962). Auto-suspension of transported sediments: turbidity currents. *Proceedings of the Royal Society of London*, A265, 315-319.

Beaubouef, R.T., Rossen, C., & Lovell, R.W.W. (2007). The Beacon Channel: A Newly Recognized Architectural Type in the Brushy Canyon Formation, Texas, USA i*n* T.H. Nilson, R.D. Shew, G.S. Steffens and J.R.J. Studlick (Eds.), *Atlas of deep-water outcrops* (pp. 432-443). AAPG studies in Geology 56.

Best, J.L. (1992). On the entrainment of sediment and initiation of bed defects: insights from recent development within turbulent boundary layer research. *Sedimentology*, 39, 797-811.

Bouma, A.H. (1962). *Sedimentology of some flysch deposits* (168 p.). Amsterdam, NED: Elsevier.

Bridge, J.S., & Jarvis, J. (1982) The dynamics of a river bend: a study in flow and sedimentary processes. *Sedimentology*, 29, 499-541.

Campbell, R.B., Mountjoy, E.W., & Young, F.G. (1973). Geology of the McBride map-area, British Columbia (93-H). *Geological Survey of Canada,* 72, 104p.

Catuneanu, O., Abreu, V., Bhattacharya, J.P., Blum, M.D., Dalrymple, R.W., Eriksson, P.G., Fielding, C.R., Fisher, W.L., Galloway, W.E., Gibling, M.R., Giles, K.A., Holbrook, J.M., Jordan, R., Kendall, C.G.St.C., Macurda, B., Martinsen, O.J., Miall, A.D., Neal, J.E., Nummedal, D., Pomar, L., Posamentier, H.W., Pratt, B.R., Sarg, J.F., Shanley, K.W., Steel, R.J., Strasser, A., Tucker, M.E., & Winker, C. (2009). Towards the standardization of sequence stratigraphy. *Earth-Science Reviews*, 92, 1-33.

Clemenceau, G.R., Colbert, J., & Eddens, J. (2000). Production results from levee-overbank turbidite sands at Ram/Powell field, deepwater Gulf of Mexico, *in* P. Weimer, R.M.

Slatt, J. Coleman, N.C. Rosen, H. Nelson, A.H. Bouma, M.J. Styzen, & D.T. Lawrence (Eds.), *Deep-water reservoirs of the world* (pp 241-251). Gulf Coast Section SEPM 20th Bob F. Perkins Research Conference.

Coleman, J.L., Jr. (2000). Carboniferous submarine basin development of the Ouachita Mountains of Arkansas and Oklahoma, *in* A.H. Bouma, and C.G. Stone (Eds.), *Fine-grained turbidite systems* (pp. 21-32). American Association of Petroleum Geologists Memoir 72/SEPM Special Publication 68.

Coleman, S.E., & Eling, B. (2000). Sand wavelets in laminar open-channel flows. *Journal of Hydraulic Research*, 38, 331-338.

Colpron, M., Logan, J.M., & Mortensen, J.K. (2002). U-Pb zircon age constraint for late Neoproterozoic rifting and initiation of the lower Paleozoic passive margin of western Laurentia. *Canadian Journal of Earth Sciences*, 39, 133-143.

Corney, R.K.T., Peakall, J., Parsons, D.R., Elliot, L., Amos, K.J., Best, J.L., Keevil, G.M., & Ingham, D.B. (2006). The orientation of helical flow in curved channels. *Sedimentology*, 53, 249-257.

Corney, R.K.T., Peakall, J., Parsons, D.R., Elliott, L., Best, J.L., Thomas, R.E., Keevil, G.M., Ingham, D.B., & Amos, K.J. (2008). Reply to the discussion of Imran et al. on "The orientation of helical flow in curved channels" by Corney et al.. *Sedimentology,* 53, 249-257.

Cronin, B.T. (1995). Structurally-controlled deep sea channel courses: examples from the Miocene of southeast Spain and Alboran Sea, southwest Mediterranean *in* A.J. Hartley and D.J. Prosser (Eds.), *Characterization of Deep Marine Clastic Systems* (pp. 115-165). Geological Society Special Publication No. 94.

Dalziel, I.W.D. (1991). Pacific margins of Laurentia and East Antarctica-Australia as a conjugate rift pair: evidence and implications for an Eocambrian supercontinent. *Geology*, 19, 598-601.

Damuth, J.E., Flood, R.D., Kowsmann, R.O., Belderson, R.H., & Giorini, M.A. (1988). Anatomy and growth pattern of Amazon deep-sea fan as revealed by long-range side-scan sonar (GLORIA) and high resolution seismic studies. *Bulletin of the American Association of Petroleum Geologists*, 72, 885-911.

Dykstra, M., & Kneller, B. (2007). Canyon San Fernando: a deep-marine channel-levee complex exhibiting evolution from submarine-canyon confined to unconfined, *in* T.H. Nilson, R.D. Shew, G.S. Steffens and J.R.J. Studlick (Eds.), *Atlas of deep-water outcrops* (pp. 226-230). AAPG studies in Geology 56.

Dykstra, M., & Kneller, B. (2009). Lateral accretion in a deep-marine channel complex: implications for channelized flow processes in turbidity currents. *Sedimentology, 56*, 1411-1432.

Eisbacher, G.H, (1985). Late Proterozoic rifting, glacial sedimentation, and sedimentary cycles in the light of Windermere deposition, western Canada. *Paleogeography, Paleoclimatology, and Paleoecology*, 51, 231-254.

Elliott, T. (2000). Depositional architecture of a sand-rich, channelized turbidite system: the Upper Carboniferous Ross Sandstone formation, Western Ireland, *in* P. Weimer, R.M. Slatt, A.H. Bouma and D.T. Lawrence (Eds.), *Deep-water reservoirs of the world* (pp. 342-373). Gulf Coast Section SEPM 20th Bob F. Perkins Research Conference

Fisher, R.V. (1983). Flow transformations in sediment gravity flows. *Geology*, 11, 273-274.

Gabrielse, H., & Campbell, R.B. (1991). Upper Proterozoic assemblages, *in* H. Gabrielse and C.J. Lorath (Eds.), *Geology of the Cordilleran orogen in Canada* (pp. 125-150). Geological Society of America, v. G-02.

Gardner, M.H., & Borer, J.M. (2000). Submarine channel architecture along a slope to basin profile, Brushy Canyon Formation, west Texas *in* A.H. Bouma and C.G. Stone (Eds.), *Fine-Grained Turbidite Systems* (pp. 195-214). American Association of Petroleum Geologists Memoir 72/SEPM Special Publication 68.

Gardner, M.H., Borer, J.M., Melick, J.J., Mavilla, N., Dechesne, M., & Wagerlie, R.N. (2003). Stratigraphic process-response model for submarine channels and related features from studies of Permian Brushy Canyon outcrops, West Texas. *Marine and Petroleum Geology*, 23, 443-458.

Hampton, M.A. (1972). The role of subaqueous debris flow in generating turbidity currents. *Journal of Sedimentary Petrology*, 42, 775-793.

Hampton, M.A. (1975). Competence of fine-grained debris flows. *Journal of Sedimentary Petrology*, 45, 834-844.

Harlan, S.S., Heaman, L., LeCheminant, A.N., & Premo, W.R. (2003). Gunbarrel mafic magmatic event: A key 780 Ma time marker for Rodinia plate reconstructions. *Geology*, 31, 1053-1056.

Hein, F.J. and McMechan, M.E. (1994). Chapter 6: Proterozoic and Lower Cambrian strata of the Western Canada Sedimentary Basin, *in* P.G. Mossop, I. Shetse (Comps.), *Geological Atlas of the Western Canada Sedimentary Basin* (pp. 57-68), Canadian Society of Petroleum Geologists and the Alberta Research Council, Calgary.

Hoffman, P.F. (1991). Did the breakout of Laurentia turn Gondwanaland inside-out? *Science*, 252, 1409-1412.

Hunt, D. and Tucker, M.E. (1992). Stranded parasequences and the forced regressive wedge systems tract: deposition during base-level fall. *Sedimentary Geology*, 81, 1-9.

Imran J., Islam, M.A., Huang, H., Kassem, A., Dickerson, J., Pirmez, C., & Parker, G. (2007). Helical flow couplets in submarine gravity underflows. *Geology*, 35, 659-662.

Imran, J., Islam, A.M., & Kassem, A. (2008) Discussion of "The orientation of helical flow in curved channel" by Corney et al.. *Sedimentology*, 55, 235-239.

Islam, M.A., Imran, J., Pirmez, C. & Cantelli, A. (2008). Flow splitting modifies the helical motion in submarine channels. *Geophysical Research Letters*, 35, L22603, doi:10.1029/2008GL034995.

Janocko, M. (2011). Deep-water sinuous channels: their development and architecture. Ph.D. Thesis (unpublished), University of Bergen.

Jolly, R.J.H., & Lonergan, L. (2002). Mechanisms and controls on the formation of sand intrusions. *Journal of the Geological Society of London*, 159, 605-617.

Khan, Z. (2012). Origin and architecture of deep-water levee deposits: insight from the ancient rock record and experiments. Ph.D. thesis, Department of the Earth Sciences, University of Ottawa, Ottawa, 300 p.

Kastens, K.A., & Shore, A.N. (1985). Depositional processes of a meandering channel on Mississippi Fan. *Bulletin of the American Association of Petroleum Geologists*, 69, 190-202.

Keevil, G.M., Peakall, J., Best, J.L., & Amos, K.J. (2006). Flow structure in sinuous submarine channels: velocity and turbulence structure of an experimental submarine channel. *Marine and Petroleum Geology*, 24, 487-503.

Kendall, B.S., Creaser, R.A., Ross, G.M., & Selby, D. (2004). Constraints on the timing of Marinoan "Snowball Earth" glaciation by 187Re-187Os dating of a Neoproterozoic, post-glacial black shale in Western Canada. *Earth and Planetary Science Letters*, 222, 729-740.

Kilner, B., Niocaill, C., & Brasier, M. (2005). Low-latitude glaciation in the Neoproterozoic of Oman. *Geology*, 33, 413-416.

Kleverlaan, K. (1989). Three distinctive feeder-lobe systems within one time slice of the Tortonian Tabernas fan, SE Spain. *Sedimentology,* 36, 25-45.

Kneller, B.C., & Buckee, C. (2000). The structure and fluid mechanics of turbidity currents: a review of some recent studies and their geologic implications. *Sedimentology*, 47 (Suppl. 1), 62-94.

Knoll, A.H., Walter, M.R., Narbonne, G.M., & Christie-Blick, N. (2006). The Ediacaran Period: A new period for the geologic time scale. *Science*, 305, 621-622.

Kolla, V., Posamentier, H.W., & Wood, L.J. (2007). Deep-water and fluvial sinuous channels – Characteristics, similarities and dissimilarities, and modes of formation. *Marine and Petroleum Geology*, 24, 388-405.

Kuenen, P.H. (1966). Matrix of turbidites: experimental approach. *Sedimentology*, 7, 269-297.

Kuenen, P.H., & Migliorini, C.I. (1950). Turbidity currents as a cause of graded bedding. *Journal of Geology*, 58, 91-127.

Li, Z., & Davies, A.G. (2001). Turbulence closure modelling of sediment transport beneath large waves. *Continental Shelf Resources*, 21, 243-262.

Li, Z.X., Bogdanova, S.V., Collins, A.S., Davidson, A., De Waele, B., Ernst, R.E., Fitzsimmons, I.C.W., Fuck, R.A., Gladkochub, D.P., Jacobs, J., Karlstrom, K.E., Lu, S., Natapov, L.M., Pease, V., Pisarevsky, S.A., Thrane, K., & Vernikovsky, V. (2008). Assembly, configuration, and break-up history of Rodinia: A synthesis. *Precambrian Research*, 160, 179-210.

Link, P.K., Christie-Blick, N., Devlin, W.J., Elston, D.P., Horodyski, R.J., Levy, M., Miller, J.M.G., Pearson, R.C., Prave, A., Stewart, J.H., Winston, D., Wright, L.A., & Wrucke, C.T. (1993). Middle and Late Proterozoic stratified rocks of the western United States Cordillera, Colorado Plateau, and Basin and Range Province *in* J. Reed, P. Sims, R.S. Houston, D.W. Rankin, P.K. Link, W.R. Van Schmus, & M.E. Bickford (Eds.), *Precambrian: Counterminous United States* (pp. 474-690). Geological Society of America Decade of North American Geology Series C-3.

Lowe, D.R. (1982). Sediment gravity flows: II. Depositional models with special relevance to the deposits of high-density turbidity currents. *Journal of Sedimentary Petrology*, 52, 279-297.

Martinsen, O.J., & Bakken, B. (1990). Extensional and compressional zones in slumps and slides in the Namurian of County Clare, Ireland. *Journal of the Geological Society of London*, 147, 153-164.

Martinsen, O.J., Lien, T., & Walker, R.G. (2000). Upper Carboniferous Deep Water Sediments, Western Ireland: Analogues for Passive Margin Turbidite Plays *in* P. Weimer, R.M. Slatt, J. Coleman, N.C. Rosen, H. Nelson, A.H. Bouma, M.J. Styzen, & D.T. Lawrence (Eds.), *Deep-water reservoirs of the world* (pp. 533-555). Gulf Coast Section SEPM 20th Bob F. Perkins Research Conference.

Martinsen, O.J., & Collinson, J.D. (2002). The Western Irish Namurian Basin reassessed – a discussion. *Basin Research,* 14, 523-542.

Meyer, L. (2004). Internal architecture of an ancient deep-water, passive margin, basin-floor fan system, Upper Kaza Group, Windermere Supergroup, Castle Creek, British Columbia. Unpublished M.Sc. thesis, Department of Geology and Geophysics,

University of Calgary, Calgary, Alberta, 188 p.

McCann, T. (Ed.) (2008). *The Geology of Central Europe, Volume 2: Mesozoic and Cenozoic* (752 p.). Bath, ENG: Geological Society of London.

McHargue, T., Pyrcz, M.J., Sullivan, M.D., Clark, J.D., Fildani, A., Romans, B.W., Covault, J.A., Levy. M., Posamentier, H.W., & Drinkwater, N.J. (2011). Architecture of turbidite channel systems on the continental slope: Patterns and predictions. *Marine and Petroleum Geology, 28*, 728-743.

Miall, A.D. (1996). *The geology of Fluvial Deposits: Sedimentary Facies, Basin Analysis, and Petroleum Geology* (582 p.). New York, USA: Springer.

Middleton, G.V., and Hampton, M.A. (1973). Sediment gravity flows: mechanics of flow and deposition, *in* G.V. Middleton and A.H. Bouma (Eds), *Turbidites and Deep Water Sedimentation, Short Course Notes, no. 1* (pp.1-38) SEPM (Pacific Section), Los Angeles.

Mohrig, D., Whipple, K.X., Hondzo, M., Ellis, C., & Parker, G. (1998). Hydroplaning of subaqueous debris flows. *Geological Society of America Bulletin*, 110, 387-394.

Mohrig, D., Elverhoi, A., & Parker, G. (1999). Experiments on the relative mobility of muddy subaqueous and subaerial debris flows, and their capacity to remobilize antecedent deposits. *Marine Geology*, 154, 117-129.

Moores, E.M. (1991). Southwest U.S.-East Antarctic (SWEAT) connection: a hypothesis. *Geology*, 19, 425-428.

Morris, W.R., & Busby-Sperra, C.J. (1990). A submarine fan valley-levee complex in the UpperCretaceous Rosario Formation, Baja California: Implications for turbidite facies models. *Geological Society of America Bulletin*, 65, 1256-1284.

Mulder, T., & Alexander, J. (2001). The physical character of subaqueous sedimentary density flows and their deposits. *Sedimentology*, 48, 269-299.

Navarro, L.L. (2005). Depositional architecture and evolution of deep-water base-of-slope and slope channel complexes in a passive-margin setting: Isaac Formation, Windermere Supergroup (Neoproterozoic), southern Canadian Cordillera. M.Sc. thesis, Department of Earth Sciences, University of Ottawa, Ottawa, 293 p.

Nidzieko, N.J., Hench, J.L., & Monismith, S.G. (2009). Lateral Circulation in Well-Mixed and Stratified Estuarine Flows with Curvature. *Journal of Physical Oceanography*, 39, 831-851.

Normark, W.R., Barnes, N.E., & Coumes, F. (1985). Rhone Fan, Mediterranean *in* A.H. Bouma, W.R. Normark, & N.E. Barnes (Eds.), *Submarine Fans and Related Turbidite Systems* (pp. 151-156). New York, USA: Springer.

O'Byrne, C.J., Barton, M.D., Steffens, G.S., Pirmez, C., & Buergisser, H. (2007). Architecture of a laterally migrating channel-complex: Channel 4, Isaac Formation, Windermere Supergroup, Castle Creek North, British Columbia, Canada i*n* T.H. Nilson, R.D. Shew, G.S. Steffens and J.R.J. Studlick (Eds.), *Atlas of deep-water outcrops* (pp. 115-118). AAPG studies in Geology 56.

Peakall, J., Amos, K.J., Keevil, G.M., Bradbury, P.W., & Gupta, S. (2007) Flow processes and sedimentation in submarine channel bends. *Marine and Petroleum Geology*, 24, 470-486.

Plint, A.G. (2010). Wave- and storm-dominated shoreline and shallow-marine systems, Ch. 8, *in* N.P. James and R.W. Dalrymple (Eds.), *Facies Models 4* (pp. 167-199), Geological Association of Canada.

Posamentier, H.W., & Kolla, V. (2003). Seismic geomorphology and stratigraphy of depositional elements in deep-water settings. *Journal of Sedimentary Research*, 73, 367-388.

Posamentier, H.W., & Walker, R.G. (2006). Deep-water turbidites and submarine fans, *in* H.W. Posamentier and R.G. Walker (Eds.), *Facies Models Revisited*. SEPM special publication no. 84.

Postma, G., Cartigny, M., & Kleverlaan, K. (2009). Structureless, coarse-tail graded Bouma Ta formed by internal hydraulic jump of the turbidity current? *Sedimentary Geology*, 219, 1-6.

Postma, G., & Cartigny, M. (2014). Supercritical and subcritical turbidity currents and their deposits – A synthesis. *Geology,* 42, 987-990.

Postma, G., Klerverlaan, K., & Cartigny, M.J.B. (2014). Recognition of cyclic steps in sandy and gravelly turbidite sequences, and consequences for the Bouma facies model. *Sedimentology*, 61, 2268-2290.

Price, R.A. (2000). The southern Canadian Rockies: evolution of a foreland thrust and fold belt. *GeoCanada2000,* Field Trip Guidebook 13, 244p.

Pyles, D.R., Jennette, D.C., Tomasso, M., Beaubouef, R.T., Rossen, C. (2010). Concepts learned from a 3D outcrop of a sinuous slope channel complex: Beacon Channel Complex. Brushy Canyon Formation, West Texas, U.S.A. *Journal of Sedimentary Research*, 80, 67-96.

Pyles, D.R., Tomasso, M., & D.C. Jennette. (2012). Flow processes and sedimentation associated with erosion and filling of sinuous submarine channels. *Geological Society of America*, 40, 143-146.

Redbourn, L.J., Bull, J.M., Scrutton, R.A., & Stow, D.A.V. (1993). Channels, echo character

mapping and tectonics from 3.5 kHz profiles, distal Bengal Fan. *Marine Geology*, 114, 155-170.

Romans, B.W. (2003). Sedimentation patterns of a Permian basinal cycle, Upper Cutoff, Brushy Canyon, and lower Cherry Canyon formations, western Delaware Basin, west Texas and southeastern New Mexico. Masters Thesis (unpublished), Colorado School of Mines, Golden, 175 p.

Romans, B.W., Schultz, M.R., Hubbard, S.M., & Graham, S.A. (2007). Facies architecture of slope channel complexes, Tres Pasos Formation at Cerro Divisadero, Chile *in* T.H. Nilson, R.D. Shew, G.S. Steffens and J.R.J. Studlick (Eds.), *Atlas of deep-water outcrops* (pp. 132-135). AAPG studies in Geology 56.

Ross, G.M. (1988). The cryptic platform to the Windermere grit system. *Geological Society of America Abstracts with Program*, 16, p. A107.

Ross, G.M. (1991). Tectonic setting of the Windermere Supergroup revisited: Geology, v. 19, p. 1125-1128.

Ross, G.M. (2000). The Neoproterozoic Windermere Supergroup: An on-land continental margin turbidite system. *Geological Survey of Canada Open File 3932*, 2 p.

Ross, G.M., & Bowring, S.A. (1990). Detrital zircon geochronology of the Windermere Supergroup and the tectonic assembly of the southern Canadian Cordillera. *Journal of Geology*, 98, 879-893.

Ross, G.M., & Parrish, R.R. (1991). Detrital zircon geochronology of metasedimentary rocks in the southern Omineca Belt, Canadian Cordillera. *Canadian Journal of Earth Sciences*, 28, 1254-1270.

Ross, G.M., Bloch, J.D., & Krouse, H.R. (1995). Neoproterozoic strata of the southern Canadian Cordillera and the isotopic evolution of seawater sulfate: Precambrian Research, v.73, p. 71-99.

Ross, G.M. and Arnott, R.W.C. (2007). Regional geology of the Windermere Supergroup, southern Canadian Cordillera and stratigraphic setting of the Castle Creek study area, Canada, *in* T.H. Nilson, R.D. Shew, G.S. Steffens and J.R.J. Studlick (Eds.), CD-ROM, 16 p. *Atlas of deep-water outcrops.* AAPG studies in Geology 56.

Russell, H.J.S., & Arnott, R.W.C. (2003). Hydraulic jump and hyperconcentrated-flow deposits of a glaciogenic subaqueous fan: Oak ridges moraine, southern Ontario, Canada. *Journal of Sedimentary Research*, 73, 887-905.

Schwarz, E., & Arnott, R.W.C. (2007). Anatomy and evolution of a slope-channel complex set (Neoproterozoic Isaac Formation, Windermere Supergroup, southern Canadian Cordillera): Implications for reservoir characterization. *Journal of Sedimentary Research*, 77, 89-109.

Smith, M.D. (2009). Stratigraphic and geochemical evolution of the Old Fort Point Formation, southern Canadian Cordillera: the deep-marine perspective of Ediacaran post-glacial environmental change. Ph.D. thesis, Department of Earth Sciences, University of Ottawa, Ottawa, 465 p.

Sprague, A.R.G. (1985). Depositional environment and petrology of the lower member of the Pennsylvanian Atokan Formation, Ouachita Mountains, Arkansas and Oklahoma. Ph.D. thesis (unpublished), University of Texas, Dallas, 323 p.

Sullivan, M., Jensen, G., Goulding, F., Jennette, D., Foreman, L., & Stern, D. (2000). Architectural Analysis of Deep-Water Outcrops: Implications for Exploration and Development of the Diana Sub-Basin, Western Gulf of Mexico *in* P. Weimer, R.M. Slatt, J. Coleman, N.C. Rosen, H. Nelson, A.H. Bouma, M.J. Styzen, & D.T. Lawrence (Eds.), *Deep-water reservoirs of the world* (pp. 1010-1031). Gulf Coast Section SEPM 20th Bob F. Perkins Research Conference.

Sumner, E.J., Peakall, J., Dorrell, R.M., Parsons, D.R., Darby, S.E., Wynn, R.B., McPhail, S.D., Perrett, J., Webb, A., & White, D. (2014). Driven arounf the bend: Spatial evolution and controls on the orientation of helical bend flow in a natural submarine gravity current. *Journal of Geophysical Research*, 119, 898-913.

Sylvester, Z., & Lowe, D. R. (2004). Textural trends in turbidites and slurry beds from the Oligocene flysch of the East Carpathians, Romania. *Sedimentology*, 51, 954-972.

Terlaky, V. (2014). Sedimentology, stratigraphy, architecture and origin of deep-water, basin-floor deposits: Middle and Upper Kaza Group, Windermere Supergroup, B.C., Canada. Ph.D. Thesis, Department of Earth Sciences, University of Ottawa, Ottawa, 240 p.

Thomas, R.G., Smith, D.G., Wood, J.M., Visser, J., Anne Calverley-Range, E., & Koster, E.H. (1987). Inclined heterolithic stratification-terminology, description, interpretation, and significance. *Sedimentary Geology*, 53, 123-179.

Tilston, M., Arnott, R.W.C., & Rennie, C. (2012). Effects of grain size and sediment concentration on turbulence and sediment transport dynamics in unsteady turbidite currents. AAPG 2012 Long Beach, Ca, Abstracts no. 1236460.

Valentine, J.W., & Moores, E.M. (1970). Plate-tectonic regulation of animal diversity and sea-level: a model. *Nature*, 228, 657-659.

Venditti, J.G., Church, M., & Bennet, S.J. (2005). Bed form initiation from a flat bed. *Journal of Geophysical Research*, v. 110, F01009, doi: 10.1029/2004JF000149.

Venditti, J.G., Church, M. and Bennet, S.J. (2006). On interfacial instability as a cause of transverse subcritical bedforms. *Water Resources Research*, 42, doi: W07423, doi: 10.1029/2005WR004346.

Walker, R.G. (1965). The origin and significance of the internal sedimentary structures of turbidites. *Yorkshire Geological Society Proceedings*, 35, p. 1-29.

Williams, P.B., & Kemp, P.H. (1971). Initiation of ripples on a flat sand bed. *Journal of the Hydraulics Division, American Society of Civil Engineers*, 97, 505-522.

Weimer, P., Slatt, R.M., Coleman, J., Rosen, N.C., Nelson, H., Bouma, A.H., Styzen, M.J. and Lawrence, D.T. (Eds.)(2000). *Deep-water reservoirs of the world.* Gulf Coast Section SEPM 20th Bob F. Perkins Research Conference.

Weirich, F.H. (1988). Field evidence for hydraulic jumps in subaqueous sediment gravity flows. *Nature*, 332, 626-629.

Wynn, B.R., Cronin, B.T., & Peakall, J. (2007). Sinuous deep-water channels: Genesis, geometry, architecture. *Marine and Petroleum Geology*, 24, 341-387.

Zelt, F.B., & Rossen, C. (1995). Geometry and continuity of deep-water sandstones and siltstones, Brushy Canyon Formation (Permian) Delaware Mountains, Texas, *in* K.T. Pickering, R.N. Hiscott, N.H. Kenyon, F. Ricci Luchi, and R.D. Smith (Eds.), *Atlas of Deep Water Environments – Architectural Style in Turbidite Systems* (pp. 111-146). London, ENG: Chapman and Hall.

Zou, F., Slatt, R., Bastidas, R., & Ramirez, B. (2012). Integrated outcrop reservoir characterization, modeling, and simulation of the Jackfork Group at the Baumgartner Quarry area, western Arkansas: Implications to Gulf of Mexico deep-water exploration and production. *AAPG Bulletin*, 96, 1429-1448.